DNA DAMAGE SENSORS IN THE CHECKPOINT RESPONSE

by

Elizabeth Jean Little

A Dissertation Submitted to the Faculty of the

DEPARTMENT OF MOLECULAR AND CELLULAR BIOLOGY

In Partial Fulfillment of the Requirements
For the Degree of

DOCTOR OF PHILOSOPHY

In the Graduate College of

THE UNIVERSITY OF ARIZONA

2003

ProQuest Information and Learning Company
300 North Zeeb Road
P.O. Box 1346
Ann Arbor, MI 48106-1346

THE UNIVERSITY OF ARIZONA ®
GRADUATE COLLEGE

As members of the Final Dissertation Examination Committee, we certify that we have read the dissertation prepared by Elizabeth Jean Little

entitled DNA Damage Sensors in the Checkpoint Response

and recommend that it be accepted as fulfilling the dissertation requirement for the Degree of Doctor of Philosophy

Ted Weinert	Date 6/27/03
Roy Parker	Date 6/27/03
Carol Dieckmann	Date 6/27/03
Lisa Nagy	Date 6/27/03
	Date

Final approval and acceptance of this dissertation is contingent upon the candidate's submission of the final copy of the dissertation to the Graduate College.

I hereby certify that I have read this dissertation prepared under my direction and recommend that it be accepted as fulfilling the dissertation requirement.

Dissertation Director Ted Weinert	Date 6/27/03

STATEMENT BY AUTHOR

This dissertation has been submitted in partial fulfillment of requirements for an advanced degree at the University of Arizona and is deposited in the University Library to be made available to borrowers under rules of the Library.

Brief quotations from this dissertation are allowable without special permission, provided that accurate acknowledgment of source is made. Requests for permission for extended quotations from or reproduction of this manuscript in whole or in part may be granted by the head of the major department or the Dean of the Graduate College when in his or her judgment the proposed use of the material is in the interests of scholarship. In all other instances, however, permission must be obtained from the author.

SIGNED: 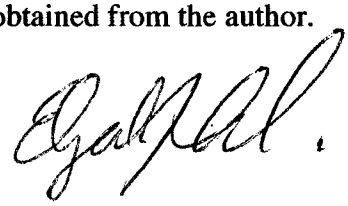

ACKNOWLEDGMENT

I'd like to acknowledge my advisor Ted Weinert for the financial support, which helped me through the trials and tribulations of not only learning, but also introducing and adapting biochemical techniques into his laboratory. I would also like to thank my committee members Roy Parker, Lisa Nagy, Carol Dieckmann, and Lynn Manseau for their support. All of the past and present members of the Weinert lab forwarded this work in one way or another. In addition, the Dieckmann lab was particularly supportive during the end of my tenure as a graduate student. One person of notable mention from the Department of Molecular and Cellular Biology is Catherine McLellan, Ph.D. who inspired me to "get it done". I would also like to thank the Tucson Yoga community for supporting me during the last few years of finishing my degree, especially Rachel King for inspiring morning discussions. My parents Howard and Mary Jo Little should have their own advanced degrees in support, and without them this would not have been possible. Spot Little encouraged me to stay enthusiastic regardless of the day or the page I was on, and Bogart Little was curled under my chair in her own show of support for the majority of my writing. And lastly, I would like to thank Marcus Needham for loving me during the most difficult part of my dissertation.

TABLE OF CONTENTS

TABLE OF CONTENTS - *Continued*

TABLE OF CONTENTS - *Continued*

LIST OF FIGURES

LIST OF FIGURES - *Continued*

LIST OF TABLES

ABSTRACT

The DNA damage checkpoint response detects DNA damage and responds to the damage by promoting DNA repair, transcriptional regulation, and cell cycle arrest. Prior to the beginning of this dissertation the checkpoint sensor proteins in *S. cerevisiae* were identified as Ddc1, Mec3, Rad9, Rad17 and Rad24. However, none of the sensors had been shown to bind DNA directly, an anticipated function of checkpoint sensors. To characterize these proteins a biochemical approach was taken to test whether any of the checkpoint sensor proteins could detect DNA.

The associated DNA binding properties of Rad24 and Rad9 were identified and characterized for the first time. Both of these checkpoint sensor proteins have an affinity for ssDNA, a common intermediate DNA structure of most DNA repair processes. In addition, the DNA damage checkpoint mutant protein Rad24-1 is defective for binding to ssDNA, suggesting that Rad24 DNA binding is required for its function in the checkpoint response.

The potential exonuclease activity of Rad17 was tested using purified protein and various DNA substrates. This study was based on reports that the Rad17 homolog Rec1 from *U.maydis* is a 3'->5' DNA exonuclease, and genetic data that indicated that Rad17 has a role in telomere degradation. Exonuclease assays with Rad17 protein preparations and ssDNA found an associated weak exonuclease that was not significantly above background levels.

Conserved residues of Rad17 thought to be required for exonuclease activity and checkpoint activity were mutated and studied for their affect on the DNA damage

checkpoint. These studies imply that in addition to the region of Rad17 that is homologous to PCNA, the long carboxy-terminal region of Rad17 is also required for its checkpoint activity.

Collectively, these studies suggest that the common DNA repair intermediate structure, single-stranded DNA, is recognized in a Rad9 and Rad24 dependent manner to initiate the DNA damage checkpoint response. This suggests that the initiation of the checkpoint response is the recognition of a single DNA structure instead of the many different structures of primary DNA damage by free radicals, UV, γ-radiation, alklylation, double strand breaks, and base mismatches.

CHAPTER 1

PRODUCTIVE PROTEIN INTERACTIONS ACTIVATE DNA DAMAGE CHECKPOINT RESPONSE IN *SACCHAROMYCES CEREVISIAE.*

Introduction

The ability of an organism to protect its genome from the DNA damage is important to the maintenance of a species. Should the genomic integrity of an organism be compromised, mutations can arise that are deleterious to the organism in addition to potentially affecting the viability of future progeny. Unfortunately, the genome is naturally unstable, and by simply duplicating its genome an organism can create mutations due to replication errors. In addition, the intracellular environment of the cell is prone to forming free radicals that damage DNA. Compounding this, the external environment presents challenges to the DNA in the form of various DNA damaging agents, such as radiation and mutagenic chemical compounds.

To prevent the accumulation of mutations, cells have developed several methods to protect their genome. First, cells utilize high fidelity DNA replication enzymes for nearly accurate duplication of their genomes. Secondly, cells have numerous DNA repair mechanisms that repair DNA when errors have been made during DNA replication, or when the genome has been damaged. And lastly, the cells have the ability to slow down or stop the cell cycle when faced with DNA damage or incomplete replication, thereby allowing time for repair. This mechanism of cell cycle delay is one aspect of a coordinated cellular response to DNA damage known as the DNA damage checkpoint

response. Cells that are defective in the DNA damage checkpoint or DNA repair processes have reduced viability in response to DNA damage.

The observation that DNA damage affects cell cycle progression was first made in prokaryotes (George et al., 1975). This was termed the SOS response and enhances cell survival in the face of environmental stress. A similar cell cycle progression control was found to be inactive in the cells of ataxia telangiectasia patients, which are defective in the ataxia-telangiectasia mutated gene (ATM)(Painter and Young, 1980). Later, cell cycle controls were also found in yeast where the majority of progress has been made characterizing the DNA damage checkpoint response (Weinert and Hartwell, 1988).

Initiation of the DNA damage checkpoint response.

The misregulation of the timing of events during the cell cycle can result in lethality. For example, if a cell has not finished replicating its genome and proceeds to mitosis, the result could be that both the mother and daughter cell inherit incomplete genomes. Therefore, cells have developed several checkpoints throughout the cell cycle in which they can control cell cycle progression in response to DNA perturbations.

The G1/S DNA damage checkpoint prevents the replication of damaged DNA, this prevents the fixing of mutations and potentially wasting energy duplicating an erroneous genome (Siede et al., 1994). In *S.cerevisiae* the G1/S DNA damage checkpoint delays the cell cycle in response to most forms of DNA damage (Gerald et al., 2002), this is in contrast to the robust arrest that results from the activation of the G2/M DNA damage checkpoint (Weinert et al., 1994). The S-phase checkpoint response slows the rate of replication due to replication blocks (Paulovich et al., 1997). The G2/M DNA

damage checkpoint prevents the separation of genomes following DNA damage and ensures that the daughter cell will inherit a complete and undamaged genome. This is the primary DNA damage checkpoint in *S.cerevisiae* and will serve as the model DNA damage checkpoint for this review.

The DNA damage checkpoint response substrate.

Although little is known regarding the actual DNA substrate that activates the DNA damage checkpoint response, it has been suggested that the DNA damage checkpoint pathway is activated by the detection of the single-stranded DNA (ssDNA), a common DNA repair intermediate of most repair pathways (Garvik et al., 1995). This suggests that it is not primary DNA damage that is detected by checkpoint proteins, rather it is already processed DNA that checkpoint proteins sense (Siede et al., 1994). For example, UV dimers are recognized by DNA repair proteins and excised from the DNA leaving behind a ssDNA gap (Batty and Wood, 2000). However, it is also possible that it is not only the ssDNA, or DNA primer-template junctions that lie on either side of this gap, but that both of these structures that are recognized by checkpoint proteins. Similar DNA repair intermediate structures are also formed during mismatch repair and recombination repair (Batty and Wood, 2000).

Organization of the DNA damage checkpoint response.

The DNA damage checkpoint pathway is thought to consist of sensors, signal transducers, and effectors (Melo and Toczyski, 2002; Nyberg et al., 2002; Zhou and Elledge, 2000). Checkpoint sensors bind DNA damage and subsequently send the DNA damage checkpoint response signal through kinase transducers. Checkpoint transducers

activate the checkpoint effector proteins via phosphorylation, which carry out the functions of the response.

However, as more biochemical data has become available, the separation of roles among the checkpoint sensors and transducers has become blurred. For example, the central kinase regulator of the checkpoint response Mec1 is considered both a sensor and a transducer due to reported weak DNA binding activity as well functioning in signal transduction via activation of downstream checkpoint kinases (Rouse and Jackson, 2002b). In addition, the putative checkpoint sensor proteins Ddc1, Mec3 and Rad17 have not been shown to interact directly with DNA (Lindsey-Boltz et al., 2001). Therefore, this and other data suggest a different view regarding checkpoint organization and that perhaps the checkpoint response utilizes a DNA-Protein scaffold from which to signal the checkpoint response.

DNA-Protein scaffold formation.

Data suggest that the DNA damage checkpoint response initiates by formation of what could be considered a DNA-protein scaffold. The primary role of the checkpoint DNA-protein scaffold would be to co-localize molecules that participate in the checkpoint response to DNA (Burack and Shaw, 2000). A primary aspect of the scaffold model is that multiple protein inputs are required to signal cell cycle arrest. One rationale for this could be that arresting the cell cycle might be costly to the cell. To stop cell cycle progression, several processes are affected such as spindle elongation and cytokinesis. Once stopped, the coordination regarding the reactivation of these processes may be difficult, and if not done accurately, deleterious to the cell. Therefore, the cell may utilize

more than one input for the activation of the checkpoint response to avoid unwarranted activation and increase the accuracy of checkpoint response activation (Rouse and Jackson, 2002a).

Three checkpoint proteins have been implicated directly in DNA substrate recognition independent of each other and therefore can be considered to form the checkpoint DNA-protein scaffold. It should be noted that the order of assembly is not known nor implied (Figure 1-1). The first checkpoint protein to be considered as a scaffold member is Rad24, which forms a complex with the four proteins Rfc2-5 and whose human orthologs have been shown to bind both ssDNA and primer-template junctions (Lindsey-Boltz et al., 2001; Shiomi et al., 2002). The second checkpoint protein that binds to ssDNA as well dsDNA ends is Ldc1, which interacts with the central checkpoint regulatory kinase Mec1 (Rouse and Jackson, 2002b). And the last checkpoint to be considered is Rad9, which in this study has been shown to have an associated ssDNA binding activity. It should be noted that these three proteins are able to bind DNA substrates under physiological salt conditions. This is in contrast to other proteins involved in the checkpoint response that have also been shown to bind to DNA but whose interactions with DNA are sensitive to physiologic salt concentrations and may reflect a DNA scanning activity of these proteins to promote their localization to DNA. Scanning activity has been suggested for proteins involved in DNA replication, non-homologous end joining and mismatch repair (Hall et al., 2001; Kelman and Hurwitz, 1998).

The hypothesis of a DNA-protein checkpoint scaffold consisting of three independent complexes comes from genetic, chromatin-immunoprecipitation (ChIP), co-immunoprecipitation, and green fluorescent protein localization (GFP) studies (Kondo et al., 2001; Melo et al., 2001). The culmination of these studies show that Ldc1 is localized to DNA in a Rad24 and Rad9 independent manner (Kondo et al., 2001). In addition, the DNA binding complex Rad24-RFC interacts with the checkpoint proteins Ddc1, Mec3 and Rad17 and localizes them to the DNA in a Ldc1 and Rad9 independent manner. Ddc1 DNA localization is dependent on Rad17 and Rad24, but is independent of Mec1 and Rad9 (Kondo et al., 2001; Melo et al., 2001). Rad9 localizes to sites of DNA damage, but its dependency on the presence of other checkpoint proteins has not been reported. However, genetic data suggest Rad9 functions in a separate pathway from Rad24 to promote cellular resistance to DNA damage (Lydall and Weinert, 1995). In addition, research including the *Xenopus* homologs of Mec1 and Rad24, Xatr and Xrad17 respectively show that during the S-phase response, the Rad9 analog Claspin is recruited to chromatin independently of Xatr and Xrad17 (Lee et al., 2003). This suggests that Rad24-RFC, Ldc1 and Rad9 bind to DNA to form a protein scaffold upon which checkpoint kinases and their substrates are brought together to interact and signal the checkpoint response.

Rad24-RFC complex

Rad24 forms a pentameric complex with the four small RFC proteins Rfc2-5 that is similar to the DNA replication complex RFC, which contains Rfc1-5 (Green et al., 2000; Lindsey-Boltz et al., 2001). During DNA replication, RFC localizes to primer-

template junctions to initiate a series of protein interactions that result in DNA polymerase localization to the DNA (Waga and Stillman, 1998). In its own RFC-like complex with Rfc2-5, Rad24 is thought to function similarly to Rfc1 as the primary DNA binding component of the complex(Waga and Stillman, 1998). However, based on what is known regarding Rad24-RFC and RFC substrate affinities, it is possible that both Rad24-RFC and RFC could compete for binding to primer-template junctions or single-stranded DNA (Lindsey-Boltz et al., 2001; Shiomi et al., 2002; Tsurimoto and Stillman, 1991). How the cell is able to reconcile this may be based on other protein interactions that favor binding of Rad24-RFC over RFC that allow time for checkpoint-controlled DNA repair mechanisms to decide the fate of primer-template junctions. It has been suggested that the checkpoint machinery then takes on the responsibility of DNA repair by detecting persistent DNA damage that cannot be easily repaired (Rouse and Jackson, 2002a). Therefore, although RFC may be present initially at sites of persistent DNA damage, the DNA damage checkpoint response may be able to override RFC mediated DNA repair.

Functions of Rfc2-5 in the DNA damage checkpoint response.

The four small RFC subunits Rfc2-5 are required for both the S-phase and DNA damage checkpoint responses and are essential for viability (Cullmann et al., 1995; Krause et al., 2001; Naiki et al., 2000; Noskov et al., 1998; Schmidt et al., 2001; Shimada et al., 1999; Sugimoto et al., 1996). In addition they also have distinct functions and interact individually with other proteins involved in DNA replication and repair. Both Rfc5 and Rfc4 interact with ssDNA binding protein Replication Factor A (RPA)(Kim and

Brill, 2001; Yuzhakov et al., 1999). This interaction promotes RFC localization to primer-template junctions and likely does the same for the Rad24-RFC complex. Rfc5 has also been shown to interact directly with the DNA replication protein proliferating nuclear cell antigen (PCNA)(Cai et al., 1998; Mossi and Hubscher, 1998). Intriguing structural modeling analysis using human protein sequences of the checkpoint proteins suggests that Rad24, Rfc3 and Rfc5 could interact with the checkpoint PCNA homologs Rad17, Mec3 and Ddc1 respectively (Venclovas et al., 2002).

RFC-like complexes are formed via a pre-complex assembly method that appears to be an economical way for the cell to form different complexes of proteins that have very similar but distinct functions. As previously mentioned, Rad24 forms a separate complex with the smaller RFC subunits that is distinct from the RFC complex. Rad24 interacts genetically and biochemically with Rfc5, and studies have shown that Rfc5 is required to load Rad24 into the complex in a manner similar to how Rfc1 is added to the RFC complex (Uhlmann et al., 1996). This is a critical for the formation of the complexes because neither Rad24 nor Rfc1 is able to bind the core complex without Rfc5 (Lindsey-Boltz et al., 2001).

Ldc1

Ldc1 is required for both the DNA damage and S-phase checkpoint responses and for the function of the PIK kinase Mec1, the central kinase regulator of the checkpoint responses (Rouse and Jackson, 2000; Wakayama et al., 2001). There are a few similarities between Lcd1 and the non-homologous end joining (NHEJ) repair protein Ku. Both kinase "adaptor" proteins interact with their respective PIK kinase at sites of

DNA damage, and in the instance of Ku the PIK kinase is DNA-PK. Interestingly, both Lcd1 and Ku have varying affinities for different DNA structures, but have a high affinity for dsDNA ends (Dynan and Yoo, 1998; Rouse and Jackson, 2002b). Although, Lcd1 has a higher affinity for dsDNA ends, it may be the case that it is recruited to the checkpoint scaffold or primer-template junctions via weaker DNA interactions, and becomes incorporated into the scaffold by its interactions with RPA, Rad24-RFC or the Ddc1/Mec3/Rad17 complex. Interestingly, Ldc1 dependent DNA binding is not increased by the presence of UV lesions in dsDNA, further supporting the hypothesis that primary DNA lesions do not activate the DNA damage checkpoint response (Rouse and Jackson, 2002b).

Rad9

Rad9 is the canonical checkpoint protein required for both S-phase and DNA damage checkpoint responses(Paulovich et al., 1997; Weinert and Hartwell, 1988). Several observations imply that Rad9 functions as a sensor for the checkpoint response. This is based on studies that have shown that the checkpoint kinase Rad53 is phosphorylated in a Rad9 dependent manner, thereby placing Rad9 upstream of a signal transducer (Gilbert et al., 2001). In addition, the hypothesis that Rad9 functions as a sensor is supported by genetic data that suggests that Rad9 functions in a separate DNA repair process that the *RAD24* genetic epistasis group has been implicated in (Lydall and Weinert, 1995). This suggests that Rad9 may localize to the DNA independently of Rad24-RFC to function as part of the checkpoint scaffold to promote activation of the checkpoint response and DNA repair.

In this study, Rad9 has been shown to associate with ssDNA binding activity implying that along with Lcd1 and Rad24-RFC, Rad9 could localize to the DNA to form the checkpoint scaffold to initiate the response. Interestingly, the functional ortholog of Rad9 in humans is the tumor suppressor BRCA1 (Paull et al., 2001). BRCA1 binds DNA of varying structures including ssDNA, which would imply that it could associate with ssDNA and the human checkpoint scaffold via direct interactions with DNA.

Following DNA damage, Rad9 becomes hyperphosphorylated in a Mec1 dependent manner to promote Rad9-Rad9 and subsequently Rad9-Rad53 interactions (Emili, 1998; Vialard et al., 1998). Rad9-Rad9 oligomerization is thought to be mediated through its two BRCT domains (Soulier and Lowndes, 1999). The Rad9 oligomer then serves as an interface for activation of the checkpoint effector kinases Rad53 and Chk1 (Navas et al., 1996; Sanchez et al., 1999). Studies of Rad9 in which mutations were made in the Rad9 BRCT domains to disrupt their overall structure are defective for Rad9 dependent activation of Rad53 and cell cycle arrest following DNA damage (Soulier and Lowndes, 1999). Thus, the Rad9 oligomerization step may serve as an additional regulatory step to avoid inadvertent activation of effector kinases by Rad9. However, recent work by Kara Nyberg (dissertation, 2003) suggests that dimerization of Rad9 occurs independent of DNA damage, and that rather the BRCT domains are function in the checkpoint response to increase the local concentration of Rad9. In addition, these studies indicate that Rad9 BRCT domains contribute to Rad9 protein stabilization and may also serve a negative regulatory role for Rad9 in regards to cell cycle arrest.

RPA

If ssDNA serves as the DNA lattice upon which the checkpoint scaffold assembles, then it is almost certain that the ssDNA binding protein RPA would also be present. The evolutionarily conserved single-stranded DNA binding protein complex RPA is required for DNA replication, UV DNA repair, and homologous recombination repair (Wold, 1997). RPA is required during DNA replication at the step of origin unwinding prior to DNA polymerase loading and is also required for DNA replication priming and fork elongation (Waga and Stillman, 1998). Thus, virtually any form of DNA metabolism that results in the formation of single-stranded DNA includes RPA.

RPA is a heterotrimeric complex consisting of the three proteins Rfa1, Rfa2 and Rfa3, which have molecular weights of 70, 32, and 14 kDa respectively(Wold, 1997). Rfa1 is required for the G1/S DNA damage checkpoint response (Longhese et al., 1996) and Rfa2 functions in both the G1/S DNA damage checkpoint and the S-phase checkpoint responses (Santocanale et al., 1995). Rfa2 and Rfa3 are probably also required for the G2/M DNA damage checkpoint response, however the identification of this requirement is hindered by the fact that Rfa1-3 are essential genes that may require unique mutants to identify their roles in the G2/M checkpoint response.

RPA is phosphorylated in a cell cycle dependent manner and is also induced following DNA damage (Wold, 1997). The DNA damage dependent phosphorylation of the RPA subunits Rfa1 and Rfa2 is checkpoint dependent. Rfa1 radiation-induced phosphorylation is dependent on Mec1, Mec3, Rad9 and Rad53 (Brush and Kelly, 2000). Rfa2 radiation induced phosphorylation requires Mec1 and Mec3 (Brush et al., 1996).

The purpose of RPA phosphorylation is unclear. However, several reports suggest that the phosphorylation of Rfa2 reflects a switching of RPA from functioning in DNA replication to homologous recombination repair(Liu et al., 2000a; Wold, 1997).

RPA may contribute to scaffold formation by promoting Rad24-RFC binding. This is supported by the finding that the human Rad24 homolog, hRad17 localizes to DNA in an RPA dependent manner (Lee et al., 2003). In addition, as previously mentioned, both Rfc5 and Rfc4 interact with RPA and further emphasizes the active role that the small RFC subunits have in scaffold formation (Kim and Brill, 2001). How RPA influences Rad 24-RFC DNA binding can be inferred from another function of RPA in DNA replication initiation where RPA is thought to recruit RFC to primer-template junctions (Yuzhakov et al., 1999). It has been suggested that RPA increases the substrate specificity of RFC for primer-template junctions by occluding RFC from binding to ssDNA(Tsurimoto and Stillman, 1991). RPA may have a similar function in the checkpoint response by guiding Rad-24-RFC to primer-template junctions. Productive interactions with the checkpoint scaffold activate signal transduction.

Once the checkpoint sensors detect DNA damage, the signal is transduced through a series of pathways consisting of phospho-inositide kinases (PIK), and another separate family of checkpoint kinases (CHK) that function downstream of the PIK related kinases (Figure 1-2). These kinases are thought to activate, through phosphorylation, the effectors of the checkpoint response to arrest the cell cycle. The substrates of the transducer kinases are proteins that function in DNA repair, cell cycle control, and transcription regulation.

Ddc1/Mec3/Rad17 complex

It appears as though the primary role of Rad24-RFC in the checkpoint response is to recruit the heterotrimeric protein complex comprised of the three checkpoint proteins Ddc1, Mec3, and Rad17 (Figure 1-1) (Kondo et al., 1999). Ddc1, Mec3, and Rad17 are required for DNA damage and S-phase checkpoint responses and are also thought to function in the same unknown repair pathway that Rad24 has been implicated in (Longhese et al., 1997; Lydall and Weinert, 1995; Paulovich et al., 1997; Weinert et al., 1994). Molecular modeling of these three proteins indicates that Ddc1, Mec3, and Rad17 are structural orthologs of the replication protein PCNA that forms a homotrimeric protein complex (Venclovas and Thelen, 2000). To initiate DNA replication, RFC recruits PCNA to primer-template junctions. In turn, PCNA recruits DNA polymerase δ and ε to the DNA that function in DNA replication or DNA repair respectively. In a similar manner, it is thought that Rad24-RFC recruits the Ddc1/Mec3/Rad17 complex to the DNA. Subcellular localization studies using GFP-tagged checkpoint proteins show that Ddc1, Mec3, and Rad17 localize to the DNA in a Rad24 dependent manner (Melo et al., 2001). In addition, human checkpoint Rad24-RFC and Ddc1/Mec3/Rad17 were visualized using transmission election mircroscopy, which revealed them to be indistinguishable from RFC and PCNA respectively (Shiomi et al., 2002). This supports the hypothesis that these three checkpoint proteins act in a similar way as RFC and PCNA, whereby DNA loading of PCNA is RFC dependent.

The presence of Rfc1 in the RFC complex is critical for loading of the PCNA complex, and suggests that the primary role for Rad24 is to load the Ddc1/Mec3/Rad17

onto DNA. In their study, Gomes and Burgers found that although the Rfc2-5 core complex could load PCNA, it could only do so using ATPγS, the non-hydrolyzable form of ATP (Gomes and Burgers, 2001). However, the full RFC complex could load and form a stable complex with PCNA in the presence of ATP and ATPγS. This suggests that the presence of Rfc1 stabilizes PCNA onto RFC regardless of ATP turnover. Gomes proposes that the significance of this may be that only RFC interacts productively with PCNA. The Rfc2-5 core complex either alone, or in a complex with an alternative large subunit such as Rad24, binds PCNA poorly and actively dissociates bound PCNA to allow binding of alternative PCNA-like complexes. This suggests a stepwise assembly model that utilizes ATP to ensure that the checkpoint Rad24-RFC complex finds Ddc1/Mec3/Rad17 prior to binding to DNA (Gomes et al., 2001).

Studies involving human checkpoint protein homologs show that the RAD24-RFC complex is able to bind the Ddc1/Rad17/Mec3 complex using co-immunoprecipitation and glycerol density gradient sedimentation (Lindsey-Boltz et al., 2001; Rauen et al., 2000). However, there is no indication the RAD24-RFC complex is able to actually load Ddc1/Mec3/Rad17 onto ssDNA, dsDNA, or primer-template junctions. It is important to note that Rad24-RFC and Ddc1/Mec3/Rad17 complexes may assemble on different DNA structures not yet tested. Alternatively, because RPA has a role in RFC loading onto primer-template junctions, it is possible that RPA also plays a role in the loading of both Rad24-RFC and Ddc1/Mec3/Rad17 onto DNA. The purpose of localizing the Ddc1/Rad17/Mec3 complex to DNA may be to recruit other proteins to sites of DNA damage. This is analogous to how PCNA not only recruits

DNA polymerases to the DNA, but also interacts with a large number of other proteins involved in DNA repair and cell cycle progression (Hammarsten and Chu, 1998).

Ldc1 and Mec1 complex.

Mec1 is required for all checkpoint responses and is the central kinase regulator that is thought to function first in a pathway of checkpoint kinases whose activation leads to cell cycle arrest(Abraham, 2001). Mec1 is a member of a family of PIK related kinases, which includes DNA-PK that functions in the non-homologous end joining DNA repair pathway. Although DNA-PK can weakly bind DNA independently of Ku, its association with DNA is greatly enhanced by Ku (Hammarsten and Chu, 1998). Similarly, although Mec1 associates with DNA weakly alone, its association with DNA is stronger when interacting with Lcd1 (Rouse and Jackson, 2002b). DNA-PK association with both DNA and Ku stimulates kinase activity, which suggests that Mec1 kinase activity may require both DNA and Lcd1 for full kinase activation (Dynan and Yoo, 1998).

Mec1-Lcd1 can respond to DNA damage independently of both *RAD9* and the *RAD24* epistasis groups(Rouse and Jackson, 2002b). Lcd1 is phosphorylated in a Mec1 dependent manner following DNA damage independently of the two checkpoint epistasis groups (Edwards et al., 1999; Paciotti et al., 2000). This suggests that the Mec1-Ldc1 complex is activated by DNA damage directly and therefore could interact with the DNA independent of the other checkpoint proteins. However, chromatin interaction is not completely independent of all checkpoint proteins, because the Mec1 *Xenopus* ortholog

Xatr requires RPA to associate with chromatin (Lee et al., 2003). However, it is unknown if the RPA dependent association directly affects Xatr or its binding partner Xatrip.

Figure 1-2 summarizes the DNA damage induced Mec1 dependent phosphorylation of checkpoint proteins and the possible function of the phosphorylation (Figure 1-2). RPA is phosphorylated following DNA damage and may be intended as a way to possibly switch the RPA molecules in the scaffold from replication to repair mode (Liu et al., 2000a). Rad9 hyperphosphorylation results in Rad9 oligomerization to subsequently interact with and promote activation of the checkpoint kinase Rad53 (Gilbert et al., 2001).Ddc1 becomes hyperphosphorylated, but the function of this phosphorylation is unclear (Paciotti et al., 1998). And lastly, Lcd1 phosphorylation is Mec1 dependent, but once again, the purpose of this is unknown (Paciotti et al., 2000; Rouse and Jackson, 2002b).

Rad9 and Rad53 interactions.

In *S.cerevisiae*, the checkpoint kinase Rad53 is required for both S-phase and DNA damage checkpoint responses (Sanchez et al., 1996; Sun et al., 1996). Rad53 belongs to the Chk2 family of checkpoint kinases, which also includes Dun1, a kinase that functions downstream of Rad53 in the DNA damage checkpoint response(Allen et al., 1994; Zhou and Elledge, 1993). Mec1 signals checkpoint activated cell cycle arrest through two independent signaling pathways, one that requires Rad53 and Dun1, and another, which requires Chk1 and the anaphase inhibitor Pds1(Gardner et al., 1999; Sanchez et al., 1999). Loss of either Rad53 or Chk1 results in a moderate checkpoint induced cell cycle arrest defect, in which cells arrest their cell cycle but cannot maintain

arrest following DNA damage (Gardner et al., 1999). Cells deficient for both Rad53 and Chk1 have a complete cell cycle arrest defect and proceed directly to mitosis following DNA damage (Sanchez et al., 1999).

Activation of Rad53 is Lcd1, Mec1 and Rad9 dependent (Gilbert et al., 2001; Rouse and Jackson, 2000; Wakayama et al., 2001). Following DNA damage, Rad53 is thought to associate with the checkpoint scaffold through interactions with Rad9. Rad53 binds Rad9 via two (forkhead-associated) FHA domains at phosphorylated threonine residue sites in Rad9 (Liao et al., 2000). Rad53 interaction with Rad9 results in an *in trans* auto-phosphorylation of Rad53 molecules (Xu et al., 2002). This suggests an activation scenario for Rad53, where Mec1 activates both Rad9 and Rad 53 directly by phosphorylation. Another possible scenario is that Mec1 is only required to phosphorylate Rad9 for Rad9 oligomerization, which in turn results in the subsequent activation of Rad53 (Toh and Lowndes, 2003).

The Rad9 and Rad53 interaction model suggests a method for the cell to amplify the signal for full cell cycle arrest. Once Rad9 oligomerizes, it interacts with Rad53, and Rad53 subsequently oligomerizes with itself (Xu et al., 2002). Rad53 auto-activation yields Rad53 molecules that have a lower affinity for the Rad9 scaffold (Gilbert et al., 2001). This leaves the Rad9 scaffold open for additional Rad53 molecules to interact and become activated, resulting in a positive feedback loop that allows for amplification of the DNA damage checkpoint response signal. This suggests a method by which the DNA damage checkpoint response is able to invoke a full cell cycle arrest with a small amount of DNA damage, such as a single double-strand break.

Rad 9 and Chk1 interactions.

The checkpoint kinase Chk1 is required for full G2/M cell cycle arrest following DNA damage (Liu et al., 2000b; Sanchez et al., 1999). In conjunction with Pds1, Chk1 functions in a separate branch of the checkpoint pathway parallel to the Rad53 branch (Gardner et al., 1999; Sanchez et al., 1999). Like Rad53 mutants, Chk1 single mutants have an abrogated cell cycle arrest defect similar to Rad53 (Sanchez et al., 1999). Although the mechanisms of Chk1 activation are not as well studied as those of Rad53, Chk1 activation appears to be similar to that of Rad53. Activation of Chk1 is dependent on Mec1 and Rad9 (Sanchez et al., 1999). In addition, Chk1 interacts with itself which is reminiscent of the Rad53 *in trans* auto-activation (Liu et al., 2000b). These findings suggest a similar role for Chk1 activation and amplification as suggested for Rad53.

The primary function of Chk1 in the DNA damage checkpoint response appears to be the regulation of the anaphase inhibitor Pds1 (Wang et al., 2001) and not DNA repair as *chk1*Δ cell are mildly UV sensitive (Sanchez et al., 1999). Chk1 physically interacts with and phosphorylates the anaphase inhibitor Pds1 to increase Pds1 protein abundance (Wang et al., 2001).

Termination of the Checkpoint.

The checkpoint scaffold model suggests that the checkpoint is also able to terminate the response through direct monitoring of DNA repair by utilizing the DNA damage substrate as a center for activation of the checkpoint response. DNA repair results in the elimination of the checkpoint DNA substrate by being restored to fully

duplexed DNA, and the subsequent disassembly of the DNA-protein scaffold. Therefore, the repair of the DNA damage can directly terminate the checkpoint response.

Dissertation overview

At the onset of this dissertation, the majority of the checkpoint sensor proteins in *S.cerevisiae* had been identified as Ddc1, Mec3, Rad17, Rad24 and Rad9. Further characterization of these genes placed them in two epistasis groups, with Rad9 comprising one, and Ddc1, Mec3, Rad17 and Rad24 belonging to the other (Longhese et al., 1997; Lydall and Weinert, 1995). These two groups were determined based on UV and alkylation damage sensitivities and suggested that there are two separate repair pathways mediated by checkpoint proteins. Although genetic data localized the sensors to the DNA, we decided to test for whether the sensors could detect DNA using a biochemical approach.

To test whether any of the sensors could directly bind DNA, the five proteins were purified from yeast extracts and tested for DNA binding using mobility gel shift analysis. Using this approach both Rad9 and Rad24 were found to have associated DNA binding activities with an affinity for single stranded DNA. This correlates well with the two proteins representing separate repair pathways, where at least one component from each of the two pathways would be expected to recognize DNA damage. The finding that single stranded DNA was the preferred substrate supports the hypothesis that this, an intermediate DNA structure of most repair pathways, is a DNA substrate recognized by checkpoint proteins. This alleviates the checkpoint response from having to evolve specific sensor proteins for every form of primary DNA damage such as UV dimers or

double stranded DNA breaks. This also implies that DNA damage processing is required prior to checkpoint activation.

Interestingly, the checkpoint protein Rad17 has been implicated in DNA processing in two ways. First, Rad17 is homologous to the 3'->5' exonuclease Rec1 from *U.maydis*(Lydall and Weinert, 1995; Thelen et al., 1994). And secondly, the accumulation of single stranded DNA at telomeres in the *cdc13-1* conditional mutant background is dependent on the Rad24 epistasis group that includes Rad17 (Lydall and Weinert, 1995). We chose to directly test Rad17 for exonuclease activity using DNA degradation assays with purified Rad17. In addition, point mutations were constructed throughout Rad17 to determine if a conserved residue in a proposed exonuclease domain and another conserved region of the protein were important for Rad17 checkpoint function. However, the low exonuclease activity detected in these assays was not significantly above background levels. The addition of the checkpoint proteins Ddc1 and Mec3, two protein that form a trimeric complex with Rad17, did not stimulate nuclease activity nor did the addition of DNA substrates with various secondary structures.

What is gained from this dissertation is the hypothesis that multiple checkpoint proteins directly bind to a common intermediate DNA repair structure to activate the checkpoint response. Another checkpoint protein that has been shown to directly bind DNA is Lcd1. Thus potentially all three checkpoint proteins Lcd1, Rad9, and Rad24 are required to bind to sites processed of DNA damage to activate the checkpoint response.

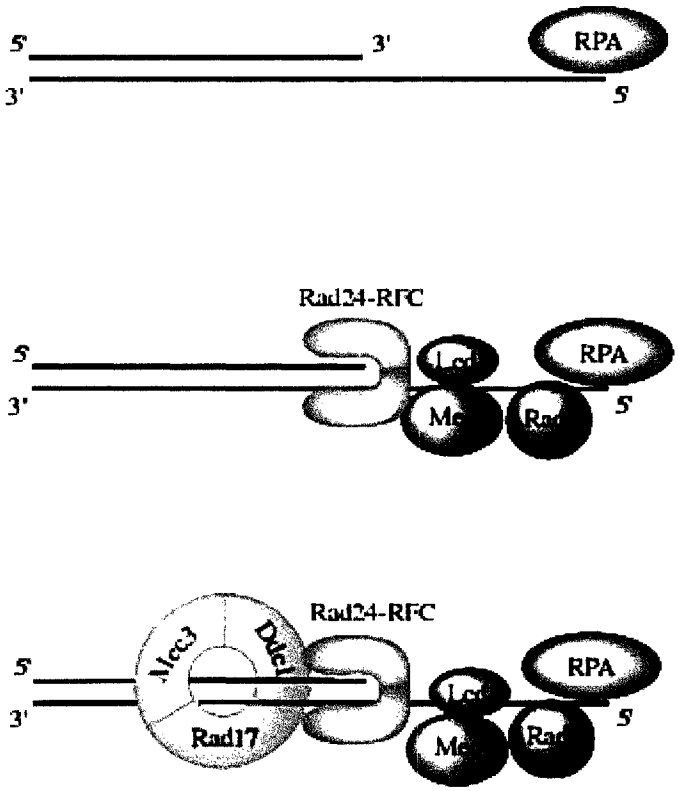

Figure 1-1. DNA damage checkpoint protein scaffold assembly on processed DNA damage.

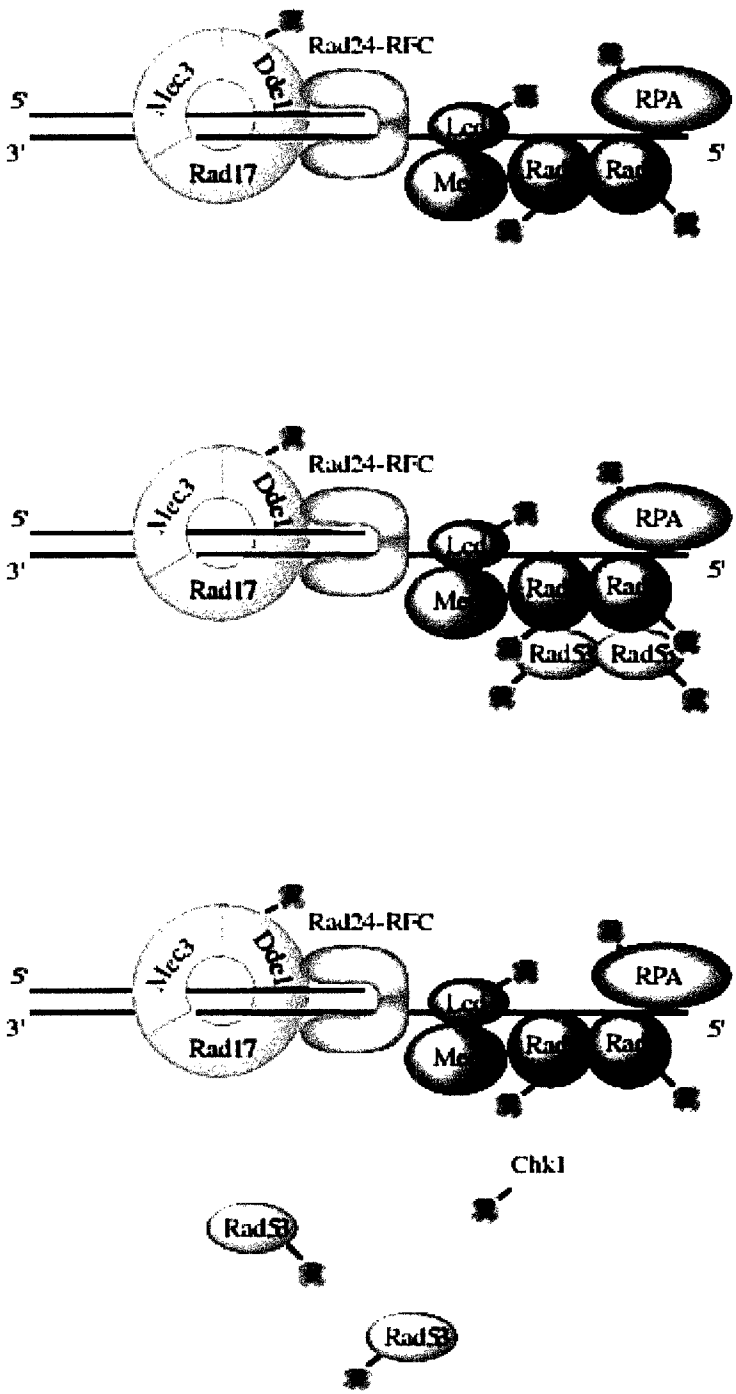

Figure 2. Activation of checkpoint effector kinases by interactions with DNA-protein scaffold

Table 1-1. Activities of DNA damage checkpoint response proteins. *These reported activites include studies of homologs and have not been shown to occur for all of the homologs listed.*

Protein	Functional class
Rfa1/Rfa2/Rfa3	ssDNA binding protein complex.
Rfc2-5	Forms complex with Rad24.
Rad24	DNA binding, and interacts with the Ddc1/Mec3/Rad17 complex.
Ddc1/Mec3/Rad17	Potentially functions to recruit checkpoint kinase substrates and DNA repair proteins to the checkpoint scaffold.
Ldc1	Binds to dsDNA and potentially to primer-template junctions, interacts with and is required for Mec1 checkpoint activity.
Rad9	Associated ssDNA binding activity includes it in the scaffold, interacts with and is required for Rad53 activation.
Mec1	Central kinase activator for the checkpoint repsonse.
Rad53	Effector kinase activated through Rad9 interactions and functions upstream of the checkpoint kinase Dun1.
Chk1	Effector kinase that requires Rad9 for activation and phosphorylates the anaphase inhibitor Pds1.

Table 1-2. DNA damage checkpoint response proteins are conserved in eukaryotes.

Protein	*S.cerevisiae*	*S.pombe*	Humans
RFC structural ortholog	Rad24	Rad17	Rad17
PCNA structural ortholog	Ddc1 Mec3 Rad17	Rad9 Hus1 Rad1	Rad9 Hus1 Rad1
BRCT domain containing	Rad9	Crb2	BRCA1
PIK kinase associated	Lcd1	Rad26	ATRIP
PIK kinase	Mec1 Tel1	Rad3 Tel1	ATR ATM
Effector kinase	Rad53 Chk1	Cds1 Chk1	Chk2 Chk1

CHAPTER 2

THE CHECKPOINT PROTEIN RAD24 HAS AN ASSOCIATED SINGLE-STRANDED DNA BINDING ACTIVITY.

Summary

In *S.cerevisiae*,RAD24 is required for the DNA damage checkpoint response and functions redundantly with *CHL12* in the replication checkpoint response that slows S-phase when DNA damage is present during DNA replication. Rad24 and Chl12 are homologous to replication factor C (RFC) proteins, and both checkpoint proteins form distinct RFC-like protein complexes that include the four smaller RFC protein subunits. Rad24 and Chl12 are thought to be responsible for the DNA substrate specificity for their respective RFC-like complex, much like Rfc1 is the primary DNA binding component of the RFC protein complex. To test whether Rad24 could bind to DNA directly, as has been shown for Rfc1, Rad24 was purified from yeast extracts and assayed for DNA binding using gel mobility shift analysis with various DNA substrates.

In this study, Rad24 associated DNA binding was found to have a higher affinity for single-stranded DNA when compared to double-stranded DNA. In addition, Rad24 does not recognize DNA nicks or DNA ends, suggesting that Rad24 can detect single-stranded DNA gaps. Rad24 DNA binding does not show a preference for a primer-template junctions suggesting that Rad24 activity may require other proteins to specifically recognize primer-template junctions. Finally, the *rad24-1* checkpoint mutant was sequenced and was found to result in a carboxy-terminal truncation of the Rad24 protein. The Rad24-1 mutant protein has no associated DNA binding activity.

These data suggest that Rad24 detects single-stranded DNA, the common repair intermediate for most DNA repair processes for its role in the activation of the DNA damage checkpoint response.

Introduction

Cells that they can take many courses of action in response to DNA damage. They can repair the DNA damage, arrest their cell cycle to allow time for repair, and in the instance of multicellular organisms, they can choose to undergo programmed cell death. These processes prevent the accumulation of cellular mutations that can lead to cancer. However, first and foremost, cells must detect the DNA damage before they can choose the appropriate set of responses for the amount and type of DNA damage present.

DNA repair pathways utilize sensor proteins to detect primary DNA damage that has not yet been processed. For example, the Rad14 protein in *S.cerevisiae* functions in the UV repair process and binds directly to UV dimers (Batty and Wood, 2000). The function of a sensor protein following DNA damage is to recruit other DNA repair proteins to the site of damage to facilitate repair. Similarly, the DNA damage checkpoint response that arrests the cell cycle following DNA damage is thought to utilize sensors that detect DNA damage. In *S.cerevisiae*, several proteins have been identified that are required for the G2/M DNA damage checkpoint, which prevents cells from entering mitosis following DNA damage. Of these proteins, the five that are thought to be potential sensors of DNA damage are Rad9, Rad17, Rad24, Mec3 and Ddc1. Genetic data and protein sequence analysis of these proteins involved in DNA replication suggest that they function as sensors for the DNA damage checkpoint (Longhese et al., 1997; Lydall and Weinert, 1995; Venclovas and Thelen, 2000).

The five potential sensor genes fall into two different epistasis groups with *RAD9* as its own group, and *DDC1*, *MEC3*, *RAD17* and *RAD24* belonging to the *RAD24*

epistasis group. Genetic studies suggest that the two groups have different functions in DNA repair(Longhese et al., 1997; Lydall and Weinert, 1995). *S.cerevisiae* strains that carry deletions in any one of the five sensor genes are completely defective in the G2/M checkpoint response. However, strains that contain mutations in both the *RAD9* and *RAD24* epistasis groups are more sensitive to DNA damage than any single mutant from either of the epistasis groups. An explanation for this is that both groups are required for checkpoint activation but have different functions in regard to DNA damage repair (Paulovich et al., 1997). If the two groups do function in different repair processes they may also require their own method for detecting DNA damage. Therefore, a member of the *RAD24* group and Rad9 itself could bind to DNA. Rad9 associated DNA binding is described in Chapter 3. The biochemical characterization of these sensor proteins is an area of ongoing research.

Biochemical studies on potential DNA damage checkpoint sensors suggest that they have similarities to their replication protein homologs. During DNA replication, replication factor C (RFC) recruits proliferating nuclear cell antigen (PCNA) to DNA primer-template junctions, PCNA in turn recruits DNA polymerase to the DNA (Waga and Stillman, 1998). Following this study, additional reports have shown that Rad24 functions in a similar manner to its replication homolog Rfc1. Rad24 and Rfc1 both form pentameric complexes with four small RFC subunits, Rfc 2-5(Gerik et al., 1997; Green et al., 2000). In addition, the human form of the Rad24-RFC complex binds to both single-stranded DNA (ssDNA) and DNA primer-template junctions (Lindsey-Boltz et al., 2001). The Rad24-RFC complex has also been shown to interact with the PCNA homologs

Ddc1, Mec3 and Rad17, which suggests that Rad24-RFC recruits the Ddc1/Mec3/Rad17 complex to sites of ssDNA (Shiomi et al., 2002).

Previous studies suggest that ssDNA serves as the DNA structure by which the checkpoint is activated (Garvik et al., 1995). It would be parsimonious for the cell to have a DNA damage checkpoint response to detect ssDNA, because ssDNA is a common intermediate DNA structure of many different DNA repair pathways. It would be more costly for the cell to require many different proteins to act as sensors for specific DNA lesions that are caused by DNA damaging agents, and other aberrant structures that arise due to faulty DNA replication or repair.

In this study, the checkpoint sensor proteins of the *RAD24* epistasis group were purified from *S.cerevisiae* using non-denaturing conditions and affinity chromatography. These proteins were tested for DNA binding activity using gel mobility shift assays, and substrate specificity was determined by testing DNA substrates that contain various DNA structures. Determining the substrate may help identify what form of DNA damage activates the checkpoint and what repair processes these checkpoint proteins function in. In addition, characterizing the DNA damage checkpoint substrate may lead to insights into what DNA processing needs to occur for the checkpoint to release its arrest and allow the cell cycle to continue.

Results

Over- production of checkpoint proteins.

The checkpoint genes belonging to the *RAD24* epistasis group were amino-terminally fused to the Glutathione S-transferase epitope and each fusion protein was tested for *in*

vivo activity for both UV tolerance and cell cycle arrest following DNA damage in their respective mutant strain background (see Table 2-1). Cells containing the temperature sensitive mutation *cdc13-1* accumulate ssDNA at their telomeres when shifted to the restrictive temperature of 36°C. This ssDNA is recognized as DNA damage and activates the DNA damage checkpoint response. The GST-Ddc1 protein restored the UV resistance and *cdc13-1* DNA damage checkpoint cell cycle arrest defect when overexpressed in a *ddc1*Δ strain,(Fig. 2-1). As shown in Fig. 2-2, the GST-Mec3 fusion protein does not fully restore UV resistance in a *mec3*Δ mutant. However, it does complement the DNA damage checkpoint defect of the *mec3*Δ mutant in response to *cdc13-1* damage. As shown in Fig. 2-3, GST-Rad17 is able to fully complement the *rad17*Δ strain in both of these assays, suggesting that the GST epitope tag does not interfere with Rad17 cellular activities in response to UV damage tolerance, and DNA damage checkpoint activation following *cdc13-1* DNA damage. And lastly, GST-Rad24 partially restored the UV resistance of the *rad24*Δ mutant and fully complemented the DNA damage checkpoint response defect in the presence of *cdc13-1* DNA damage, (Fig. 2-4).

The checkpoint protein fusions were overproduced using galactose induction in a protease-deficient yeast strain. The proteins were then purified using affinity chromatography with a glutathione sepharose column and confirmed using SDS-polyacrylamide gels, Coomassie staining and Western blot analysis, (Fig. 2-5). As shown, the proteins migrated at their predicted molecular weights, and a 70kD contaminating protein was detected. Previous studies using GST epitope have also reported a contaminating protein of the same size that co-purifies with the epitope.

Single Stranded DNA Binding Activity of GST-Rad24

To examine whether any of the members of the *RAD24* epistasis bind DNA, each was tested using mobility shift analysis and a ssDNA substrate. The 35 base long oligonucleotide substrate was labeled with ^{32}P phosphate at the 5' end. Fig. 2-6, lane 8 shows that only a GST-Rad24 dependent DNA binding activity was detected and was not associated with GST, GST-Ddc1, GST-Mec3 and GST-Rad17 preparations, Fig. 2-6, lanes 4-7. To test whether Ddc1, Mec3 or Rad17 required all three proteins to potentially form the reported hetero-trimeric complex to bind to DNA, the proteins preparations were combined and tested for DNA binding. As shown in Fig. 2-6, lane 10, no DNA binding is associated when Ddc1, Mec3 or Rad17 are combined in the mobility shift assay. To test whether Ddc1, Mec3 or Rad17 could interact with Rad24 in the mobility shift assay to produce a new slower migrating band indicating a super complex formation, all four checkpoint proteins were added to the same reaction. As shown in Fig. 2-6, lane 11, the Rad24 dependent DNA binding activity was unaffected by the presence of Ddc1, Mec3 or Rad17, implying that these proteins do not interact in this assay. If Ddc1, Mec3 or Rad17 had interacted with Rad24 a shift in the Rad24 binding would have been expected to be observed, possibly resulting in a band shift to a slower mobility owing to the increase in size of the protein complex.

It is known that the 5' phosphorylated end of the substrate is physiologically relevant and occurs in cells during DNA replication. DNA 5' ends occur during Okazaki fragment maturation, HO breaks and recombination repair. To test whether this was a necessary aspect of the DNA structure that contributed to GST-Rad24 binding affinity,

the same substrate was 3' end labeled. As shown in Fig. 2-7, the presence of the 5' phosphate is not required for DNA binding by GST-Rad24.

GST-Rad24 Has a Hierarchy of Affinities for DNA Base Composition.

To further examine the DNA binding preferences of GST-Rad24, a series of competition assays were performed. This type of assay is a steady state assay in which protein was added to a mixture of substrates that contained both the 5' labeled substrate used in the previous experiments and increasing concentrations of unlabeled competitor DNA of equal length. As shown in Fig. 2-8, GST-Rad24 binding activity has higher preferences for both poly-dT and poly-dC in comparison to its very low affinity for the poly-dA oligonucleotide.

The analogy of Rad24 with Rfc1 in regard to binding primer-template junctions suggests that GST-Rad24 binding would be structure-specific and not dependent on the DNA sequence. However, the affinity of GST-Rad24 different base compositions can be has also been observed in other DNA binding proteins whose function is thought to be to recognize DNA structures and not DNA sequences. DNA binding proteins that bind to DNA structures that are not thought to recognize DNA sequences such as RecA, have also been shown to have DNA composition preferences. In addition, others have observed that the RFC complex also has base composition preferences (Tsurimoto and Stillman, 1991). In addition, analysis of the poly-dA oligonucleotide using denaturing and non-denaturing gel electrophoresis indicate no unusual secondary structures as had been observed with a poly-G substrate of the same length (data not shown).

GST-Rad24 Binds to Primer-Template Junctions with Either 5' or 3' Overhangs.

To determine if GST-Rad24 DNA binding has a higher affinity for DNA primer-template junctions in comparison to ssDNA, a competition assay was performed with two hairpin substrates (Fig. 2-9A). The hairpin substrates are structurally similar to primer-template junctions formed during replication and have been used by other labs to test for primer-template binding by RFC (Tsurimoto and Stillman, 1991). However, in addition to the 5' overhang substrate, a DNA hairpin substrate with a 3' overhang of the same sequence but reversed directionality was also tested. This was done to test GST-Rad24 binding specificity for primer-template junctions that are recognized by replication proteins. If GST-Rad24 is not specific for primer-template junctions, it may also be able to bind to a substrate of the reverse sequence. The ssDNA control contains only the sequence of the ssDNA overhang with the same polarity of the primer-template junction. As shown in Fig. 2-10, GST-Rad24 has a slightly higher affinity for the hairpin structures when compared to the ssDNA control substrate. However, GST-Rad24 binding showed no preference regarding the directionality of the hairpin substrates. This was somewhat unexpected because the DNA binding component of the RFC complex, Rfc1, has been reported to bind specifically primer-template junctions with a higher affinity when compared to ssDNA (Uhlmann et al., 1997). An RFC binding preference for primer-templates of an opposite directionality has not been reported. Interestingly, RFC as a complex does not show a high degree of specificity for primer-template junctions when compared to ssDNA until PCNA interacts with RFC(Tsurimoto and Stillman, 1991).

GST-Rad24 Has a Higher Affinity for ssDNA than dsDNA.

To determine what degree of specificity GST-Rad24 has for ssDNA, a hairpin substrate 35 base pairs long was constructed that when folded intra-molecularly forms a fully duplexed hairpin. In a competition assay with this dsDNA substrate and a ssDNA substrate containing one strand of the dsDNA version, GST-Rad24 affinity for dsDNA was tested. GST-Rad24 dependent binding activity is significantly lower for dsDNA in comparison to the ssDNA substrate (Fig. 2-11). Other labs have observed that RFC has a similar degree of affinity for ssDNA when compared to dsDNA in the absence of PCNA. (Lindsey-Boltz et al., 2001; Tsurimoto and Stillman, 1991)

GST-Rad24 has a Minimal Binding Size Requirement.

To further characterize GST-Rad24 binding activity, the minimal binding size requirement was tested using competition assays and ssDNA substrates that varied only by length. The substrates used were poly-dT oligonucleotides of 15, 20, 25, 30 and 35 nucleotides in length. The use of a mono-nucleotide sequence avoided sequence and base composition biases that would occur by simply shortening the length of a heterologous ssDNA substrate. When competed with these substrates the minimal binding size requirement for GST-Rad24 was between 20-25 nucleotides in length for a high affinity interaction compared to the 15 nucleotide long substrate, (Fig. 2-12). This is intriguing because the 20 nucleotide-long binding requirement is within the size of the gap produced in UV excision repair (Batty and Wood, 2000).

GST-Rad24 Has a Higher Affinity for Gapped Substrates.

The substrates tested in this study all have 3' and/or 5' free ends. To determine if free ends play a role in GST-Rad24 binding, DNA substrates were constructed that contain

two hairpins, one at each end, leaving either a nick or a 35 base long ssDNA gap in the middle of the structure. As shown in Fig. 2-13, the 35 base long ssDNA control and the gapped substrate are bound with equal affinity by GST-Rad24. To determine if the 35 base long gap was the requirement for the double hairpin substrate to be bound by GST-Rad24, nicked or fully double-stranded substrates were tested. GST-Rad24 has a lower affinity for both these substrates in comparison to the ssDNA and gapped substrates. This suggests that GST-Rad24 does not have an affinity for free ends, but rather has an affinity for the ssDNA component of these double hairpin constructs.

Characterization of the Rad24-1 Mutant

The first *RAD24* mutant was characterized initially in the screen for radiation sensitive mutants. Following that study, Weinert et. al. found the mutant *rad24-1* was defective in the G2/M DNA damage checkpoint. In this study, the *rad24-1* gene was PCR amplified and sequenced to determine the mutation at the gene level. The change in the mutant gene is a Trp-Stop non-sense mutation, which results in a carboxy-terminal truncation of the Rad24 protein (Fig. 2-15A).

The *rad24-1* gene was cloned downstream of the GST epitope in the expression vector previously used to express the checkpoint proteins in this study, and tested for its ability to complement a *rad24*Δ strain. Previous characterization of the *rad24-1* mutant strain indicates it is a complete loss of function mutant when compared to the deletion strain. In addition, the *rad24-1* mutant is both sensitive to DNA damaging agents and is defective in the DNA damage checkpoint function when compared to the deletion strain. The checkpoint defect of this mutant was assayed using *cdc13-1* DNA damage and

sensitivity to UV was also tested (Fig. 2-4). Interestingly, when GST-Rad24-1 was overexpressed it had a hypomorphic phenotype in regards to its ability to complement in either assay.

Rad24 contains several regions of homology with the RFC proteins as indicated by the boxes in Fig. 2-15 (A) (Lydall and Weinert, 1997). In the *rad24-1* mutant, these regions of RFC homology are intact, however the carboxy-terminal domain thought to be a DNA binding domain for RFC1 is not present (Uhlmann et al., 1997). This suggests that the defect in *rad24-1* may be an inability to bind to DNA. Therefore, to examine GST-Rad24-1 DNA binding activity, the protein was purified and assayed using mobility gel electrophoresis and a ssDNA substrate. GST-Rad24-1 was purified using the same method as the other checkpoint proteins in this study and the results of the purification are shown in Fig. 2-14. Polyacrylamide gel electrophoresis and Coomassie Blue staining and Western blot analysis using anti-GST antibodies confirmed the presence of the epitope tagged protein. No DNA binding activity was associated with GST-Rad24-1 as shown in Fig. 2-15 (B).

GST-Rad24-1 may not bind to DNA for several potential reasons. The DNA binding domain of Rad24 may be located in the carboxy-terminal portion of the protein or perhaps the overall structure of the DNA binding domain is affected by the loss of the carboxy-terminus. Nevertheless, the data suggest that the DNA binding activity of Rad24 is linked to its checkpoint function and DNA damage resistance.

Does Rad 24 directly bind to DNA?

To test for whether Rad24 directly binds to DNA, mobility gel shift analysis was performed using anti-GST polyclonal antibodies. The addition of antibodies to reactions could result in three different outcomes. One result could be observation of the super-shift where the observed it DNA binding activity moves through the gel at a slower rate due to the added size of the antibody binding it to the DNA binding protein. A second outcome is referred to as interference, where the antibody blocks of the DNA binding activity of the protein by directly binding the active site of the DNA binding protein or otherwise inhibiting protein DNA-binding activity. And thirdly, it is been observed that not all antibodies are effective in this sort of assay, possibly due to the antibody epitope being embedded internally in the protein because the assays are non-denaturing (Jennifer Hall, University of Arizona, personal communication). When tested using an anti-GST antibody no change in the Rad24 dependent mobility shift was observed (Fig. 2-16). Two reasons for this result are that the antibody does not recognize a non-denatured GST epitope tag or that Rad24 does not directly bind to DNA.

GST cleavage from Rad 24 does not substantially alter the Rad 24 dependent mobility shift.

To test whether cleavage of GST from Rad 24 would alter the rate of mobility of the band shift observed in these assays, GST was cleaved enzymatically from Rad24. This was achieved by taking advantage of the thrombin cleavage site located between GST and Rad 24. As shown in Figure 2-17(A), no significant change in mobility was observed between the GST -Rad24 and GST-Rad24 treated with thrombin reactions. Thrombin

cleavage did occur as shown in the silver stain gel in Fig. 2-17(B), where the addition of thrombin resulted in the formation of a new protein band of the correct size of GST and Rad24 alone. However, it should be noted that this gel represents the results of protein purification procedures prior to further optimization whose results are shown in Figure 2-5. Nevertheless, the GST control lanes in the mobility gel shift analysis do not contain any Rad24 dependent binding activity suggesting that the purification procedure was effective enough to discern between the GST control and Rad24 dependent DNA binding activity.

There are several problems with interpreting this type of analysis that depends on the molecular weight of the protein. Personal communications with Mark Dodson, (University of Arizona) suggest that proteins do not necessarily migrate through gels based on their molecular weights under non-denaturing conditions. This may be due to overall protein structure or the overall protein charge, where proteins that have a negatively charged characteristic migrate faster than proteins that have a more positively charged character in. In addition, the difference in mobility between a monomer and dimer of a protein is limited in this assay as shown by single-stranded binding protein from *E.coli* as shown in Figure 2-16. The size of an SSB monomeric complex is 76kDa, and the size of the dimeric complex is 152kDa. The mobility difference between these two complexes is very small. Thus the change of Rad24 dependent DNA binding from potential 104 to 76kDa would be expected to be even less discernable. Therefore, as alluring as this information may be, it cannot be interpreted alone.

DNA-protein cross-linking analysis of GST-Rad24 binding activity.

To test if Rad24 was directly responsible for binding to DNA, DNA-protein cross-linking assays were performed in collaboration with Kirsten Krause (Dieckmann lab, University of Arizona). These assays use short-wave UV to cross-link the proteins covalently to radio-labeled substrates. To assay GST-Rad24, a mobility gel shift reaction was treated with UV and analyzed using SDS-PAGE gel and phosphorimagery. As shown in Figure 2-18(A) and (B), the DNA-protein banding pattern was observed that is nearly identical to the yeast single-stranded binding protein RPA. Comparison of DNA cross-linked to RPA (gift from Tim Formosa) with GST-Rad 24 results in an almost identical DNA-protein banding pattern. RPA is a hero trimeric protein complex containing three proteins with molecular weights of 70kDa, 32kDa, and 14kDa. The multiple bands seen are likely to be combinations of the to three proteins complexed to a 10.7kDa DNA substrate. Interestingly, GST-Rad24-1 protein preparation did not show the activity seen in the GST-Rad24 preparation (Fig. 2-18C).

However, if GST-Rad 24 directly binds to DNA its molecular weight would be 114.4 kDa, a size that would migrate within the banding pattern of RPA. Although it could be anticipated that because GST-Rad 24 is in excess of RPA, and therefore would expected to result in a strong band, it is possible that GST-Rad24 does not cross-link as readily as RPA to DNA. Thrombin cleavage of GST from Rad24 would not be informative because if Rad24 alone was cross-linked to the DNA it would migrate at 87 kDa, within the banding patter of RPA. This data suggest that Rad 24 interacts with RPA

and that also the DNA binding activity associated with the GST-Rad 24 is also RPA, the does not rule out the possibility that Rad 24 directly binds to DNA.

Discussion

Rad24 is required for cell cycle arrest following DNA damage, and genetic data suggest that Rad24 functions in UV and alkylation DNA damage repair processes (Lydall and Weinert, 1995). Further supporting the model that Rad24 functions in DNA damage repair, studies in yeast have localized Rad24 intra-cellularly to sites of DNA damage (Melo et al., 2001). This same study showed that Ddc1, Mec3 and Rad17 localized to the DNA in a Rad24 dependent manner. Therefore, the observation from this study that Rad24 binds DNA supports the hypothesis that Rad24 functions as a checkpoint sensor protein that recruits Ddc1, Mec3 and Rad17 to the DNA. The data presented in this study suggest that Rad24 either binds to or associates with a protein that binds to DNA. To better understand the substrate specificity of Rad24, a GST epitope tagged Rad24 fusion protein was over-expressed and purified from yeast using non-denaturing affinity chromatography. Substrate competition assays were used to determine the specificity of Rad24 binding to secondary DNA structures.

Rad24 Associated Binding Prefers ssDNA.

Rad24 dependent DNA binding has a higher affinity for ssDNA than dsDNA. This was not suprising because both the human homolog of Rfc1 and the human Rad17-RFC complex been reported to have higher affinities for ssDNA when compared to dsDNA(Tsurimoto and Stillman, 1991; Uhlmann et al., 1997). This ssDNA activity

would enable the protein to be present at sites of DNA repair processing during which ssDNA gaps are formed during DNA damage repair processes.

The Rad24 dependent binding activity bound to DNA primer-template junctions of either directionality and with ssDNA with equal affinity. This suggests that Rad24 binding activity could recognize both primer-template junctions that lie on either side of a gapped DNA substrate formed during DNA repair processes and the ssDNA alone. However, during substrate recognition in the cell, RPA would likely be present thus Rad24 would likely bind to either of the primer-template junctions. The presence of the primer-template junctions in the substrates used in this study did not decrease the affinity of Rad24 for them. This substrate recognition activity by Rad24 associated binding would allow it to not only function during many forms of DNA repair but also suggests a model of how to terminate the checkpoint response. The completion of repair by a polymerase from the gapped ssDNA substrate to a fully dsDNA substrate would destroy both the ssDNA substrate and primer-template junctions that Rad24 would be expected to bind, and subsequently signal the completion of repair. Thus, without a DNA substrate to continually activate the checkpoint response, the checkpoint response would terminate and the cell cycle would be allowed to continue.

The minimal binding size of Rad24 DNA associated binding is between 20 and 25 nucleotides long, which is sufficient for Rad24 to bind to the ssDNA intermediate structure formed during UV repair. However, once again, Rad24 may have to compete with RPA for ssDNA, but still be able to bind to the primer-template junctions formed during DNA repair without obstruction by RPA.

And finally, Rad24 does not show a high affinity for a nicked DNA substrate. Nicks are formed during DNA replication, and DNA repair processes. This suggests that Rad24 DNA binding activity could not recognize DNA ligase substrates that are formed once the ssDNA gap is filled by DNA polymerases, perhaps a step which terminates the checkpoint response. A lack of affinity for nicked substrate is consistent with the model that Rad24 DNA binding activity has a higher specificity for ssDNA or primer-template junctions formed prior to the completion of the DNA repair.

In this study, the Rad24 protein was found to associate with DNA binding activity alone and without the presence of the RFC subunits. This correlates well with a report by Uhlmann et al that showed Rfc1 was the only protein of the RFC complex that could bind directly to DNA in the presence of physiological salt conditions (Uhlmann et al., 1997). In addition, Rfc1 bound to primer-template junctions and ssDNA with apparent equal affinity using hairpin substrates that formed via intramolecular interactions. These findings are in agreement with what has been observed using the same DNA hairpin substrates with the complete RFC complex (Tsurimoto and Stillman, 1991).

Rad24 DNA Binding Substrate Specificity Analysis of Rad24 and its Human Homolog, hRad17.

To imply that hRad17-RFC, and therefore Rad24-RFC, could bind directly to primer-template junctions is contrary to what is known about RFC DNA binding. RFC binds to ssDNA and DNA primer-template junctions equally in the absence of the single stranded DNA binding protein RPA (Tsurimoto and Stillman, 1991). It has also been shown that although RPA blocks RFC from binding to ssDNA, RPA cannot occlude RFC

from primer-template junctions. By blocking RFC from binding to ssDNA, RPA prevents RFC from binding to ssDNA in an unproductive manner and guides it to binding to primer-template junctions, a DNA substrate for which RPA cannot out compete RFC (Tsurimoto and Stillman, 1991).

However, the DNA binding analysis of Rad24 is complicated. Biochemical analysis using the complete human Rad24-RFC complex, hRad17-RFC, reported that the complex bound with a two-fold higher affinity to primer-template junctions when compared to ssDNA (Lindsey-Boltz et al., 2001). A primary problem with the assays done to address hRad17-RFC DNA binding activity is that the authors used DNA substrates that relied on inter-molecular interactions to form primer-template junctions. As previously mentioned, the difficulty of using two separate ssDNA substrates to construct a primer-template junction substrate has been shown by others (Naureckiene and Holloman, 1999). In the case of hRad17-RFC, by comparing DNA affinities between two reactions, with one containing both a 100 base long substrate and a 50 base long substrate, and another reaction only containing the 50 base long substrate would not be a straight forward comparison. The first reaction would contain 2 times more DNA molecules than the latter reaction. Given that intermolecular interactions occur at a low efficiency, the first reaction could be misinterpreted as a two fold higher binding activity for the two DNA substrate reaction when compared with the single substrate reactions. This two-fold effect for a primer-template junction when compared to a ssDNA substrate is what was observed when hRad17-RFC was tested with substrates intended to form

through intermolecular interactions (Lindsey-Boltz et al., 2001). A more conservative interpretation of these results is that hRad17-RFC binds to ssDNA.

Rfc1 is thought to act as the primary DNA binding component of the RFC complex (Uhlmann et al., 1997). This implies that Rad24 is also the primary DNA component of the Rad24-RFC complex. Nevertheless, it would not be unexpected for other protein-protein interactions to modulate this activity. Contrary to how RPA prevents RFC from binding to ssDNA, the replication protein PCNA increases the affinity of RFC for ssDNA. Therefore, it may be possible that the Ddc1/Mec3/Rad17 complex may affect the ssDNA affinity of Rad24-RFC for ssDNA for a different DNA substrate.

Characterization of the rad24-1 Mutation.

Sequencing of the original *RAD24* mutation, *rad24-1*, revealed that the mutant protein contains a carboxy-terminal truncation that includes all of the RFC homology boxes identified in Rad24. To further characterize this mutant, Rad24-1 was epitope tagged with GST and purified using the same methods as GST-Rad24. Rad24-1 protein preparations did not contain any associated DNA binding activity when assayed using mobility shift analysis. DNA binding assays of different Rfc1 truncation mutants revealed that it contains two DNA binding domains, one at the amino-terminus and another at the carboxy-terminus (Uhlmann et al., 1997). Because Rad24 does not contain the amino-terminal ligase domain also found in Rfc1 that binds ssDNA, Rad24 would be expected to have a DNA binding domain located at its carboxy-terminus, similar to Rfc1. The finding that the Rad24-1 protein has no associated DNA binding suggests that Rad24 also

contains a DNA binding domain at its carboxy-terminus. There are several other explanations for the DNA binding defect found in Rad24-1 protein. The carboxy-terminal truncation could disturb the overall folding of the protein. Another explanation that cannot be completely ruled out is the possibility of a protein that co-purifies with Rad24 whose DNA binding is truly being examined in these assays, and that the Rad24-1 protein cannot form a complex with this unknown DNA binding protein.

Over-expression of GST-Rad24-1 results in a partial checkpoint defect in response to UV and *cdc13-1* DNA damage. However, when *rad24-1* is expressed from the genomic copy alone it shows a complete loss of function phenotype. Further analysis of *rad24-1* is required to determine the true defect of the mutant protein.

DNA-Protein Cross-linking Analysis Suggests that GST-Rad24 Associates with RPA.

The observation that Rad 24 probably interacts with RPA was not unanticipated. During DNA replication Rfc1 associates with RPA and hRad17 has been shown to localize to DNA in an RPA dependent manner (Lee et al., 2003; Yuzhakov et al., 1999). In addition, RPA is required for both the S-phase checkpoint and the DNA damage checkpoints. What is suggested by this data is certainly in interaction between Rad 24 and RPA. However this data does not rule out the possibility of Rad 24 directly binding to DNA.

The Role of Rad24 in the Activation of the DNA Damage Checkpoint Response.

The ability of Rad 24 dependent DNA binding activity to recognize primer-template junctions and ssDNA suggests a model in which Rad 24-RFC loads Ddc1/Mec3/Rad17 onto the DNA to activate the checkpoint pathway and facilitate the

repair. This is analogous to how RFC loads PCNA on primer-template junctions to facilitate replication by recruiting DNA polymerases (Waga and Stillman, 1998). The Rad24-RFC and Ddc1/Mec3/Rad17 complexes may recruit unknown proteins to facilitate their roles in the as of yet unidentified DNA repair process that these proteins are thought to have a role in (Lydall and Weinert, 1995).

Further analysis needs to be done to determine if Rad24 DNA binding activity is indeed specific to ssDNA, or if other proteins play a role in the DNA binding to promote primer-template junction specificity. The different degrees of affinity that Rad24 DNA binding has for dsDNA, ssDNA and primer-template junctions may function to localize Rad24 to the DNA. The dsDNA affinity may keep Rad24 localized generally to the DNA and the ssDNA affinity may closely associate Rad24 with sites of DNA repair. In addition, Rad24 localization to primer-template junctions may be aided by the interaction of other proteins such as RPA and Ddc1/Mec3/Rad17. These affinities for other forms of DNA may decrease the amount of time Rad24 requires to act in a timely manner for the DNA damage checkpoint response.

Materials and Methods

Yeast strains and media.

Standard media conditions were used that included yeast extract-peptone and 2% dextrose (YEPD) and –ura dropout media for strains containing plasmids (Sherman, 1986).

Checkpoint mutants strains used in this study are isogenic with W303 and constructed using standard genetic techniques (Table 2-1). Mutations were previously

described for *mec3Δ, rad17Δ, and rad24Δ* (Lydall and Weinert, 1995, 1997: Weinert and Hartwell, 1993), and *ddc1Δ* (Longhese et al., 1997). The *cdc13-1* and *cdc15-2* have been used in previous studies(Gardner et al., 1999; Lydall and Weinert, 1995). The protease deficient strain containing *pep4, prb1*, and *prc1* was a gift from A.Adams. Yeast transformations were performed according to the LiAc TRAFO method (Schiestl and Gietz, 1989).

Plasmid constructions.

To construct plasmid ELP17 a *GST* containing fragment was PCR amplified from DL-C209 using the primers BGST5, 5'CAGGAAACAGGATCCATGTCCCCTA3' and NGST3, 5'CTTTGGCATATGCGGCGATCC3'. The *GST* BamHI-NdeI fragment was fused to the *GAL1* gene within the DLC-218 polylinker (Lydall and Weinert, 1997). DLC-218 is based on the pRS416 vector. The ELP18 *GST-RAD17* fusion plasmid was constructed by fusing a NdeI-NotI *RAD17* containing fragment from DLC-258 downstream of the *GST* gene in ELP17. Plasmid ELP37 was constructed by PCR amplification of *MEC3* using the primers MEC35, 5'AGTCATATGAAATTAAAATTGATAGTA3' and MEC33, 5'CCGCGCGGCCGCTTACAAGCCCTTCGATCTTGC3'. The PCR NdeI-NotI fragment was fused downstream of *GST* in ELP17. ELP38 was constructed by PCR amplification of the *DDC1* gene using the primers DDC152, 5'GACTAGTATGTCATTTAAGGCAACTATC3' and DDC13, 5'TACTAGTTTAGTCAAATATACCCCTTAC3'. The *DDC1* PCR containing SpeI-SpeI fragment was fused downstream of the *GST* gene in ELP17 that had been digested

with SpeI and Klenow filled. ELP39 was constructed by fusing a SpeI-NotI fragment containing *RAD24* that had been PCR amplified using the primers RAD24F2, 5'ACTGCATACTAGTATGGATAGTACGAATTTGAAC3' and RAD24GR2, 5'ATCGGAGCGGCCGCATGTGCATAGATTTGTGTGG3', downstream of the *GST* gene in ELP17.

G2/M cell cycle arrest assaying using *cdc13-1* DNA damage induction.

G2/M cycle arrest assays were performed as described (Lydall and Weinert, 1995). Yeast cells containing plasmids were grown for two days at 30°C in -ura dropout media and 2% raffinose. Overnight cultures were inoculated 1:50 dilution into -ura dropout media and 2% raffinose at 30°C. The following day cells were checked for cell density with a hemocytometer. Cells were counted as follows: one cell was counted as one and a budded cell counted as two. Cultures were adjusted to $6x10^6$ cells/ml if the cultures had not grown past $1.5x10^7$. α-factor (Sigma; St. Louis, MO) was then added to a final concentration of 20n*M*, except in the case of ddc1Δ cells which did not contain the bar1 mutation in which case the α-factor final concentration was 400n*M*. Cells were washed starting at t= -40 minutes to the zero time point and resuspended into YEP and 2% galactose media. At the zero time point cells were shifted to 36°C the restrictive temperature for *cdc13-1* and *cdc15-2*. Aliquots of the cultures were taken at the designated time points and fixed by adding 0.5 mls of cell culture to 1 ml 95% ethanol. Cell cycle arrest assays were quantitated by analyzing the nuclei of the cells to determine if nuclear division has occurred resulting in two nuclei, or if the G2/M checkpoint had been activated resulting in one visible nucleus. Nuclear morphologies were quantitated

by scoring at least 100 cells that had been stained with 4,6-diamino-2-phenylindole (DAP1, 0,2 μg/ml) (Pringle et al., 1989) and visualized with a fluorescent microscope.

Cell survival following UV exposure.

Saturated cultures were grown as previously described in the section on cell cycle arrest assay. Cell cultures were adjusted to $2x10^6$ cells/ml grown for 6 hours with shaking at 23°C. Cells cultures were then adjusted to a final concentration of 2000 cells/ml. Duplicate 100μl aliquot were then plated in duplicate on YEPD agarose plates and the plates were allowed time to dry (approx. 20 min.). Plated cells were then exposed to appropriate does of UVC using a Stratalinker 1800. The plates were then incubated at 23°C for and counted on day 3 to determine viability. A control plate that had not been exposed to UVC defined 100% viability.

Protein preparation.

Protease deficient yeast cells containing plasmids were grown for two days at 30°C in 5.5 mls -ura dropout media and 2% raffinose. Eleven mls of saturated culture was inoculated into 1 liter of -ura and 2% raffinose and allowed to grow to midlog at 30°C with vigorous shaking. Once cells had reached midlog ($4-6x10^6$ cells/ml), protein expression was induced with 2% for 6 hours. Cells were pelleted, resuspended in 50% glycerol, flash frozen using liquid nitrogen, and stored in 50ml Falcon tubes at –70°C. Cell pellets were thawed on ice, pelleted, and resuspended in 4x the volume of the pellet of lysis buffer was added (50mM Tris-HCl [pH 7.4], 100mM NaCl, 2mM EDTA,1% NP-40, 1mM 2-mercaptoethanol, Aprotinin 2μg/ml, Leupeptin 2μg/ml, Pepstatin 1μg/ml). An equal volume to the lysis buffer of glass beads was added and cells lysed by vortexing at 4°C.

Glass beads were washed with lysis buffer and the wash added to the supernatant. Cell lysates were clarified by centrifugation at 10,000 x g and then passed over glutathione cellulose (Pharmacia) column (200µl bed volume) twice. Columns were washed with 10 column volumes with lysis buffer and GST fusion proteins eluted using elution buffer (30mM Hepes-K+[pH7.8], 7mM $MgCl_2$, 0.5 mM DTT, 10mM reduced glutathione). Protein preparations were separated on SDS-polyacrylamide gel electrophoresis (PAGE) of either 7.5% or 10% acrylamide concentration. The bis-acrylamide/acrylamide ratio was 1:37.5 respectively and visualized using Coomassie blue staining.

Western blotting.

Proteins were electroblotted onto nitrocellulose membrane and blocked for 1 hour in blocking solution (PBS-T and 5% w/v powder non-fat dry milk). The membranes were then washed once with PBS-T and then incubated for 1 hour with primary goat anti-GST antibody (Pharmacia) in PBS-T and 2.5% w/v powdered non-fat dry milk. Blots were then washed 3 times for 5 minutes each wash with PBS-T and then incubated for 1 hour with rabbit anti-goat HRP conjugated secondary antibody (Sigma) in PBS-T and 0.3% w/v powder non-fat dry milk. The blots were then washed 3 times for 5 minutes each wash with PBS-T. Pierce Super Signal chemilumenescent substrate was used to detect the proteins.

Gel mobility shift assays.

Gel mobility shift assays contained 200-400ng of fusion protein,30mM Hepes-K (pH7.8), 7mM $MgCl_2$, 0.5 mM DTT, 10mg/ml BSA, 20mM EDTA, 100mM NaCl, and 4fmoles of DNA substrate P^{32} labeled with Polynucleotide-Kinase (Roche Applied Science) in a

40μl volume. Reactions were incubated at 30°C for 20min and loaded onto a 5% acrylamide gel. Gels were dried onto Wattman paper and analyzed using a Molecular Dynamics 445 S1 PhoshporImager and the IP Lab Gel H program. Super shift assays were performed by adding 1μl of goat anti-GST antibody (Pharmacia) to mobility shift reactions and run on non-denaturing gels.

DNA-Protein Cross-linking.

Assays were performed by placing mobility gel shift reactions onto parafilm paper and placed on ice. A short wave hand held UV lamp was placed 3 cm from the reactions. Times of exposure varied from 2 to 8 minutes. Following cross-linking 10 μl of 5x SDS-PAGE gel loading buffer was adding to the 40 μl reactions, and run on 7.5-10% SDS-PAGE gels. Gels were dried on Wattman paper and analyzed using Dynamics 445 S1 PhoshporImager and the IP Lab Gel H program.

Sequencing of *rad24-1.*

To determine the mutation in the rad24-1 gene, the gene was PCR amplified from the mutant strain using the primers RAD24F, 5'GCAAACACGCATTGATATCTG3' and RAD24R, 5'TGTGGAATATTTCCTGGGGT3'. The PCR product was sequenced and revealed a G->A mutation at nucleotide 1340. This results in a Trp->Stop mutation that causes a truncated mutant protein.

Figure 2-1. Complementation of both cell cycle arrest defect and UV senstivity of a *ddc1*Δ strain by the GST-Ddc1 fusion protein. (A) GST-Ddc1 is able to restore the cell cycle arrest defect of a *ddc1*Δ strain following *cdc13-1* DNA damage. (B) GST-Ddc1 restores UV tolerance for a *ddc1*Δ strain.

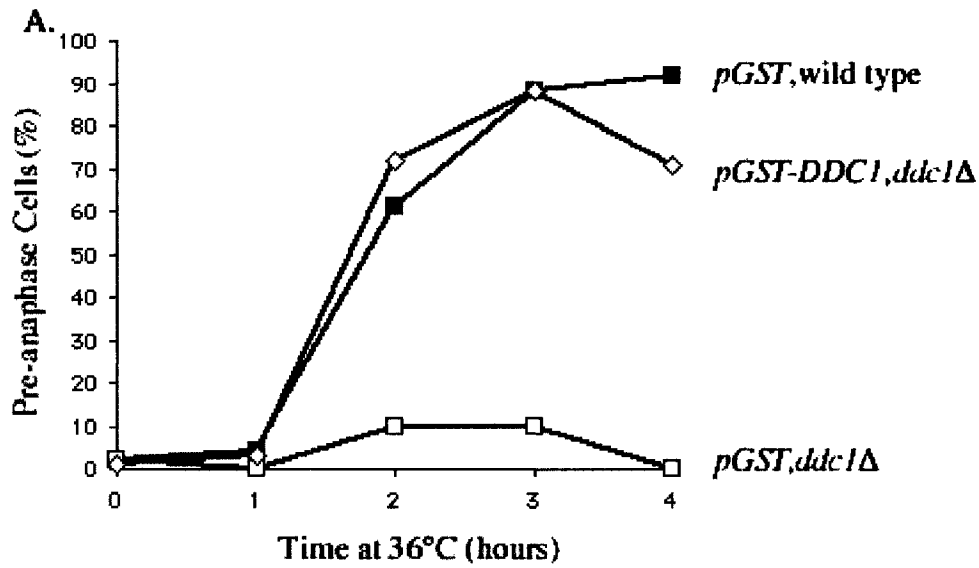

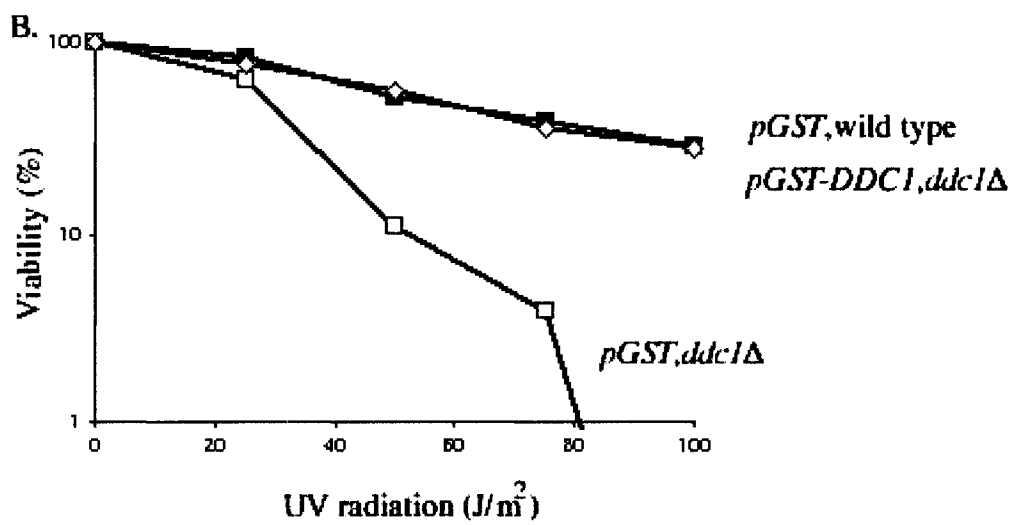

Figure 2-2. Complementation of both cell cycle arrest defect and UV senstivity of a *mec3Δ* strain by the GST-Mec3 fusion protein. (A) GST-Mec3 is able to restore the cell cycle arrest defect of a *rmec3Δ* strain following *cdc13-1* DNA damage. (B) GST-Mec3 partially restores UV tolerance for a *mec3Δ* strain.

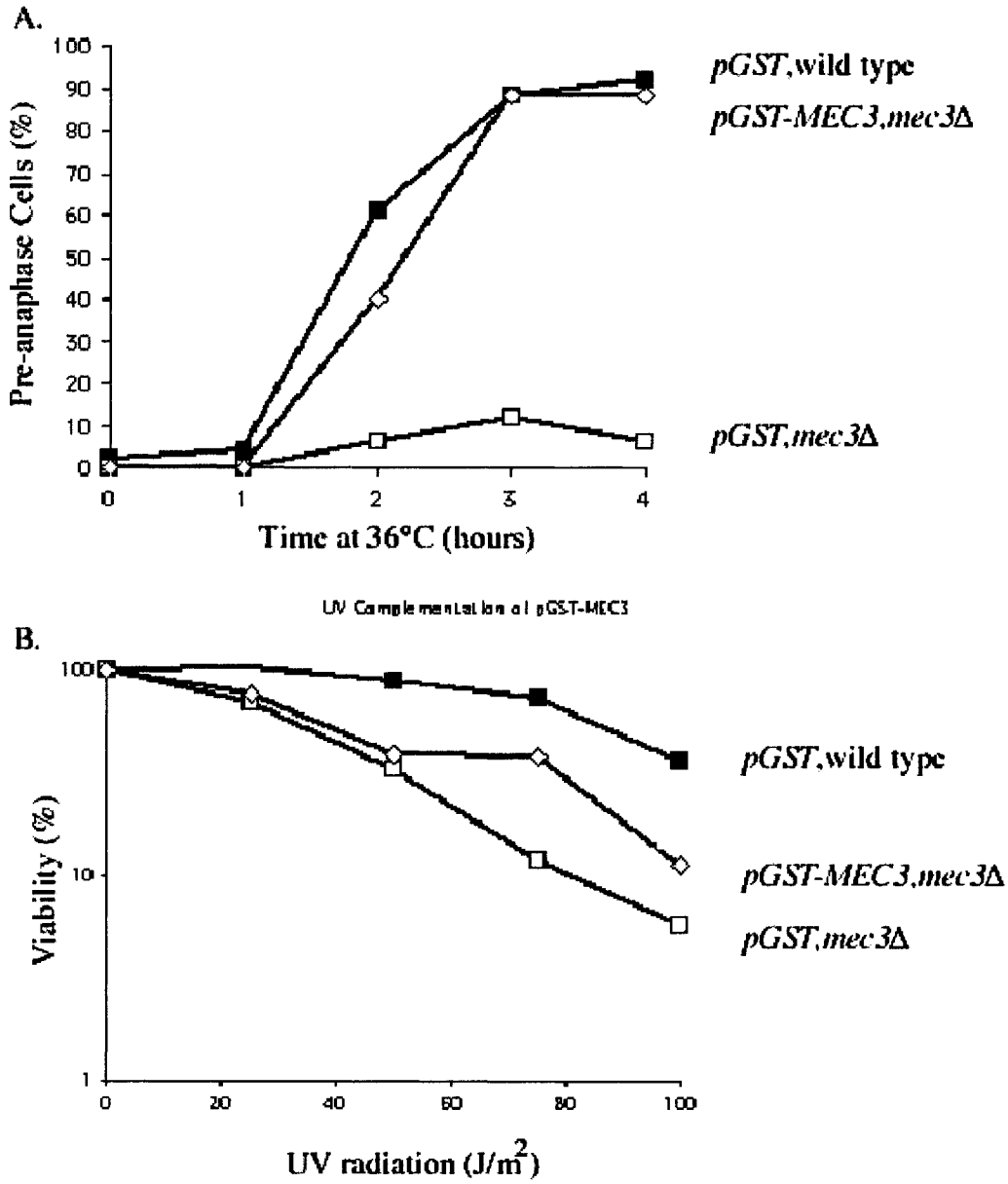

Figure 2-3. Complementation of both cell cycle arrest defect and UV senstivity of a *rad17Δ* strain by the GST-Rad17 fusion protein. (A) GST-Rad17 is able to restore the cell cycle arrest defect of a *rad17Δ* strain following *cdc13-1* DNA damage. (B) GST-Rad17 restores UV tolerance for a *rad17Δ* strain.

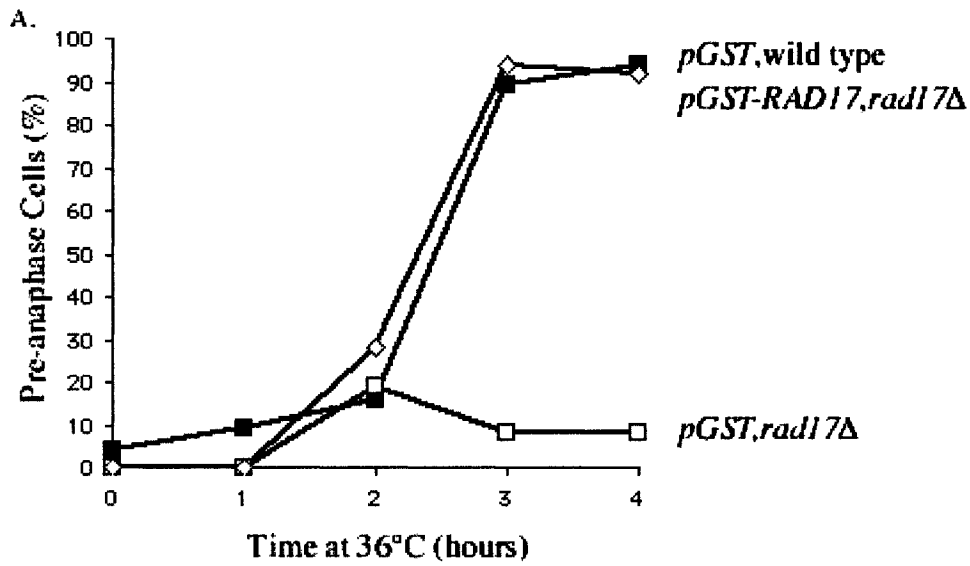

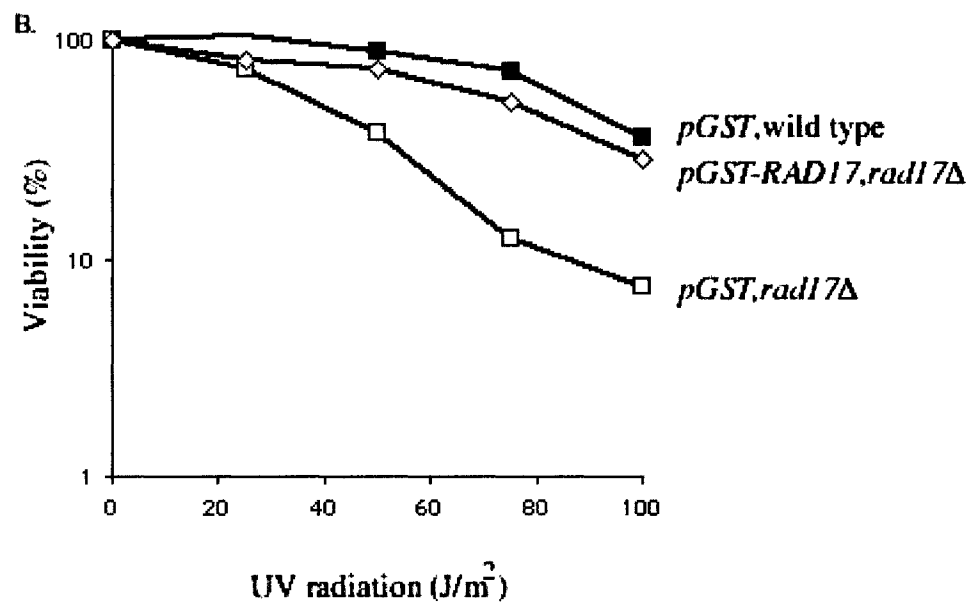

Figure 2-4. Complementation of both cell cycle arrest defect and UV senstivity of a *rad24Δ* strain by the GST-Rad24 and GST-Rad24-1 fusion proteins. (A) GST-Rad24 is able to restore the cell cycle arrest defect of a *rad24Δ* strain following *cdc13-1* DNA damage. When tested under the same conditions the GST-Rad24-1 fusion protein is not able to complement the cell cycle defect of a *rad24Δ* mutant. (B) GST-Rad24 and GST-Rad24-1 partially restore the UV tolerance of a *rad24Δ* strain.

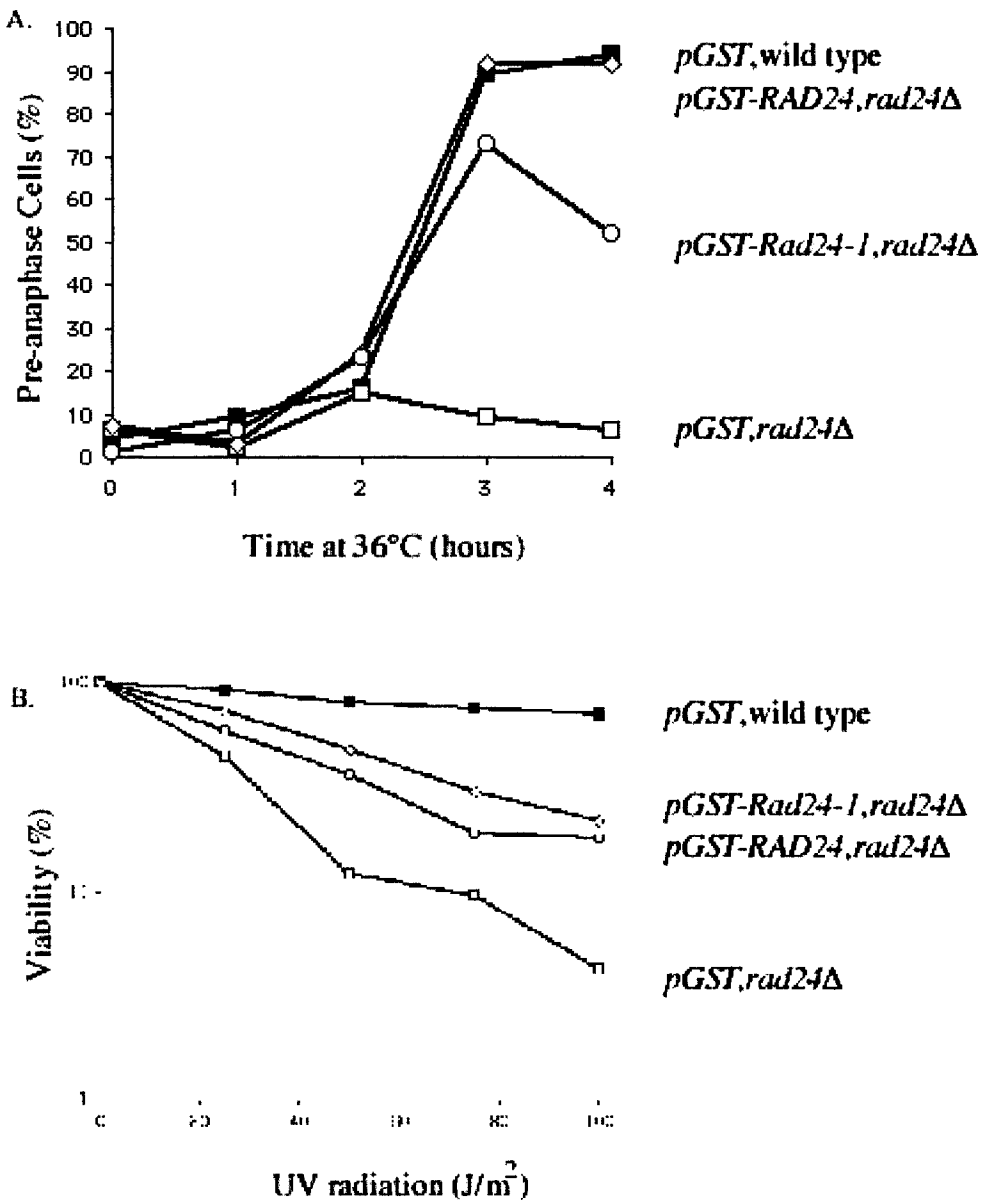

Figure 2-5. GST purification of fusion proteins. Recombinant GST fusion checkpoint proteins were separated by SDS/PAGE and stained with Coomassie blue. Sizes of molecular weight markers are indicated. Western blots with antibodies specific for the GST epitope tag are shown to the right of the respective Coomassie blue gel.

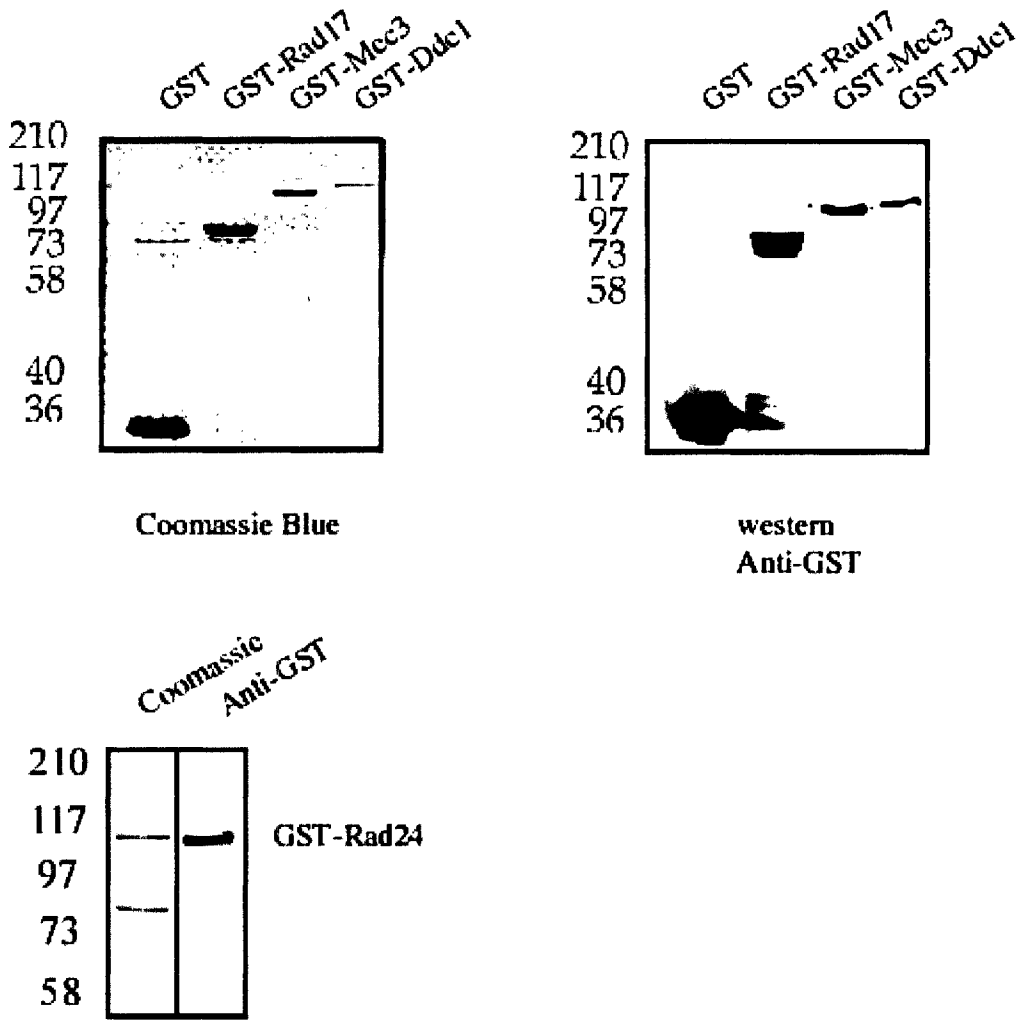

Figure 2-6. GST-Rad24 dependent DNA binding activity. Gel mobility shift assays were performed with with protein preparations mixed with a ^{32}P-labeled gapped DNA substrate (Figure 3-6) for 20 min at 30°C using standard condition with the exception of 10mM NaCl and crosslinked with 0.5% glutaraldehyde before electrophoresis in a 5% polyacrylamide gel and 0.5xTBE (90mM Tris/64.6mM boric acid/2.5mM EDTA, pH8.3). GST-Rad24 associated DNA binding activity (lane 7) was not detectable in the GST, GST-Ddc1, GST-Mec3 and GST-Rad17 reactions (lanes 3-7). A reaction containing the three checkpoint proteins that form a heterotrimeric complex similiar to PCNA, GST-Ddc1, GST-Mec3, GST-Rad17, did not result in DNA binding activity (lane 10). Combining all four checkpoint recombinant proteins had no effect on the mobility shift (lane 11). Crosslinking was shown to not be necessary (lane 9).

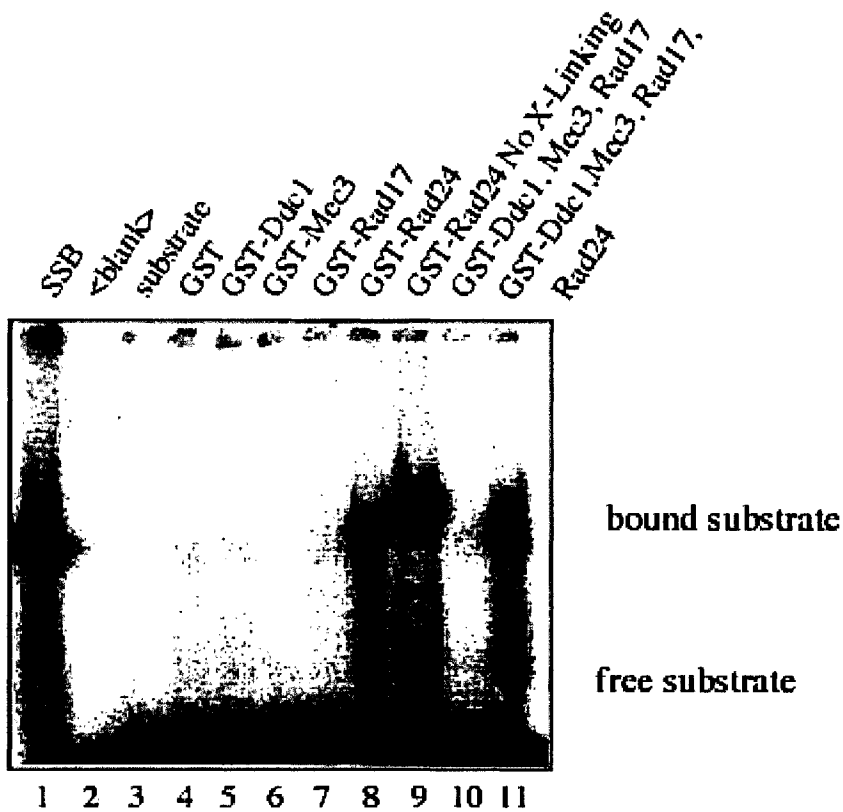

Figure 2-7. Rad24 dependent DNA binding does not require the presence of a 5' phosphate. DNA probes were 5' phophorylated with polynucleotide kinase and ^{32}P, or 3' end labeled with terminal transferase and ^{32}P. GST protein preparations do not bind to either probe (lanes 1 and 3) and both GST-Rad24 protein preparations bind to 5' or 3' end labeled probes (lanes 2 and 4).

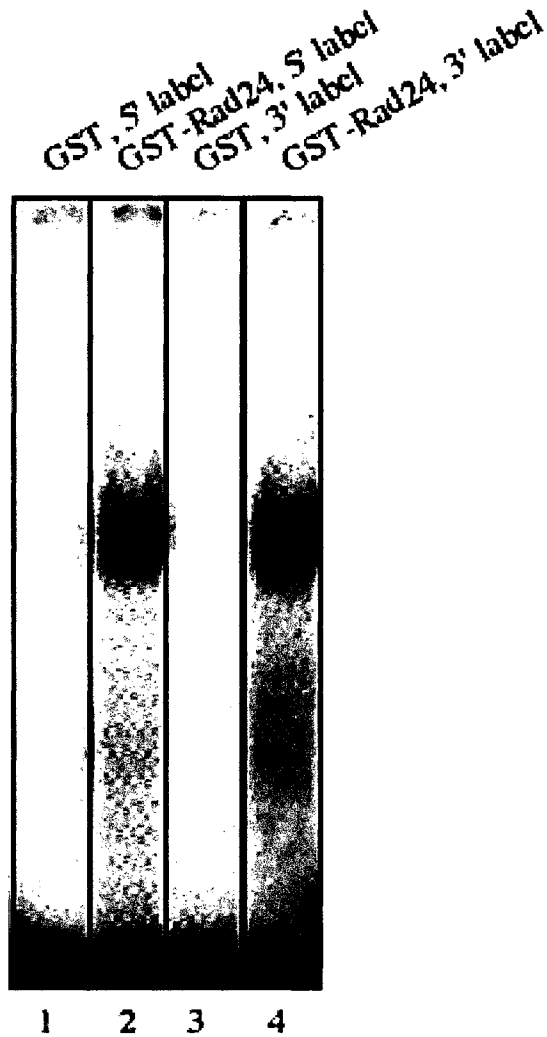

Figure 2-8. Rad24 dependent DNA binding preference hierarchy. (A) Gel mobility shifts were performed using ^{32}P labeled ssDNA substrate with varying amounts of unlabeled competitor DNAs present at the start of the reactions. Poly-A DNA was added in lanes 2-5, poly-dT DNA was added in lanes 7-10, poly-dC DNA was added in lanes 12-15, and identical linear DNA was added in lanes 17-20. The amounts of competitor varied from no competitor to 10 fold excess of labeled DNA. (B) Quantitative analysis of Rad24 dependent DNA binding to the linear DNA in the presence of DNA competitor DNAs.

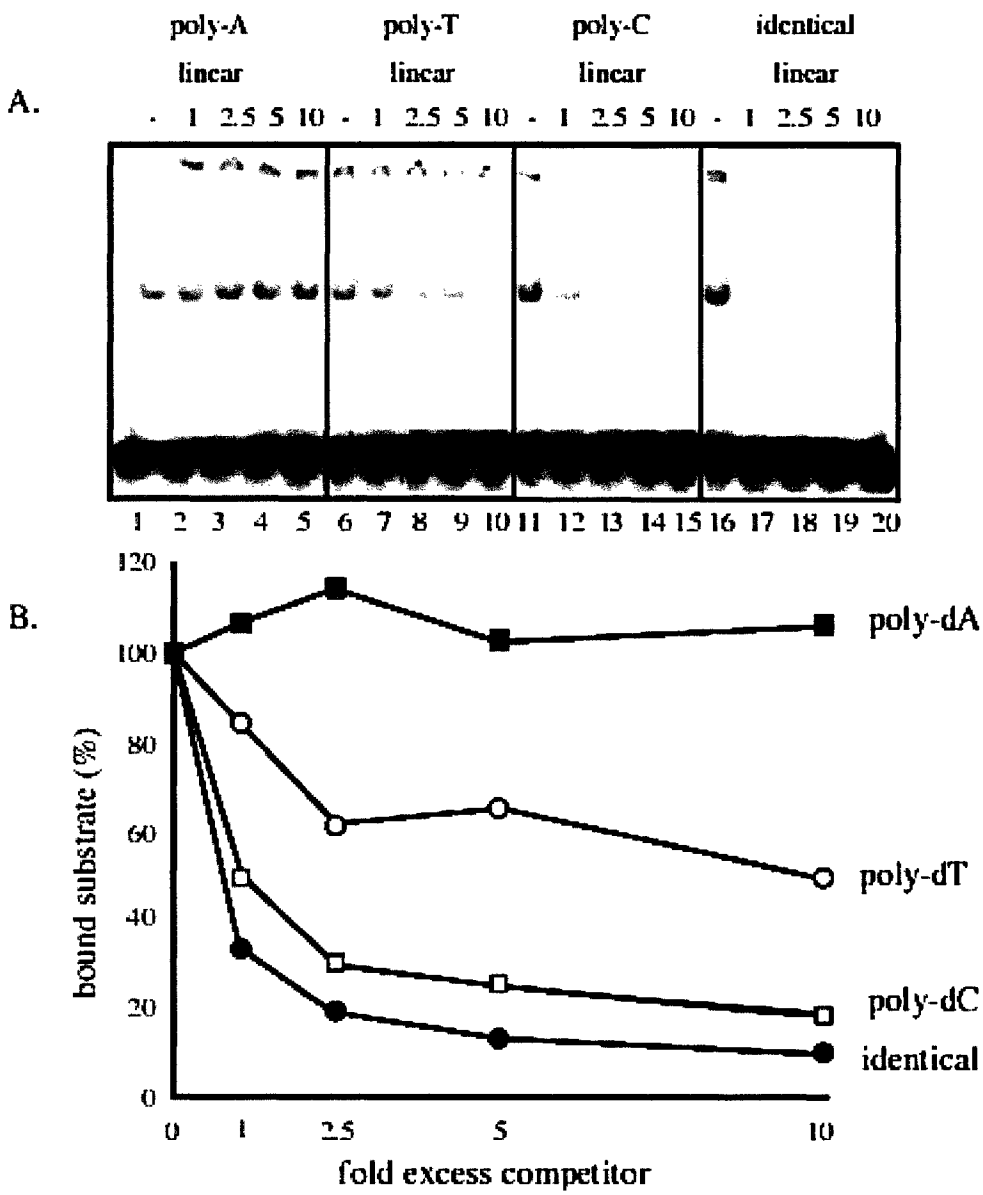

Figure 2-9. Secondary structures of DNA substrates used in this study. (A) Hairpin substrates that form intramolecular secondary structures at a higher efficiency than DNA substrates that form secondary DNA structures by intermolecular interactions. The two hairpin substrates resemble either a primer-template junction that can be recognized by replication proteins, or a primer-template of the opposite orientation. (B) Structure of DNA substrate that contains a gap 35 nucleotides long and no double-stranded ends. (C) Structures of DNA substrates containing either a nick or duplex DNA without double-stranded ends. For substrate sequences see Table 1-2.

A. DNA Hairpin substrate with 3' or 5' free end (29 nts. ssDNA).

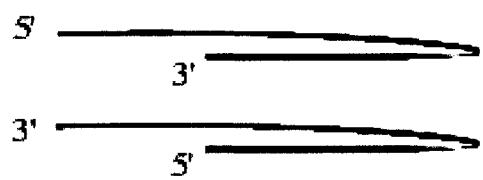

B. Gapped hairpin substrate.

C. Nicked hairpin substrate, ligated to form duplexed DNA substrate.

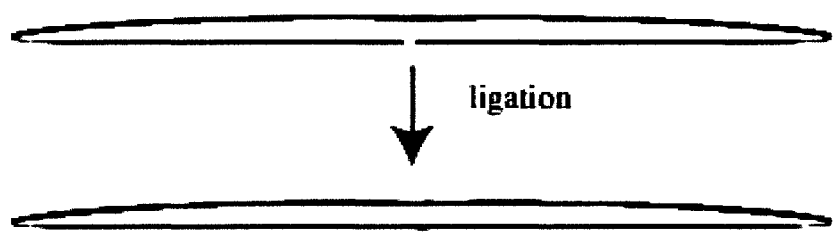

Figure 2-10. Rad24 dependent DNA binding activity is unaffected by secondary DNA hairpin structures. (A) Gel mobility shifts were performed using ^{32}P labeled linear substrate not identical to the linear unlabeled competitor DNA. Linear competitor DNA is the same length and sequence as the ssDNA regions of the hairpin substrates, and the same directionality of the 5' free end hairpin substrate. Linear DNA was added in lanes 2-6, 5' free end hairpin DNA was added in lanes 7-11, and 3' free end hairpin DNA was added in lanes 12-16. Lane 1 is a substrate-only control. The amounts of competitor varied from no competitor to 10-fold excess of the concentration of labeled DNA. (B) Quantitative analysis of the reactions performed in (A).

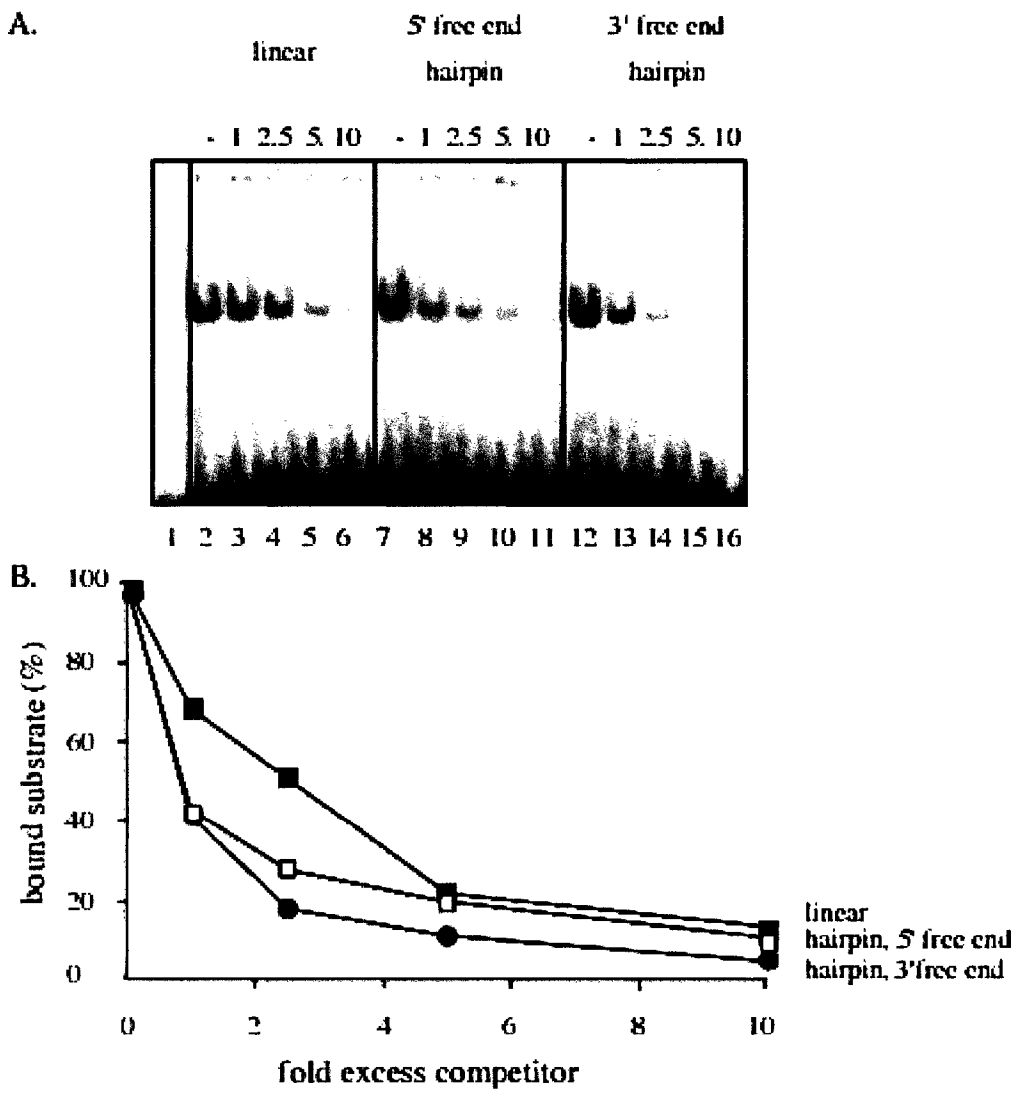

Figure 2-11. Rad24 dependent DNA binding has a lower affinity for duplex DNA. (A) Gel mobility shifts were performed using ^{32}P labeled linear substrate. Unlabeled competitor DNA was identical, complementary, or duplexed in sequence and structure of the labeled substrate. Duplex DNA was constructed through intra-molecular interactions that form a hairpin structure. Identical linear competitor DNA was added in lanes 2-4, complementary linear DNA lanes 6-8, and hairpin DNA lanes 10-12. (B) Quantitative analysis of Rad24 dependent DNA binding to linear DNA in the presence of competitor DNAs.

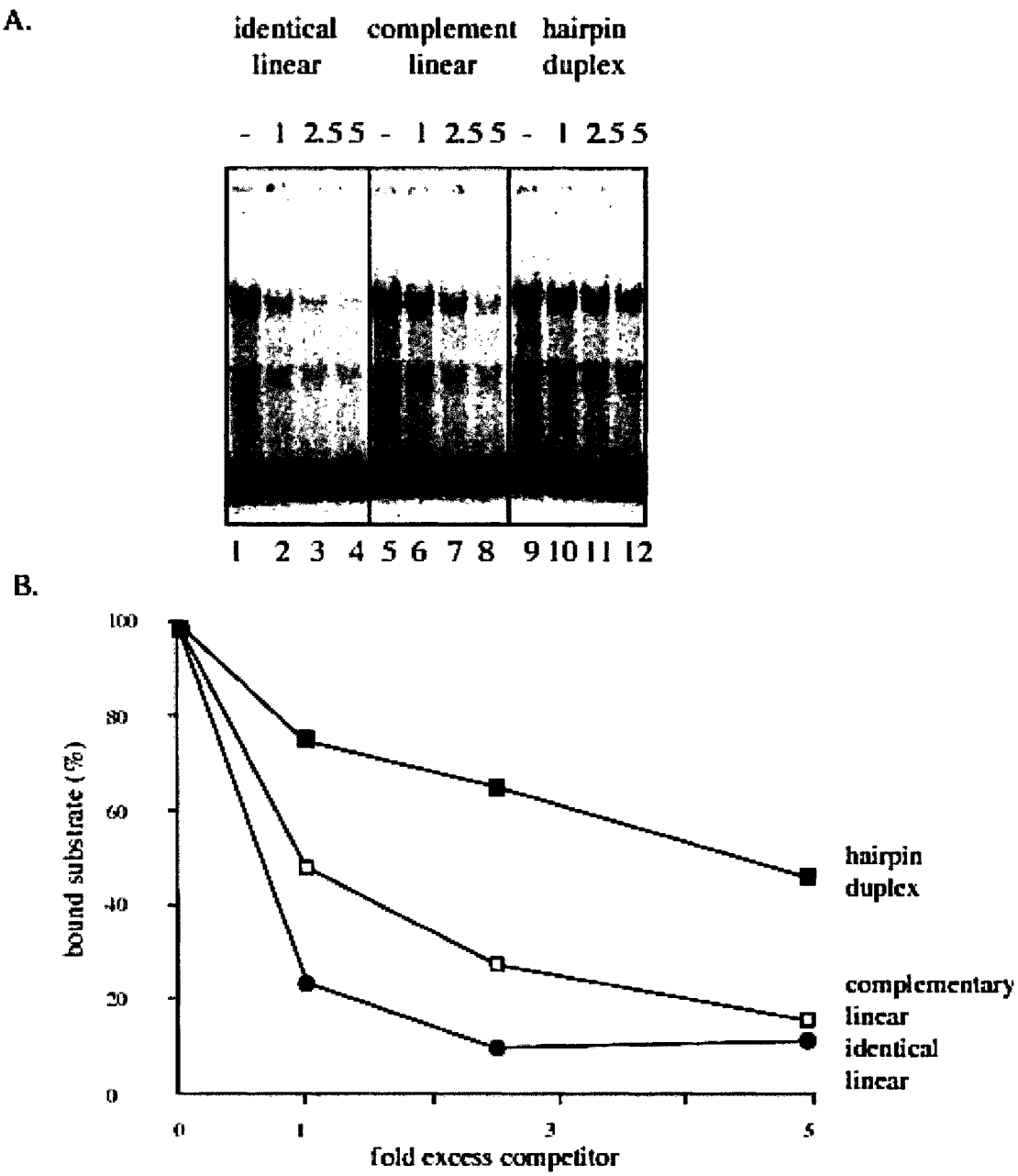

Figure 2-12. Rad24 dependent DNA binding has a substrate size preference. (A) Gel mobility shifts were performed using a heterologous 35 base long ^{32}P labeled substrate. Unlabeled competitor DNAs varied only by length and were only constructed with poly-dT. Linear 15 base long poly-dT DNA was added in lanes 2-5, 20 base long poly-dT DNA was added in lanes 7-10, 25 base long poly-dT DNA was added in lanes 12-15, 30 base long poly-dT DNA was added in lanes 16-20, and 35 base long poly-dT DNA was added in lanes 22-25.
(B) Quantitative analysis of Rad24 dependent DNA binding to linear DNA of varying lengths in the presence of competitor DNAs.

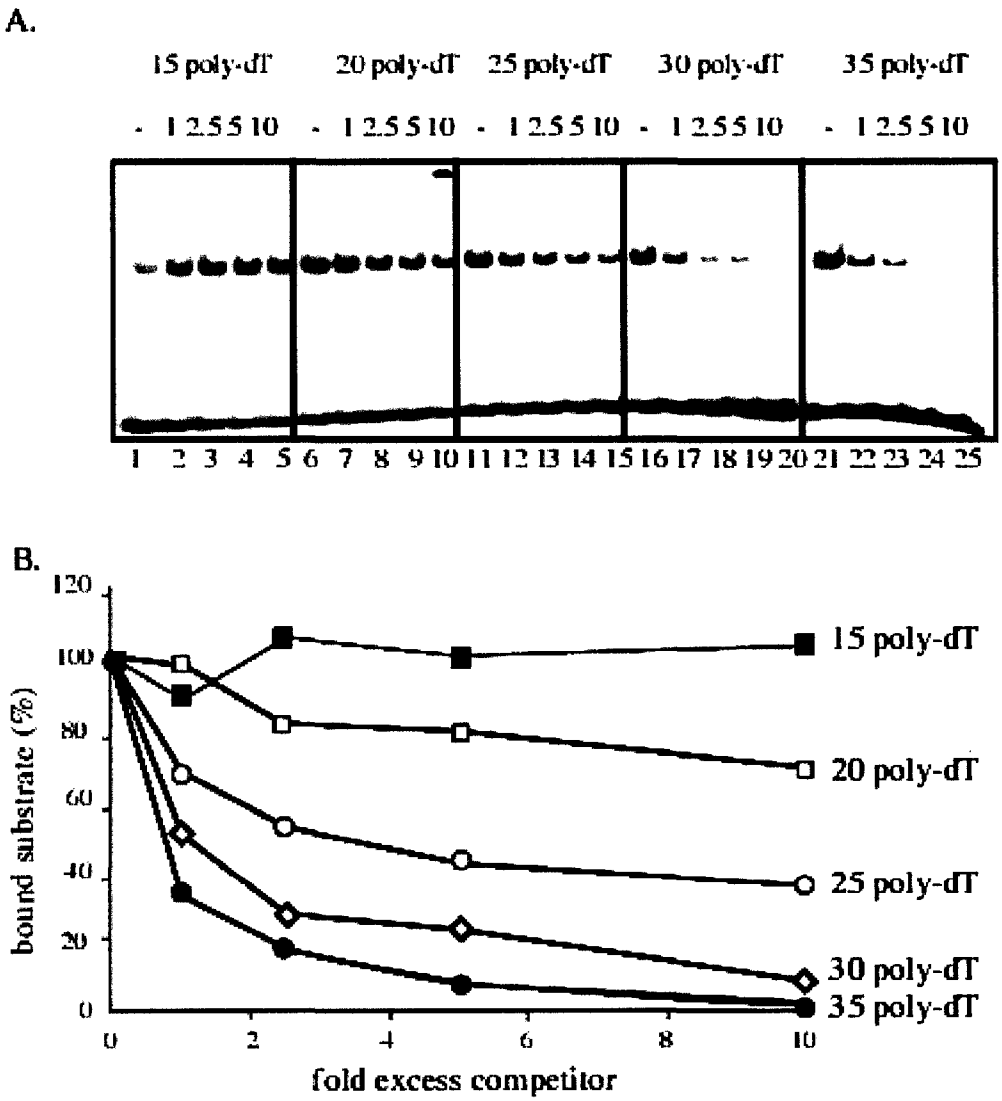

Figure 2-13. Rad24 dependent DNA binding does not bind to nicked or duplex DNA. (A) Gel mobility shifts were performed using the 35 base long ^{32}P labeled heterologous subustrate. Unlabeled competitor DNA containing a nick, gap or duplex contain two hairpin structures instead of dsDNA ends. Linear DNA was added in lanes 2-5, gapped DNA in lanes 7-11, nicked DNA in lanes 12-15, and duplex DNA in lanes 17-20. (B) Quantitative analysis of Rad24 dependent binding to DNA substrates with varying secondary DNA structures.

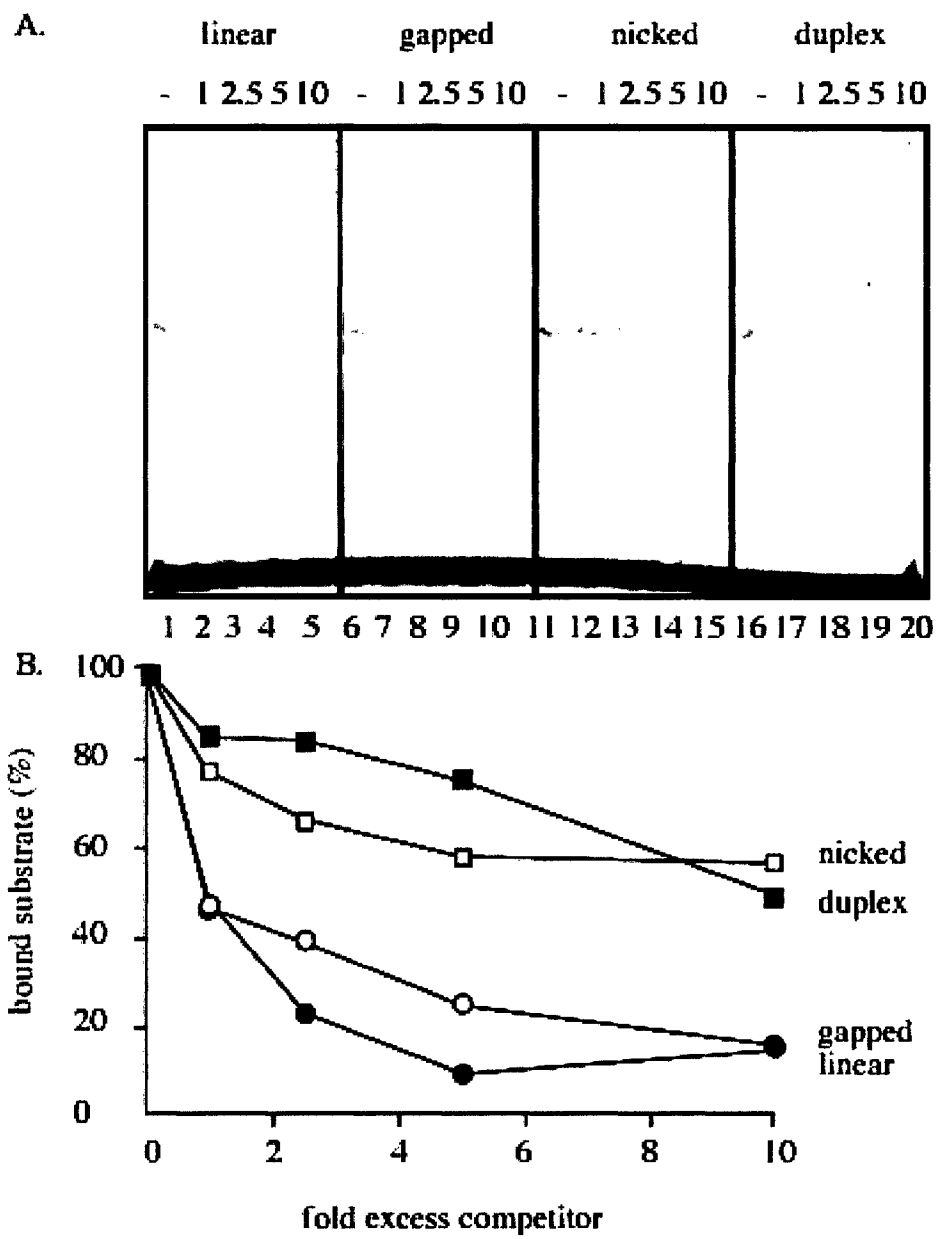

Figure 2-14. GST purification of fusion proteins. Recombinant GST fusion checkpoint proteins were separated by SDS/PAGE and stained with Coomassie blue. Sizes of molecular weight markers are indicated. The western blot with antibodies specific for the GST epitope tag is shown to the right of the Coomassie blue gel. Asterisks indicate co-purifying proteins that associate with the GST epitope control alone.

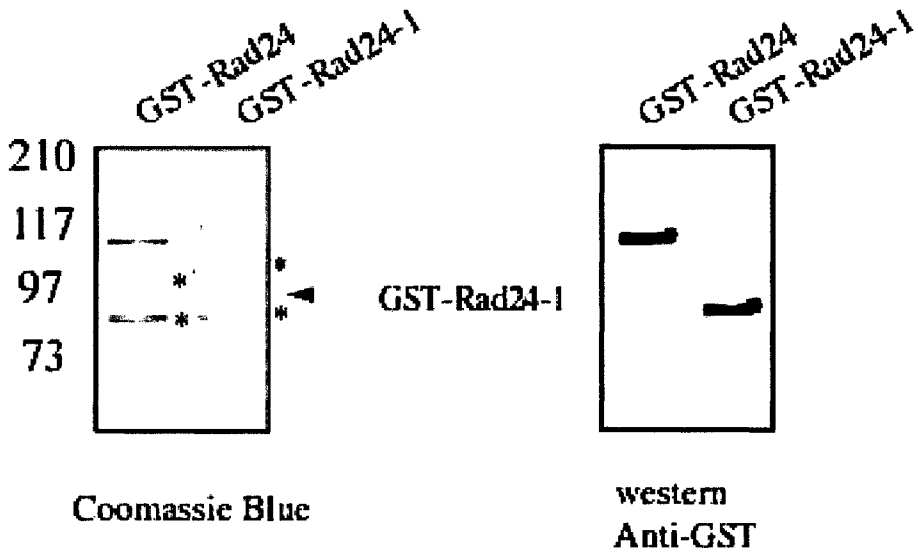

Figure 2-15. Structure and DNA binding defect of the Rad24-1 checkpoint mutant protein. (A) The *rad24-1* mutation was PCR amplified and sequenced. Sequence analysis revealed that the *rad24-1* mutation is a non-sense mutation, resulting in a carboxy-terminal truncation. The Rad24-1 mutation lies downstream of the regions of Rad24 that are homologous to RFC proteins as shown in boxes II-VIII. (B) Gel mobility shift analysis was performed using ^{32}P labeled linear DNA, and GST-Rad24 or GST-Rad24-1 protein preparations. No Rad24 dependent DNA binding is detected in the Rad24-1 protein preparation.

A. The DNA damage checkpoint mutant *rad24-1*

Tryptophan ⟶ Stop
(446 a.a.)

Rad24p homology to RFC motifs are marked by boxes.

B.

Figure 2-16. Addition of anti-GST polyclonal antibody to mobility gel shift reactions does not result in a change in Rad24 dependent DNA binding reactions. Lane 1 is a ^{32}P labeled linear substrate alone control. Lane 2 contains the *E.coli* single-stranded DNA binding protein. Lane 3 is GST alone control reaction, and lane 5 contains GST and anti-GST antibody. Lane 6 contains GST-Rad24 and lane 8 contains GST-Rad24 and anti-GST antibody. Lanes 4 and 7 are tested different parameters that do not pertain to the addition of antibodies to mobility gel shift reactions.

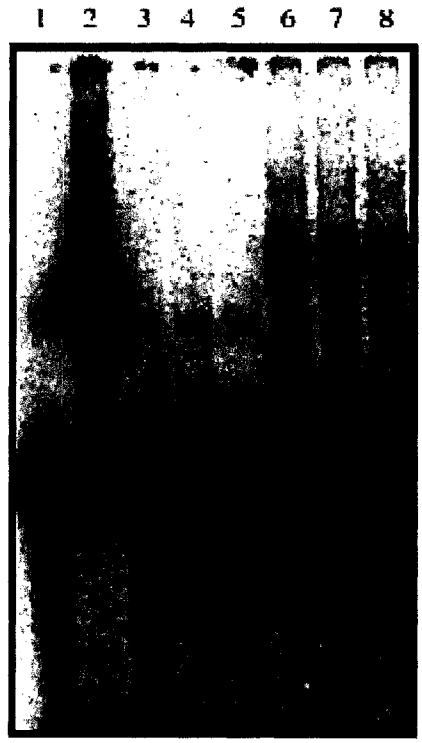

Figure 2-17. Thrombin cleavage of the GST epitope from Rad24 did not result in a substantial change in mobility. Lane 1 is an *E.coli* single-stranded binding protein reaction that served as a positive control. Lane 2 is a DNA^{32}P labeled linear substrate control, lane3 is a GST control, lane 4 is GST treated with thrombin, lane 5 is a GST-Rad24 reaction, and lane 6 is GST-Rad24 treated with thrombin. Thrombin cleavage was done at room temperature for 2 hours.

A.

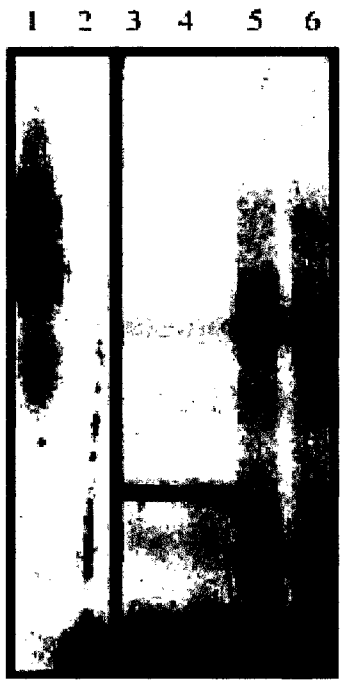

B.

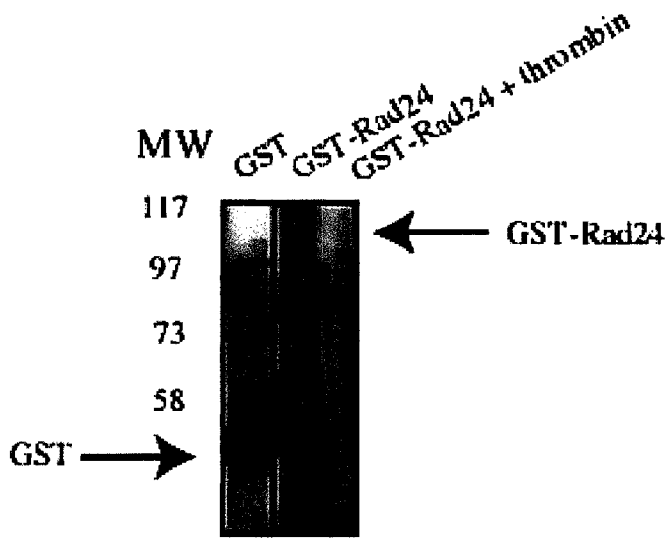

Figure 2-18. DNA-protein cross-linking assays of GST-Rad24, GST-Rad24-1 and RPA with a ^{32}P labeled 35 base long ssDNA substrate. Mobility gel shift reactions containing protein and DNA substrate were cross-linked using short wave UV, run on SDS-PAGE gels, and analyzed using as a phosphorimager (A) Separate RPA and GST-Rad24 reactions. (B) RPA and GST-Rad24 reactions run side by side on an SDS-PAGE gel. The control lane contains reaction buffer and DNA only. (C) The GST-Rad24-1 protein preparation does not contain this activity.

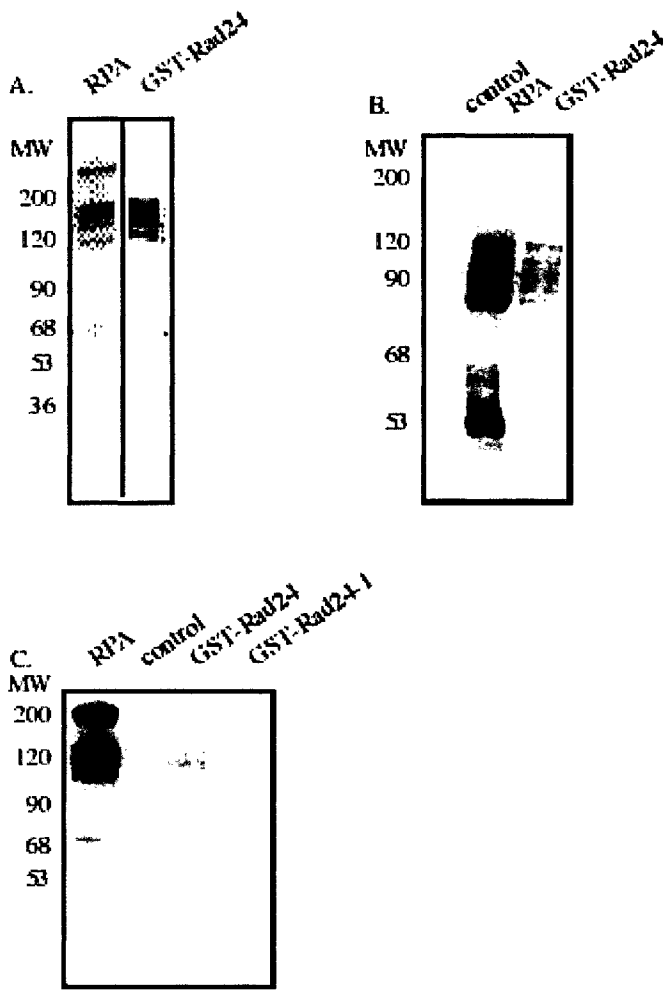

Table 2-1. Strains used in this study.

Strain	Genotype	Source
DLY408	*Mat**a**, bar1, cdc13-1, cdc15-2 his3, trp1, ura3, ade2,*	D.Lydall
DLY410	*Mat**a**,bar1, rad24::TRP1, cdc13-1,cdc15-2 ura3, leu2*	D.Lydall
DLY534	*Mat**a**,bar1, rad17::LEU2, cdc13-1,cdc15-2 ura3, trp1*	D.Lydall
DLY740	*Mat**a**, bar1, mec3ΔG::ura3::LEU2, cdc13-1,cdc15-2, his3*	D.Lydall
	*Mat**a**, ddc1Δ::KanMX4, cdc13-1,cdc15-2, leu2, his3*	This study

Table 2-2.

Oligonucleotides used in this study.

gapped substrate	
EXO22	CAGGTACTTTGAACGAATGCAT
EXO35	TAGTTAATCATTGGCTCTTGTATTCGCGTATCTTG
EXO80	ATCATGCATTCGTTCAAAGTACCTGTCAAACTATT ATTCCGAGCACAAGATACGCGAATACAAGAGCCA ATGATTAACTA
	hairpin oligonucleotide with 5' free end
HPF96	TTTTTTTTTTTTTTTTTTTTTTTTTTTAGATCCCCGG GTACCGAGCTCGAATTCGTAATCATATGATTACGA ATTCGAGCTCGGTACCCGGGGATC
hairpin oligonucleotide with 3' free end	
HPR96	CTAGGGGCCCATGGCTCGAGCTTAAGCATTAGTAT ACTAATGCTTAAGCTCGAGCCATGGGCCCCTAGAT TTTTTTTTTTTTTTTTTTTTTTTTT
hairpin single stranded region sequence	
HP45	TTTTTTTTTTTTTTTTTTTTTTTTTTTAGATCCCCG GGTACCGAG
EXO35 complement	
EXO35R	CAAGATACGCGAATACAAGAGCCAATGATTAA CTA
EXO35 hairpin	
EXO35HP	TAGTTAATCATTGGCTCTTGTATTCGCGTATCTTG CAAGATACGCGAATACAAGAGCCAATGATTAACT A

Table 2-2 continued.

gapped substrate with hairpin ends	
P115	GATCCGGTAGGCGTAATCATATGATTACGCCTACC GGATCTAGTTAATCATTGGCTCTTGTATTCGCGTAT CTTGGTCCGGACACCATCTATCATATGATAGATGG TGTCCGGAC
nicked and duplex substrate with hairpin ends	
P150	GAGCCAATGATTAACTAGATCCGGTAGGCGTAATC ATATGATTACGCCTACCGGATCTAGTTAATCATTG GCTCTTGTATTCGCGTATCTTGGTCCGGACACCAT CTATCATATGATAGATGGTGTCCGGACCAAGATAC GCGAATACA

CHAPTER 3

THE CHECKPOINT PROTEIN RAD9 HAS AN ASSOCIATED SINGLE-STRANDED DNA BINDING ACTIVITY.

Summary

In *S.cerevisiae*, the *RAD9* dependent DNA damage checkpoint response arrests cell cycle progression in G2 following DNA damage. This checkpoint dependent arrest allows time for DNA repair prior to mitosis. Genetic studies suggest that Rad9 functions in a separate DNA repair pathway. The finding that Rad24 was the only member of its genetic epistasis group that could bind to DNA suggested that it was the DNA damage sensor for its DNA repair pathway. This also suggested that Rad9 may be the DNA binding component of its repair pathway. Therefore, Rad9 was purified from yeast extracts and tested for DNA binding using mobility gel shift analysis.

Rad9 was found to have an associated DNA binding with a higher affinity for single-stranded DNA when compared to double-stranded DNA. Rad9 associated DNA binding activity also has a base composition preference that are similar to those observed for Rad24 associated DNA binding. The minimum single-stranded DNA substrate length that Rad9 binds is 20-25 nucleotides long, short enough to interact with the 29 base long ssDNA repair intermediate formed during UV excision repair.

Rad9 associated binding recognizes single-stranded DNA, a DNA repair intermediate structure that is formed during most DNA repair processes. Thus, Rad9 may also function as a direct sensor of the DNA substrate that activates the DNA damage checkpoint and function directly on DNA to mediate repair. This biochemical activity

indicates that Rad9 has a more direct role in DNA substrate recognition for the activation of the checkpoint response than previously thought.

Introduction

Cells must maintain their genomes to ensure their viability and that of their progeny. The extra-cellular environment exposes DNA to damaging agents in the form of UV and ionizing radiation. In addition, many DNA lesions occur due to intracellular activities that make mistakes. To prevent DNA mutations that may arise from damaged DNA, cells rely on DNA damage checkpoints to detect the DNA damage and arrest cell cycle progression to allow time for repair (Weinert et al., 1994).

Proteins involved in the DNA damage checkpoint response also have roles in DNA damage repair (Lydall and Weinert, 1995) In *S.cerevisiae*, several proteins required for the DNA damage checkpoint response have also been implicated as the initial sensors of DNA damage that trigger the checkpoint response. These potential sensor proteins are Ddc1, Lcd1, Mec1, Mec3, Rad9, Rad17, and Rad24. Only Lcd1 and Rad24 have been shown biochemically to have an associated DNA binding activity that would indicate they directly detect DNA damage (Rouse and Jackson, 2002b; Shiomi et al., 2002). Both Rad24 and the Rad24 human homolog Rad17 bind to single-stranded DNA (ssDNA), primer-template junctions, and bind with a lower affinity to double-stranded DNA (dsDNA) (This dissertation) (Lindsey-Boltz et al., 2001). Rad24 ssDNA binding activity suggests that it can detect the processing of DNA damage because ssDNA is a common intermediate for most DNA repair pathways(Garvik et al., 1995). Lcd1 has a high DNA binding affinity for dsDNA ends and a lower binding affinity for ssDNA(Rouse and Jackson, 2002b).

Genetic studies suggest that Rad9 functions in its own DNA repair pathway and may be able to detect DNA damage independently of Rad24 (Longhese et al., 1997; Lydall and Weinert, 1995). Epistasis analysis indicates that *RAD9* belongs to a separate epistasis group from that of *RAD24*. The *RAD24* epistasis group also contains the checkpoint genes *DDC1*, *MEC3* and *RAD17*, and suggests that these proteins function in an unknown DNA repair pathway. *RAD9* alone represents a separate epistasis group. Cells containing a mutant belonging to either the *RAD9* or *RAD24* epistasis groups are completely checkpoint defective, cells containing mutations from both epistasis groups are more sensitive to UV and alkylation damage than single mutants. This suggests that the Rad9 protein functions in a repair process that is independent of Rad24.

One potential model for the function of Rad9 is that it can detect DNA damage and regulate repair at sites of damage. In addition to being involved in DNA repair, Rad9 may also function in the checkpoint response to recruit checkpoint kinases to the DNA to activate the checkpoint. For example, Rad53 is thought to be localized to the DNA by Rad9 to transduce the checkpoint signal through phosphorylation of protein targets that function in cell cycle arrest and DNA repair.

Rad9 contains two BRCT domains located at its carboxy-terminus. The function of these two domains has been suggested to be in dimerization of Rad9 (Soulier and Lowndes, 1999). However, recent studies by Kara Nyberg (dissertation 2003) suggest that dimerization is not a requirement for checkpoint activation and that Rad9 dimerizes independent of DNA damage. Overexpression of a Rad9 protein lacking the two BRCT domains in a *rad9*Δ strain is proficient for cell cycle arrest following DNA damage.

These studies suggest that the BRCT domains of Rad9 serve to promote the local concentration of Rad9 at sites of DNA damage so as to activate the checkpoint. In addition it has also been suggested that the BRCT domains promote Rad9 protein stability and may also have a role in the negative regulation of Rad9.

To test whether Rad9, as a sensor protein, binds directly to DNA, the protein was purified from yeast extracts and binding activity was tested using mobility gel shift analysis. DNA substrates were designed to determine the specificity of Rad9 dependent DNA binding for various DNA structures found in the cell during DNA repair and replication. The characterization of Rad9 substrate specificity may aid in indicating the points at which DNA repair Rad9 functions to facilitate both DNA repair and activation of the damage checkpoint response.

Results

In Vivo Activity of GST-Rad9.

The Rad9 protein was amino-terminally fused to the GST epitope on a yeast expression vector downstream of a galactose-inducible promoter. To test whether the GST epitope interfered with the *in vivo* activity of *RAD9*, the fusion protein was tested for both its ability to restore the checkpoint arrest and for UV resistance in a *rad9*Δ background. GST-Rad9 checkpoint function was tested using the *cdc13-1* conditional mutant that allows ssDNA damage accumulation at telomeres at the restrictive temperature of 36°C, which activates the checkpoint response. As shown in Fig. 3-1 (A), the GST epitope does not interfere with the function of Rad9 in regard to cell cycle arrest following DNA damage. The same *rad9*Δ strain was then tested for the ability of GST-Rad9 to confer

UV resistance following exposure to increasing doses of UV radiation, (Fig. 3-1, B). Once again, the GST epitope did not interfere with the ability of GST-Rad9 to complement the UV sensitivity of *rad9*Δ. These data suggest that the GST-Rad9 fusion protein is functional and that the epitope tag does not inactivate Rad9 *in vivo*, and therefore suggest that the GST epitope would not interfere *in vitro* assays.

Overexpression and Purification of Rad9.

GST-Rad9 was overexpressed using galactose induction in a yeast strain that was deficient in multiple proteases to avoid degradation during cell lysis and protein purification. Nevertheless, GST-Rad9 was very unstable following cell lysis despite the fact that the lysate was buffered with protease inhibitors as shown by Coomassie Blue and western analysis, Fig. 3-2. The protein was then purified using non-denaturing affinity chromatography with a glutathione sepharose column. SDS polyacrylamide gel electrophoresis with Coomassie Blue staining indicated a protein of the correct molecular weight following purification. Western blot analysis using anti-GST antibodies confirmed the presence of the fusion protein. A 70kD contaminating protein co-purifies with the GST epitope alone and previous studies using this epitope in *E.coli* have reported the presence of a heat shock protein co-purifying with the epitope. However, no activity has been assigned to this protein.

GST-Rad9 binds to ssDNA.

Rad9 was tested for DNA binding activity using a 35-base long oligonucleotide substrate that was labeled with ^{32}P phosphate at the 5' end. The protein and substrate were incubated together and DNA binding activity was assayed using mobility gel shift

electrophoresis. As shown in Fig. 3A, a slower migrating band was seen in the reaction including GST-Rad9, but not with the GST epitope alone. In addition, the presence of the 5' phosphate is not required for Rad9-dependent binding as shown in Fig. 3-3, where the same DNA substrate was 3' labeled with ^{32}P and terminal transferase. Rad9 binds equally to either the 5' or 3' end labeled substrates.

In addition to the dominant band, another weaker band shift is seen migrating faster may be due to dimerization activity of Rad9. As previously mentioned, BRCT domains have been shown to function in Rad9-Rad9 interactions. The slower migrating band maybe due to binding of Rad9 to itself, whereas the faster migrating band may be a monomeric form of GST-Rad9 binding to DNA. To determine if this faster migrating band was due to Rad9 dimerization, GST-Rad9 was assayed by decreasing the protein concentration to favor the formation of monomers. However, no change was detected, suggesting that this faster migrating form may not be a monomeric form of Rad9 binding to the DNA (data not shown). Alternatively, this band may be a degradation product of Rad9 that forms during purification or an alternative conformation of Rad9 binding to the DNA. It is also possible that the decrease in concentration did not affect the potential Rad9 dimer, or the band may be caused by a contaminating protein.

GST-Rad9 Shows a Preference for Base Composition of DNA Substrates.

To determine if Rad9 contains DNA sequence or base composition specificity, competition assays were used with different substrates that were the same length as the initial substrate(Mazin and Kowalczykowski, 1996). However, the substrates used to compete with the heterologous substrate were engineered to contain only poly-dT, poly-

dC, or poly-dA. To perform the assay, the competing substrates were added in increasing concentrations to reactions containing a fixed concentration of the 5' ^{32}P labeled substrate. GST-Rad9 was added to each of these reactions at the same time, and the results are shown in Fig. 3-4. Rad9 associated binding activity has a low affinity for poly-dA, and a higher affinity for poly-dT and poly-dC. However, the protein DNA binding activity is not sequence specific as indicated by the ability of poly-dC to compete effectively with the ^{32}P labeled substrate. This is interesting given that adenine is a purine and thymine a pyrimidine and not considered to be structurally similar. Nevertheless, base composition bias has been noted among DNA binding proteins that function to bind to DNA structures such as RFC, Ku, and the recombination repair protein RecA(Dynan and Yoo, 1998; Mazin and Kowalczykowski, 1996; Tsurimoto and Stillman, 1991).

Minimum Binding Site Requirement for GST-Rad9.

UV excision repair produces a ssDNA gap approximately 29 nucleotides long, and during mismatch repair ssDNA gaps of varying length are also formed(Batty and Wood, 2000). Therefore, if Rad9 has a role in detecting the active UV repair through detection of an intermediate DNA repair structure, Rad9 may be required to bind a similar length of ssDNA. To characterize the minimal binding size required for GST-Rad9, competition assays were used with ssDNA substrates that varied by size. DNA substrates did not vary by sequence or base composition in order to avoid complicating the interpretation of the results. Poly-dC substrates that were 15, 20, 25 and 30 nucleotides in length were constructed for this assay. When these substrates were tested in a competition assay the

minimal binding size requirement appeared to be approximately 20 nucleotides in length, Fig. 3-5. This size requirement is similar to that found for GST-Rad24 and is within the size of the gap produced in UV excision repair. This suggests that Rad9 could bind the gapped DNA repair intermediate structure formed during UV repair.

GST-Rad9 has a higher affinity for ssDNA than dsDNA.

ssDNA is an intermediate DNA structure common to many damage repair pathways such as UV repair, mismatch repair, and recombination repair and has been suggested to be a substrate for the DNA damage checkpoint pathway. If Rad9 is a sensor for the DNA damage checkpoint pathway, then it too may bind to ssDNA to initiate the checkpoint. To determine the specificity of GST-Rad9 for ssDNA, a substrate competition assay was used with dsDNA and ssDNA. The dsDNA substrate was constructed to form a hairpin secondary structure via intramolecular interactions. The ssDNA substrates contained either the top or bottom strand sequences of the dsDNA hairpin substrate.

Previous studies have observed that the efficiency of pairing two separate oligonucleotides to form a single dsDNA substrate is not efficient and results in a high concentration of ssDNA substrate and a low concentration of dsDNA substrate(Naureckiene and Holloman, 1999). To circumvent this problem, a hairpin substrate was constructed that base-paired with itself to form dsDNA. The competition assay was designed as previously described for the base composition assay. GST-Rad9 associated DNA binding had almost no affinity for dsDNA as shown in, Fig 3-6.

GST-Rad9 Binds to Hairpin Substrates with Either 5' or 3' Overhangs.

ssDNA flanked by either 3' or 5' primer-template junctions are formed during a number of DNA processes such as DNA replication, recombination, and UV excision repair. To examine if Rad9 has an affinity for this type of DNA secondary structure, substrates were constructed that contained dsDNA hairpins with either 3' or 5' overhangs. However, the addition of a hairpin substrate that contained the 3' overhang was to test whether binding was specific to primer-templates, or whether Rad9 was able to bind to a substrate with the reverse directionality. The ssDNA overhang region of the hairpin was used as a control in the competition assay.

When assayed with these substrates, GST-Rad9 bound to both hairpin substrates with equal affinity and had a lower affinity for the ssDNA substrate, Fig. 3-7. These results can be interpreted in two ways. One interpretation is that GST-Rad9 binding has a higher degree for these secondary structures, and in the instance of a ssDNA gap would prefer to bind to the sides of the gap as opposed to the region of ssDNA. However GST-Rad9 displayed a low but measurable degree of affinity for dsDNA. A second interpretation may be that the dsDNA region of the hairpin substrates may allow them to be more attractive as substrates as opposed to the shorter ssDNA substrate

GST-Rad9 Has a Higher Affinity for Gapped Substrates.

DNA substrates that are completely double-stranded containing either a nick or a 35 base long gap were used to test whether the free ends of the substrates tested in this study are a factor in GST-Rad9 binding, Fig. 3-8. These structures had double-stranded hairpins in place of both 5' and 3' ends. When competed, GST-Rad9 had a higher affinity for the substrate containing the 35 base long ssDNA gap compared to the nicked or double-

stranded substrates. In this assay, the absence of ends did not appear to affect DNA binding, and once again GST-Rad9 had a higher preference for a substrate that contains a region of ssDNA. As previously observed, GST-Rad9 did not have a high affinity for dsDNA and also did not appear to have a high affinity for the presence of nicks in the DNA. These data suggest that although nicked DNA does occur in the cell, Rad9 is not able to detect it as efficiently as it does ssDNA.

Super-shift Analysis of Rad9 Dependent DNA binding.

To test for whether it was truly Rad9 binding to the DNA, super-shift analysis was performed by adding anti-GST antibody to the mobility gel reactions. However, no change in the mobility shift was observed for Rad9 reactions for similar reasons as mentioned for Rad24 super-shift assays in Chapter 2 (data not shown).

Discussion

The Rad9 protein is needed to signal the DNA damage checkpoint pathway. Rad9 is required to signal cell cycle arrest and also plays a role in DNA damage repair. It has been shown previously that *rad9*Δ cells are completely defective in the G2/M checkpoint pathway following DNA damage (Weinert and Hartwell, 1988). *RAD9* has been shown to function in a DNA repair pathway distinct from the *RAD24* epistasis group that includes Rad17 and Mec3(Lydall and Weinert, 1995). Cells that have mutations in both *RAD9* and any member of the Rad24 epistasis group are more sensitive to DNA damage, and yet each of these mutants is equally defective for the checkpoint pathway. Data based on the ssDNA damage produced in the *cdc13-1* mutant indicate that Rad9 has a role in the regulation of DNA processing (Garvik et al., 1995). *rad9* cells show rapid

accumulation of ssDNA at their telomeres, which is the opposite of what is found in *rad24* mutants that do not accumulate ssDNA at their telomeres (Lydall and Weinert, 1995). Genetic data that show the checkpoint kinases cannot activate the checkpoint signaling pathway in a *rad9*Δ strain suggest that Rad9 has an upstream role in signaling the checkpoint pathway, indicating some role for Rad9 as a possible sensor of DNA damage or its involvement in processing DNA (Navas et al., 1996; Sanchez et al., 1999).

To examine the potential biochemical activity of Rad9 as a direct sensor of DNA damage, Rad9 was overexpressed in yeast cells and purified using non-denaturing affinity chromatography. Substrate competition assays were used to determine what DNA structures Rad9 could bind to, and found that Rad9 had a high affinity for ssDNA and a minimal binding site requirement of 20 nucleotides. The minimal binding size requirement of Rad9 suggests that the protein could bind to the small gap of ssDNA produced during UV repair (Batty and Wood, 2000). In addition, Rad9 had a slightly higher affinity for hairpin substrates that form primer-template junctions, suggesting that it can also bind to the primer-templates formed during mismatch, UV, and recombination repair. The directionality of the primer-template substrate had no affect on Rad9 binding. Rad9 also showed no affinity for nicked DNA, further supporting that Rad9 binds to ssDNA. These data suggest that Rad9 does not does not detect DNA ligase substrates. Therefore, Rad9 may simply bind the common DNA structure that is formed in several DNA repair pathways.

Rad9 associated DNA binding has a similar base composition preference when compared to Rad24. Rad9 has a low affinity for poly-dA, and a higher affinity for poly-

dC and poly-dT substrates. The function these base composition preferences serve for the checkpoint is unknown. However, base composition preferences by proteins that function in DNA repair or replication have been observed. The recombinational repair protein RecA and the replication protein complex RFC have base composition preferences (Mazin and Kowalczykowski, 1996; Tsurimoto and Stillman, 1991).

That Rad9 has an associated DNA binding activity independent of Rad24 suggests that Rad9 may be able to localize to sites of DNA damage independent of other checkpoint proteins. Genetic data supports a model in which Rad9 functions in a repair process separate from Rad 24. Therefore, Rad9 may recruit a subset of repair proteins to the DNA to promote repair and the checkpoint response processes. However, it is unknown what purpose the two different types of repair serve in connection with the singular checkpoint response except, for example, to have an alternative repair process if the initial repair process was not able to fully repair the DNA damage. The requirement of the cell to have to checkpoint repair processes may also reflect the complexity of DNA lesions that result from UV and MMS damage.

Materials and Methods

Yeast strains and media.

Standard media conditions were used that included yeast extract-peptone and 2% dextrose (YEPD) and –ura dropout media for strains containing plasmids(Sherman, 1986).

Checkpoint mutants strains used in this study are isogenic with W303 and constructed using standard genetic techniques (Table 2-1). The *rad9*Δ mutation has been

previously described (Weinert and Hartwell, 1993). The *cdc13-1* and *cdc15-2* have been used in previous studies ((Gardner et al., 1999; Lydall and Weinert, 1995). The protease deficient strain containing *pep4*, *prb1*, and *prc1* came from A.Adams. Yeast transformations were performed according to the LiAc TRAFO method (Schiestl and Gietz, 1989).

Plasmid constructions.

To construct plasmid ELP17 a *GST* containing fragment was PCR amplified from DL-C209 using the primers BGST5, 5'CAGGAAACAGGATCCATGTCCCCTA3' and NGST3, 5'CTTTGGCATATGCGGCGATCC3'. The *GST* BamHI-NdeI fragment was fused to the *GAL1* gene within the DLC-218 polylinker (Lydall and Weinert, 1997). DLC-218 is based on the pRS416 vector. The ELP40 *GST-RAD9* fusion plasmid was constructed by fusing a NdeI-NotI *RAD9* containing fragment downstream of the *GST* gene in ELP17.

G2/M cell cycle arrest assaying using *cdc13-1* DNA damage induction.

G2/M cycle arrest assays were performed as described (Lydall and Weinert, 1995). Yeast cells containing plasmids were grown for two days at 30°C in -ura dropout media and 2% raffinose. Overnight cultures were inoculated 1:50 dilution into -ura dropout media and 2% raffinose at 30°C. The following day cells were checked for cell density with a hemocytometer. Cells were counted as follows: one cell was counted as one and a budded cell counted as two. Cultures were adjusted to $6x10^6$ cells/ml if the cultures had not grown past $1.5x10^7$. α-factor (Sigma; St. Louis, MO) was then added to a final concentration of 20n*M*, except in the case of ddc1Δ cells which did not contain the bar1

mutation in which case the α-factor final concentration was 400n*M*. Cells were washed starting at t= -40 minutes to the zero time point and resuspended into YEP and 2% galactose media. At the zero time point cells were shifted to 36°C the restrictive temperature for *cdc13-1* and *cdc15-2*. Aliquots of the cultures were taken at the designated time points and fixed by adding 0.5 mls of cell culture to 1 ml 95% ethanol. Cell cycle arrest assays were quantitated by analyzing the nuclei of the cells to determine if nuclear division has occurred resulting in two nuclei or if the G2/M checkpoint had been activated resulting in one visible nucleus. Nuclear morphologies were quantitated by scoring at least 100 cells that had been stained with 4,6-diamino-2-phenylindole (DAP1, 0,2 μg/ml) (Pringle et al., 1989) and visualized with a fluorescent microscope.

Cell survival following UV exposure.

Saturated cultures were grown as previously described in the section on cell cycle arrest assay. Cell cultures were adjusted to $2x10^6$ cells/ml grown for 6 hours with shaking at 23°C. Cells cultures were then adjusted to a final concentration of 2000 cells/ml. Duplicate 100μl aliquot were then plated in duplicate on YEPD agarose plates and the plates were allowed time to dry (approx. 20 min.). Plated cells were then exposed to appropriate does of UVC using a Stratalinker 1800. The plates were then incubated at 23°C for and counted on day 3 to determine viability. A control plate that had not been exposed to UVC defined 100% viability.

Protein preparation.

Protease deficient yeast cells containing plasmids were grown for two days at 30°C in 5.5 mls -ura dropout media and 2% raffinose. Eleven mls of saturated culture was inoculated

into 1 liter of -ura and 2% raffinose and allowed to grow to midlog at 30°C with vigorous shaking. Once cells had reached midlog (4-6x10^6 cells/ml), protein expression was induced with 2% for 6 hours. Cells were pelleted, resuspended in 50% glycerol, flash frozen using liquid nitrogen, and stored in 50ml Falcon tubes at –70°C. Cell pellets were thawed on ice, pelleted, and resuspended in 4x the volume of the pellet of lysis buffer was added (50mM Tris-HCl [pH 7.4], 100mM NaCl, 2mM EDTA,1% NP-40, 1mM 2-mercaptoethanol, Aprotinin 2μg/ml, Leupeptin 2μg/ml, Pepstatin 1μg/ml). An equal volume to the lysis buffer of glass beads was added and cells lysed by vortexing at 4°C. Glass beads were washed with lysis buffer and the wash added to the supernatant. Cell lysates were clarified by centrifugation at 10,000 x g and then passed over glutathione cellulose (Pharmacia) column (200μl bed volume) twice. Columns were washed with 10 column volumes with lysis buffer and GST fusion proteins eluted using elution buffer (30mM Hepes-K+[pH7.8], 7mM $MgCl_2$, 0.5 mM DTT, 10mM reduced glutathione).

Western blotting.

Protein preparations were separated on SDS-polyacrylamide gel electrophoresis (PAGE) of either 7.5% or 10% acrylamide concentration. The bis-acrylamide/acrylamide ratio was 1:37.5 respectively. Proteins were then electroblotted to nitrocellulose membrane and blocked for 1 hour in blocking solution (PBS-T and 5% w/v powder non-fat dry milk). The membranes were then washed once with PBS-T and then incubated for 1 hour with primary goat anti-GST antibody (Pharmacia) at a 1:2000 dilution in PBS-T and 2.5% w/v powdered non-fat dry milk. Blots were then washed 3 times for 5 minutes each wash with PBS-T and then incubated for 1 hour with rabbit anti-goat HRP

conjugated secondary antibody (Sigma) in PBS-T and 0.3% w/v powder non-fat dry milk. The blots were then washed 3 times for 5 minutes each wash with PBS-T. Pierce Super Signal chemilumenescent substrate was used to detect the proteins.

Gel mobility shift assays.

Gel mobility shift assays contained 200-400ng of fusion protein,30mM Hepes-K (pH7.8), 7mM $MgCl_2$, 0.5 mM DTT, 10mg/ml BSA, 20mM EDTA, 100mM NaCl, and 4fmoles of DNA substrate P^{32} labeled with Polynucleotide-Kinase (Roche Applied Science) in a 40μl volume. Reactions were incubated at 30°C for 20min and loaded onto a 5% acrylamide gel. Gels were dried onto Whatman paper and analyzed using a Molecular Dynamics 445 S1 PhoshporImager and the IP Lab Gel H program. Super shift assays were performed by adding 1μl of goat anti-GST antibody (Pharmacia) to mobility shift reactions and run on non-denaturing gels.

Figure 3-1. Complementation of both cell cycle arrest defect and UV senstivity of a *rad9Δ* strain by the GST-Rad9 fusion protein. (A) GST-Rad9 for the most part restores the cell cycle arrest defect of a *rad9Δ* strain following *cdc13-1* DNA damage. (B) GST-Rad9 fully restores UV tolerance in a *rad9Δ* strain.

A.

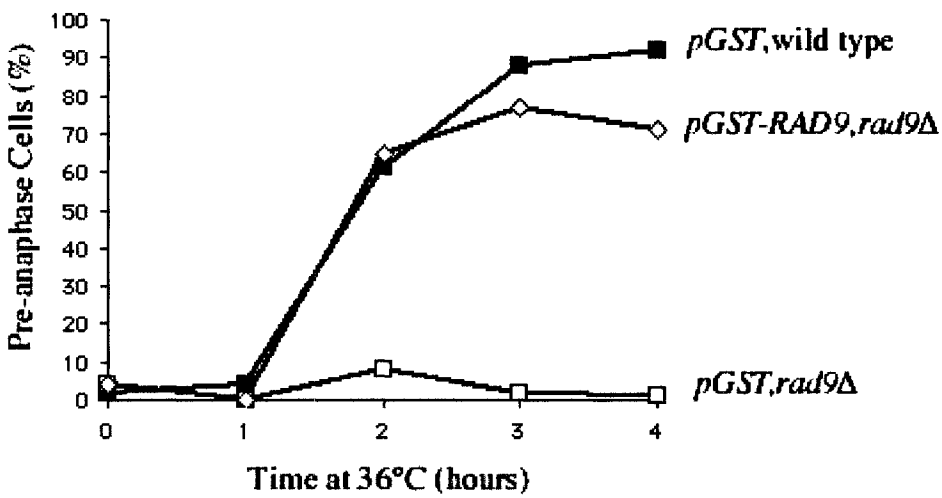

B.

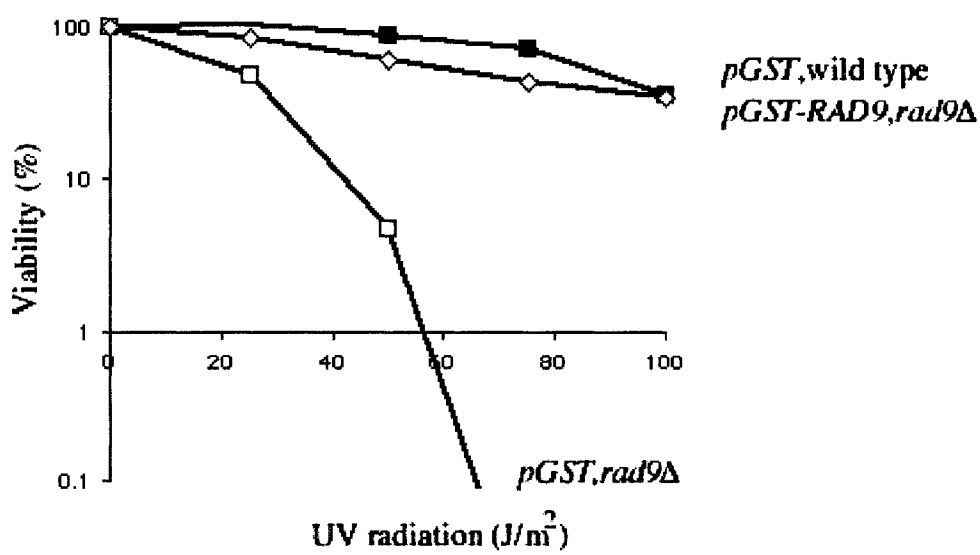

Figure 3-2. GST purification of recombinant Rad9. Proteins were separated by SDS/PAGE and stained with Coomassie blue. Size of molecular weight markers are indicated. Western blot with antibodies specific for the GST epitope is shown. Asterisks indicate unknown proteins that co-purify with the GST tag alone.

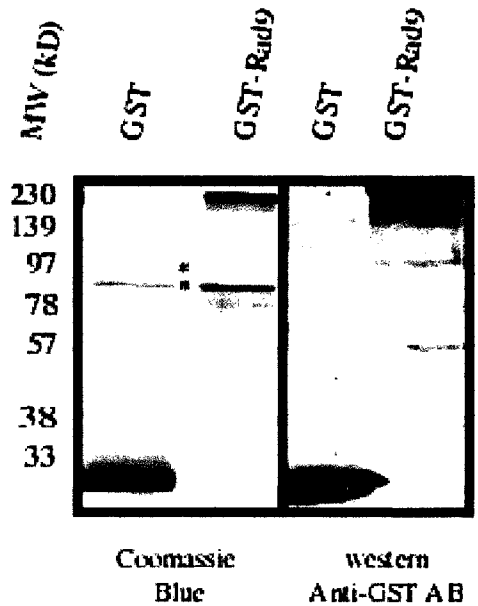

Figure 3-3. Rad9-dependent DNA binding does not require the presence of a 5' phosphate to bind to a single stranded DNA substrate. DNA probes were 5' phosphorylated with polynucleotide kinase and ^{32}P, or 3' end labeled with terminal transferase and ^{32}P. GST protein preparations do not bind to either probe (lanes 1 and 3). The GST-Rad9 protein preparation binds to both the 5' end labeled and 3' end labeled substrates (lanes 2 and 4).

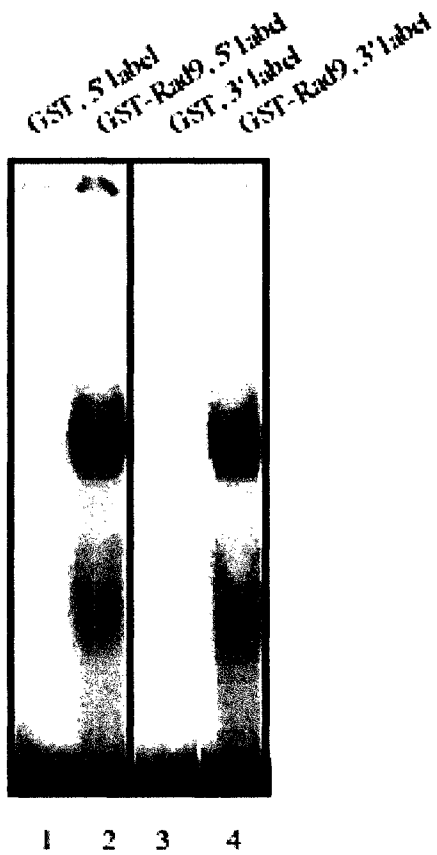

Figure 3-4. Rad9 dependent DNA binding preference hierarchy. (A) Gel mobility shifts were performed using ^{32}P labeled single stranded DNA substrate with varying amounts of unlabeled competitor DNAs present at the start of the reactions. Poly-dA DNA was added in lanes 2-5, poly-dT DNA was added in lanes 7-10, linear poly-dC DNA was added in lanes 12-15, and identical linear DNA was added in lanes 17-18. The amounts of competitor varied from no competitor to 10-fold excess of labeled DNA.

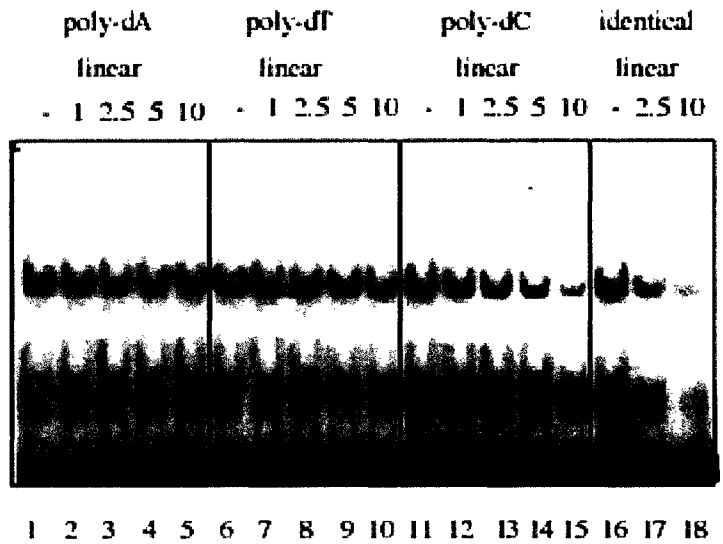

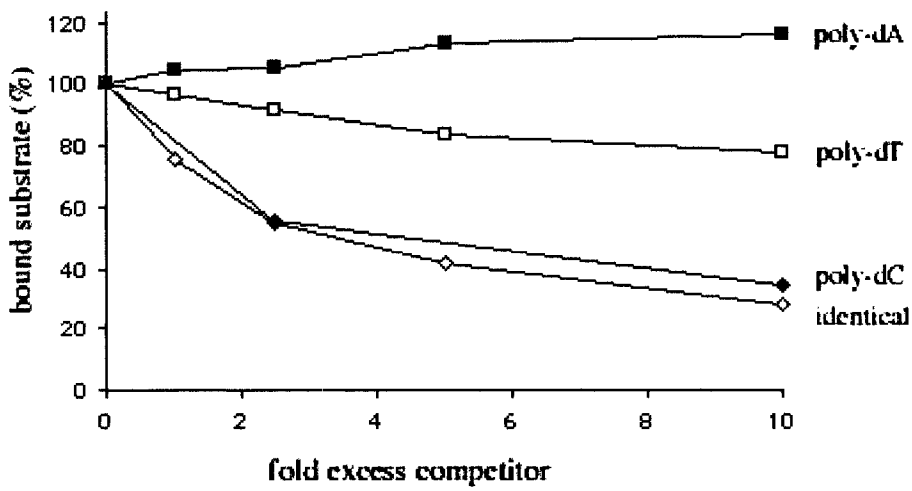

Figure 3-5. Rad9-dependent DNA binding has a substrate size preference. (A) Gel mobility shifts were performed using a heterologous 35 base long ^{32}P labeled substrate. Unlabeled competitor DNAs varied only by length and were only constructed with poly-dC. Linear 15 base long poly-dC DNA was added in lanes 2-5, 20 base long poly-dC DNA was added in lanes 6-9, 25 base long poly-dC DNA was added in lanes 11-14, and 30 base long poly-dC DNA was added in lanes 15-18. (B) Quantitative analysis of Rad9 dependent DNA binding to linear DNA of varying lengths in the presence of competitor DNAs.

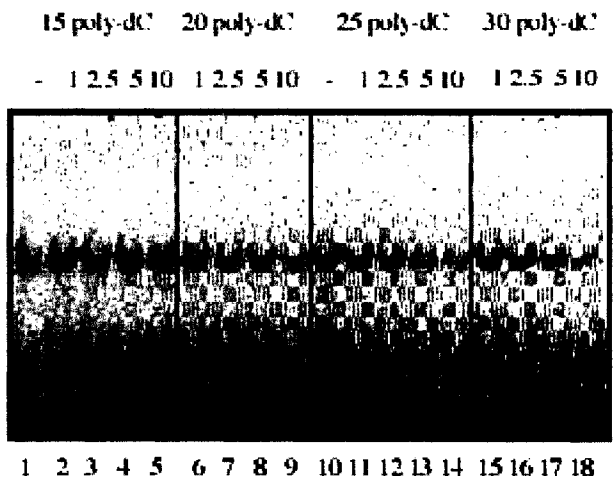

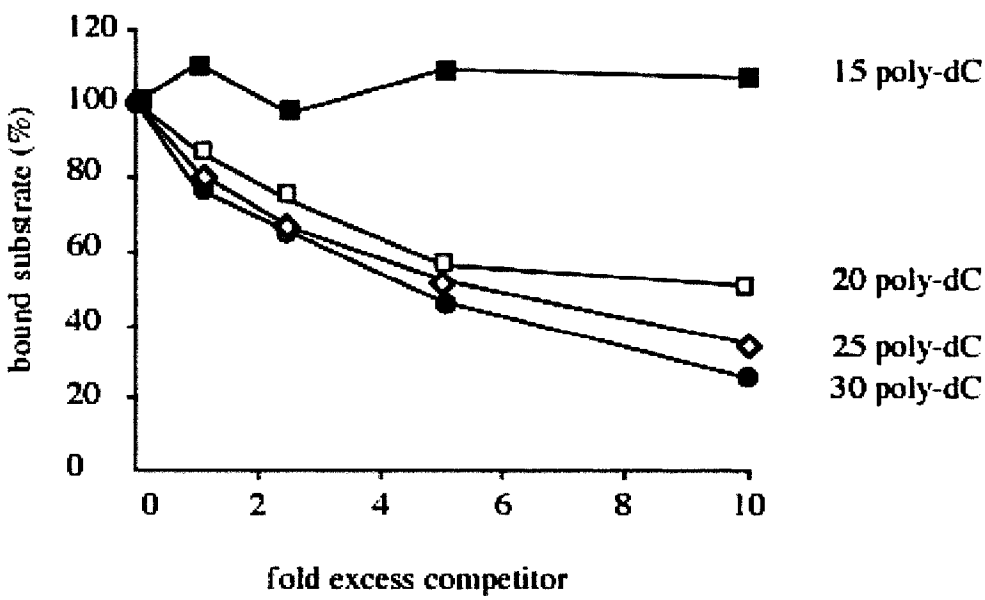

Figure 3-6. Rad9 dependent DNA binding has a lower affinity for duplex DNA. (A) Gel mobility shifts were performed using ^{32}P labeled idential linear substrate. Unlabeled competitor DNA was identical, complementary, or duplexed in sequence and structure of the labeled substrate. Duplex DNA was formed through intra-molecular interactions and formed a hairpin structure. Identical linear competitor DNA was added in lanes 2-5, complementary linear DNA lanes 7-10, and hairpin DNA lanes 12-15. (B) Quantitative analysis of Rad9 dependent DNA binding to linear DNA in the presence of competitor DNAs.

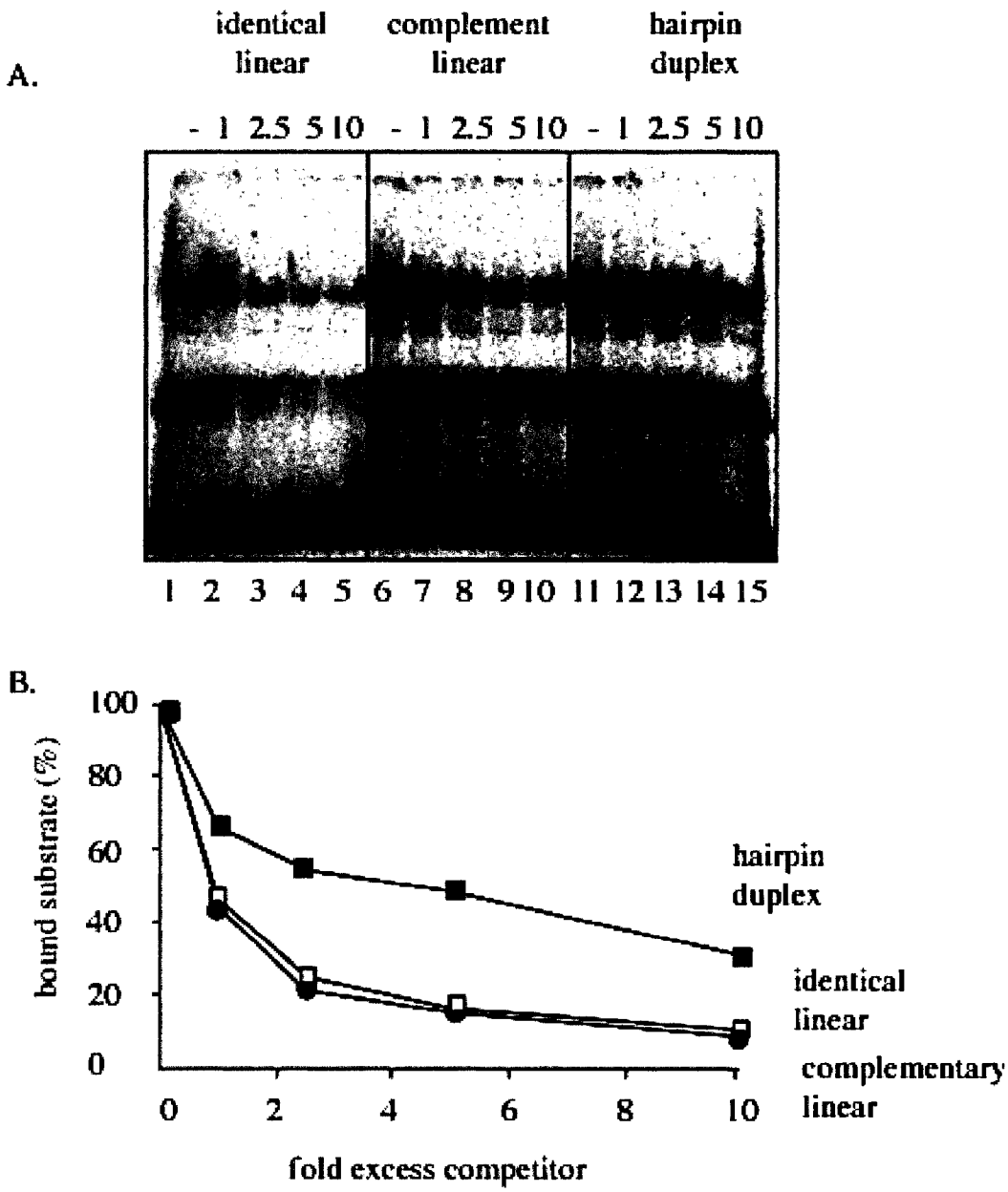

Figure 3-7. Rad9 dependent DNA binding activity is unaffected by secondary DNA hairpin structures. Gel mobility shifts were performed using ^{32}P labeled linear substrate not identical to the linear unlabeled competitor DNA. Linear competitor DNA is the same length and sequence as the ssDNA regions of the hairpin substrates, and the same directionality as the 5' free end hairpin substrate. The amounts of competitor varied from no competitor to 10 fold excess of the concentration of labeled DNA. Quantitative analysis of the reactions performed is shown below.

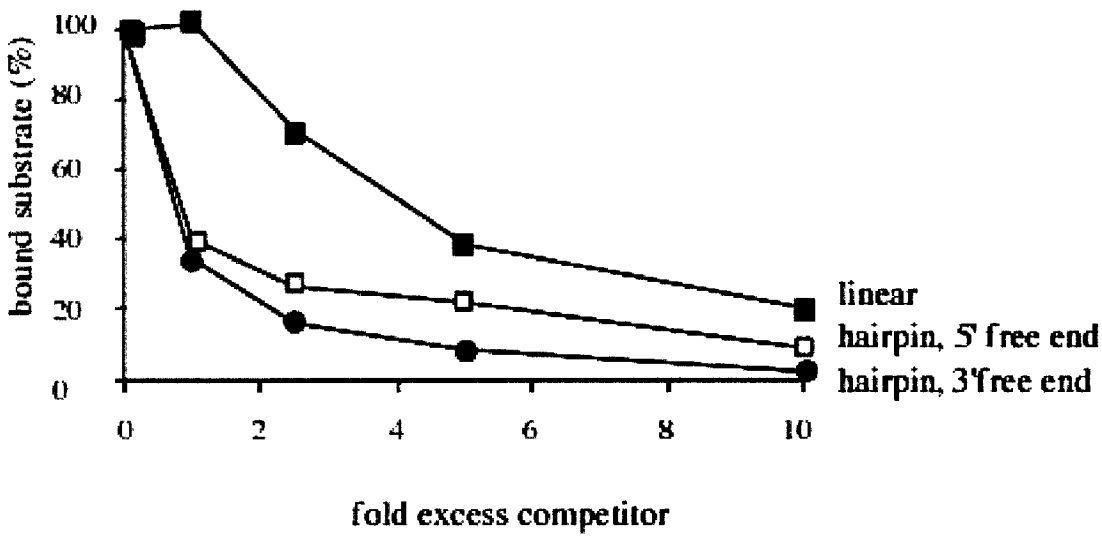

Figure 3-8. Rad9 dependent DNA binding does not bind to nicked or duplex DNA. (A) Gel mobility shifts were performed using the 35 base long ^{32}P labeled heterologous substrate. Unlabeled competitor DNA containing a nick, gap or duplex contain two hairpin structures instead of dsDNA ends. Linear DNA was added in lanes 2-5, gapped DNA in lanes 7-11, nicked DNA in lanes 12-15, and duplex DNA in lanes 17-20. (B) Quantitative analysis of Rad9 dependent binding to DNA substrates with varying secondary DNA structures.

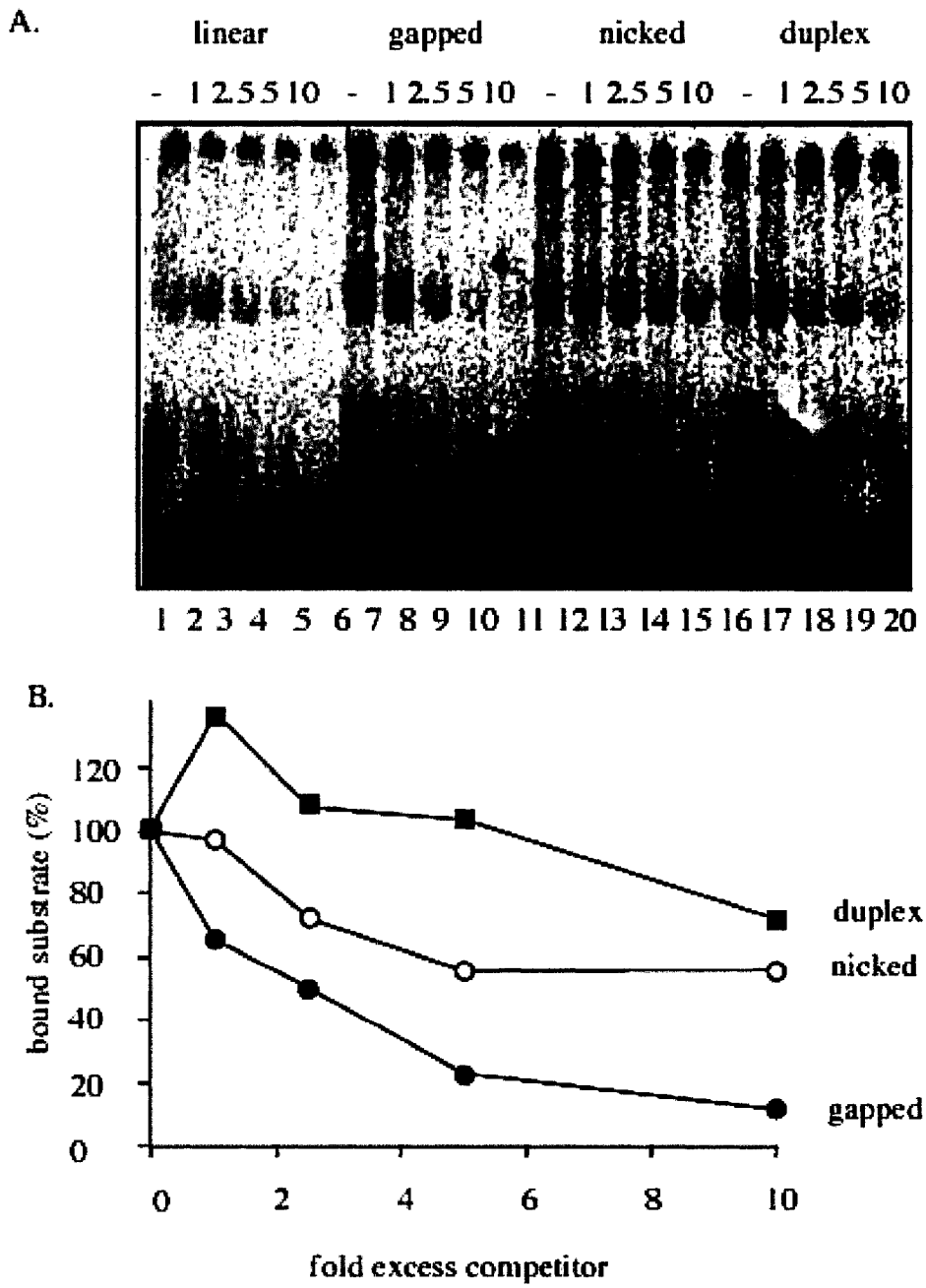

CHAPTER 4

THE CHECKPOINT PROTEIN RAD17 HAS NO SUBSTANTIAL EXONUCLEASE ACTIVITY.

Summary

The *Saccharomyces cerevisiae* protein Rad17 is required for the DNA damage checkpoint response and has previously been shown to function in DNA repair following UV or alkylation DNA damage. Rad17 has been reported to be homologous to Rec1, a 3'->5' exonuclease from *Ustilago maydis*, and may also be an exonuclease. To directly test whether Rad17 is an exonuclease, the protein was purified from yeast extracts using non-denaturing conditions, and DNA degradation assays were performed with DNA substrates of varying DNA secondary structures.

In this study, low nuclease activity was associated with Rad17 protein preparations. Unexpectedly, low nuclease activity was also associated with the checkpoint proteins Ddc1, Mec3 and Rad24. This suggests that these proteins potentially associate with an exonuclease, as Ddc1, Mec3 and Rad24 have no reported homology to nucleases. On the contrary, Rad17, Mec3, and Ddc1 are homologous to the replication protein proliferating nuclear antigen (PCNA) and Rad 24 is homologous to replication factor C (RFC) proteins which recruit PCNA to primer-template junctions for the purpose the DNA replication. Therefore, it is not surprising Ddc1, Mec3, Rad17 and Rad24 may possibly interact with and co-purify with an exonuclease such as a polymerase with a 3'->5' proofreading exonuclease activity.

Introduction

Cells stop progressing through their cell cycle following DNA damage due to activation of the DNA damage checkpoint response. The DNA damage checkpoint provides time for DNA repair processes to function and as a result prevents the accumulation of mutations. A large number of proteins required for the checkpoint response have been identified, and information about how these proteins function in the checkpoint response has come from studies done using the model organism *S. cerevisiae*. Briefly, the current model of DNA damage checkpoint pathway activation begins with initiation of the response by protein sensors that directly detect DNA damage. Subsequently, the cell cycle is signaled through kinases that act upon the targets of the checkpoint response to stop cell cycle progression.

The four checkpoint proteins Ddc1, Mec3, Rad17, and Rad24 that are thought to serve as sensors of DNA damage for the DNA damage checkpoint in *S.cerevisiae* are homologous to replication proteins (Lydall and Weinert, 1997; Venclovas and Thelen, 2000). These homology data suggest that these checkpoint proteins may function similarly to their replication homologs. Rad24 has been shown to be homologous to, and function similarly to, RFC proteins. RFC is known as the DNA clamp loader that binds to DNA primer-template junctions to load the replication protein PCNA onto DNA as one of the initiating steps of DNA replication (Waga and Stillman, 1998). Interestingly, the checkpoint proteins Ddc1, Mec3 and Rad17 are homologous to PCNA and form a trimeric protein complex(Kondo et al., 1999).

Homology data also suggest that Rad17 is a 3'->5' exonuclease(Lydall and Weinert, 1995). The Rad17 homolog Rec1 from *Ustilago maydis*, and the human homolog hRad1 have reported exonuclease activities (Parker et al., 1998; Thelen et al., 1994). However, it is not known what function these exonuclease activities serve in the cell. One model suggests that these exonucleases degrade DNA to form a DNA substrate for other checkpoint proteins to bind and activate the checkpoint response. Interestingly, Rad17 itself has not been found to be an exonuclease and a second study characterizing hRad1 reported no detectable exonuclease activity from purified hRad1 protein (Freire et al., 1998).

One reason why Rad17 exonuclease activity has not been observed may be that Rad17 requires other proteins to be a functional exonuclease. Other checkpoint proteins may stabilize Rad17 during purification, whereas Rec1 is more stable during the protein purification process and does not require other proteins for exonuclease activity. Genetic data suggests that the checkpoint proteins Ddc1, Mec3, and Rad24 may have an affect on Rad17 exonuclease activity because they belong to the same genetic epistasis group (Longhese et al., 1997; Lydall and Weinert, 1995). Biochemical analysis has also shown that Ddc1 and Mec3 directly interact with Rad17 and together Ddc1, Mec3 and Rad17 form a hetero-trimeric complex (Kondo et al., 1999). Interestingly, Rec1 is an exonuclease when purified as a monomeric protein, and does not require other proteins for its activity(Thelen et al., 1994). However, Rec1 may be able to assemble into a homo-trimeric complex similar to PCNA following purification and perhaps requires DNA interactions to form a complex with itself.

Further data that support the model that Ddc1, Mec3 and Rad17 physically function together in a protein complex come from protein sequence analysis that suggests that all three checkpoint proteins have a low degree of homology to PCNA and to each other(Venclovas and Thelen, 2000). Protein sequence analysis suggests that these proteins can form a toroidal protein structure similar to PCNA. The function of PCNA is to load DNA polymerase onto DNA and promote its processivity during replication(Tsurimoto, 1998). Therefore, a model that emerges that combines both the PCNA modeling and exonuclease activity is one in which the Ddc1/Mec3/Rad17 complex also encircles the DNA. In this model, DNA would move through the hole in the Ddc1/Mec3/Rad17 structure complex to be degraded. Precedence for an exonuclease that forms a toroidal structure comes from lambda exonuclease in which double-stranded DNA (dsDNA) is threaded through the protein structure and the 5'->3' strand is degraded(Kovall and Matthews, 1997). The 3'->5' strand then exits though the back of the lambda exonuclease as a potential substrate for recombination(Kowalczykowski et al., 1994). However, lambda exonuclease has not been shown to be homologous to Ddc1, Mec3, Rad17 or PCNA. Indeed, while the overall structure of PCNA and lambda exonuclease is toroidal, the secondary structures within the molecules are quite different.

In this study, Rad17 was initially tested for exonuclease activity without the presence of other checkpoint proteins using assay conditions similar to those used to characterize Rec1 exonuclease activity(Thelen et al., 1994). However, assays testing for Rad17 exonuclease activity revealed a low level of exonuclease activity. Therefore, Ddc1, Mec3 and Rad24 were tested for their effect on Rad17 exonuclease activity.

Multiple DNA substrates were tested to determine if different DNA secondary structures would stimulate Rad17 exonuclease activity.

Results

Rad17 was purified using the GST epitope tag system.

Both Rec1 and Rad17 are insoluble when over-expressed in bacteria with the intention of purifying them for exonuclease assays. Rec1 can be refolded into a soluble form by first solubilizing it with guanidine-Cl denaturing conditions and then gradually dialyzing away the guanidine. Problematically, when this technique was used to solubilize and refold Rad17 the protein precipitated during dialysis. To circumvent this problem we chose to purify Rad17, from yeast using the glutathione S-transferase (GST) epitope tag. The glutathione S-transferase purification method has several advantages. GST is an enzyme that binds to glutathione sepharose with a high affinity and can be eluted using mild elution conditions that decreases the probability of protein aggregation.

The over-expression of GST fusion proteins in yeast was chosen for several reasons. First, expression of yeast proteins in yeast allows for post-translational processing such as phosphorylation to occur(Leroy et al., 1994; Mitchell et al., 1993). Secondly, should the presence of other proteins be necessary for the activity of a protein, these proteins would be able to interact inside the cell and then co-purify with the protein of interest(Leroy et al., 1994). And thirdly, it is common for proteins that are insoluble when expressed in bacteria to be soluble when expressed in yeast(Mitchell et al., 1993).

GST-Rad17 was over-expressed in a protease deficient yeast background. Yeast cells containing GST-Rad17 were grown to mid-log and over-expression was induced

using 2% galactose. Cells were harvested by centrifugation, lysed with glass beads in the presence of protease inhibitors, and the protein isolated using affinity chromatography. As shown in Fig. 1-5, this method was successful in the recovery of GST-Rad17 from yeast. Both Coomassie blue staining and Western blot analysis using anti-GST antibodies confirmed the presence of the protein with the predicted molecular weight of 72kDa.

An unidentified protein co-purifies with the GST epitope and GST-Rad17 when the protein samples are analyzed using Coomassie blue or silver stain. Therefore, the GST protein preparation was tested as a control for any potential exonuclease activity from this unknown protein or other co-purifying proteins not detected by Coomassie blue protein gel staining.

GST-Rad17 was tested for exonuclease activity using varying buffering conditions. No exonuclease activity was detected for GST-Rad17 when initially tested by D.Lydall using similar buffering conditions and DNA substrate as had been successful for characterizing Rec1 exonuclease activity. This was not unexpected due to the low degree of homology, which suggests that Rad17 and Rec1 may function differently. Therefore, different buffering conditions and DNA substrates were tested for their effects on potential exonuclease activity.

The DNA substrate chosen to test for exonuclease activity was single-stranded DNA synthesized using PCR with labeled αAMP^{32}, and unlabeled dTTP, dCTP and dGTP. The ssDNA substrate made it possible to detect any exonuclease activity, whether it be 3'->5' or 5'->3' and can detect weak exonuclease activity because the substrate is

labeled along the entire length of the DNA as opposed to only the 5' end. For example, if Rad17 is a 3'->5' exonuclease, it would be required to degrade the entire length of a substrate to free the 5' end labeled nucleotide when measured by trichloroacetic acid precipitation (TCA). Therefore it would be difficult to detect 3'->5' exonuclease activity if the exonuclease has low processivity or slow nucleolytic activity. Because Rec1 has a higher preference for ssDNA over dsDNA, the PCR product was heat-denatured to disrupt the DNA duplex in the same manner as the ssDNA substrate used in Rec1 exonuclease assays (Thelen et al., 1994).

GST-Rad17 exonuclease activity was assayed using different buffering systems and pH levels with the ^{32}P labeled ssDNA substrate. Rec1 is only half as active at pH7 as at pH9, therefore pH and also buffering conditions were tested for their effect on potential Rad17 exonuclease activity. Both GST and GST-Rad17 were purified, incubated with the DNA substrate and exonuclease activity measured using TCA precipitation. ExoIII was used as a control because it is commercially available, and is useful as a control for the effectiveness of the TCA precipitation. As shown in Table 4-1, when compared with the robust activity of ExoIII, Rad17 displayed weak exonuclease activity when assayed using Tris-acetate at pH 8 and Tris-chloride at pH 9. When the exonuclease assay was repeated, GST-Rad17 exonuclease activity was once again observed using Tris-acetate buffering conditions at pH 8, Table 4-2 (A). In addition, an increase in the concentration of GST-Rad17 but not the GST epitope in exonuclease reactions resulted in an increase in exonuclease activity only in the GST-Rad17 reaction,

Table 4-2 (B). However this assay had difficulty detecting exonuclease activity over the control background signal.

The presence of DNA secondary structures in the substrates tested did not result in DNA exonuclease activity from GST-Rad17, GST-Rad24, GST-Ddc1 and GST-Mec3.

Genetic data suggest that Rad17 may require the checkpoint proteins Ddc1, Mec3 or Rad24, or all three for exonuclease activity. As previously mentioned, the *RAD24* epistasis group includes *DDC1*, *MEC3*, and *RAD17*, suggesting that they function in the same cellular process. Ddc1, Mec3 and Rad17 have been shown to physically interact with each other. To test this, Ddc1-, Mec3- and Rad24-GST fusion proteins were overexpressed and purified from yeast as previously described for GST-Rad17, and the results of the purification are shown in Fig. 1-5. Both Coomassie and Western analysis confirmed the identity of the proteins at their predicted molecular weights.

In addition to testing for the effect that the presence of other checkpoint proteins may have on Rad17 exonuclease activity, a DNA substrate was designed to test the effects that various secondary DNA structures may have on Rad17 exonuclease activity. This substrate contained several secondary DNA structures that the checkpoint proteins may encounter in the cell. Listed in Table 4-3, and shown in Fig. 4-1, the substrate was constructed using three polynucleotides and formed a ssDNA gap 20 nucleotides wide, similar to the gap formed when nucleotide excision repair is activated. In addition, this gapped substrate offered a blunt end, which is relevant in regards to non-homologous end joining DNA repair. The three oligonucleotides were labeled with ^{32}P at the 5' ends,

boiled to disrupt non-specific interactions, and slowly cooled to room temperature to promote specific intermolecular interactions in formation of the substrate.

The checkpoint proteins were then tested either alone or in combination for exonuclease activity using this DNA substrate. Protein preparations were incubated with the gapped DNA substrate using the previously mentioned exonuclease conditions, and the products of the reaction were analyzed using denaturing gels. The use of denaturing gels allowed for the detection of any potential endonucleolytic activity. Exonucleases and endonuclease have been shown to be homologous in bacteria. For example, lambda phage exonuclease is distantly related to the endonucleases EcoRV and PvuIII(Kovall and Matthews, 1998). Single stranded binding protein (SSB) was included in this assay because the reactions were also tested in parallel for DNA binding activity (Fig. 4-2). A low overall exonuclease activity is detected in all of the samples, and when the four protein samples are added together the result is only the level of exonuclease activity from of all four background levels added together. It should be noted that the gel in Figure 4-2 was warped during fixation and transfer to Wattman paper. The bottom lanes are marked that correspond with the wells at the top of the gel. The sizes of degradation products were not determined. The exonuclease activity from this assay demonstrates that there did not appear to be any synergistic exonuclease activity among the proteins, and that the overall exonuclease activity detected was not above background levels.

The effect of NaCl on exonuclease activity was also tested because the assay for exonuclease activity did not contain NaCl in the conditions used for Rec1 exonuclease assays. The presence of NaCl increased the exonuclease activity observed in these

reactions (Lane 10 of Fig. 4-2). This could be from either a direct effect on the exonuclease activity or the presence of the NaCl promoting a more stabilizing buffering condition for the gapped substrate. The absence of salt in the reactions may have had a negative affect on the ability of the oligonucleotides to form the gapped substrate by destabilizing duplex formation, although the substrates were formed initially in the presence of NaCl, which was then removed.

To determine if there was a preferential degradation of the three oligonucleotides, each of the three was labeled and incorporated into the gapped substrate (Fig.4-2, lanes 11,12 and 13). Of the three oligonucleotides, only the 80 and the 22 oligonucleotides were degraded. The common structure or sequence of these two oligonucleotides that promotes exonuclease activity is unclear. Perhaps the presence of single stranded DNA near the 5' end, regardless of directionality, is able to promote exonuclease activity. Because no degradation ladder is apparent, the directionality of the exonuclease activity is thought to be 5' to 3'. However, if the exonuclease is a 3'->5' exonuclease with an affinity for 3' ends, it would only degrade the 22 and the 80, not the 35. The interpretation of these assays is complicated because the formation of the gapped substrate using the three oligonucleotides may be inefficient, and the actual concentration of the fully formed gapped substrate was probably low.

Exonuclease activity was tested using hairpin substrates.

Ddc1, Mec3, and Rad17 were tested for exonuclease activity using oligonucleotide substrates that formed hairpin secondary DNA structures intra-molecularly. Precedence for testing exonuclease activity using this type of DNA substrate comes from Rec1

studies that tested Rec1 substrate specificity using different forms of oligonucleotide substrates and found that exonuclease activity increase when tested with a hairpin substrate that contained a 3' recessed end (Naureckiene and Holloman, 1999). Rec1 exonuclease assays included self-annealing oligonucleotides as substrates to further characterize the exonuclease activity of Rec1. These substrates provide several advantages over DNA substrates constructed using single stranded oligonucleotides to form secondary DNA structures such as double stranded DNA substrates and hairpins. Primarily, substrates that are constructed based on inter-molecular interactions have been shown to yield low amounts of duplexed oligonucleotides when incubated together in equimolar amounts. In addition, since intramolecular association is the preferred reaction, DNA duplex formation is equimolar without excess single stranded oligonucleotides that complicate the interpretations of the assay results. Interestingly, Rec1 has a higher preference for ssDNA over dsDNA in exonuclease assays that use substrates that use intra-molecular interactions to form DNA structures when compared to exonuclease assays that use either vector DNA as a dsDNA substrate and heat denatured vector DNA as a ssDNA substrate.

Rec1 has a preference for 3' recessed ends in exonuclease assays using hairpin substrates and Rad17 is expected to have the same substrate specificity as its *U.maydis* homolog. Therefore, the low exonuclease activity detected in Ddc1, Mec3, and Rad17 exonuclease assays may be stronger using a different DNA substrate. To test this, Ddc1, Mec3, and Rad17 were assayed for exonuclease activity using DNA hairpins with 3' or 5' recessed ends with identical sequences. The substrates were 5' labeled with ^{32}P using

polynucleotide kinase, boiled at 100°C for five minutes, and slowly cooled to room temperature to promote the annealing of the DNA substrate hairpin structures. When Ddc1, Mec3, and Rad17 were assayed alone or in combination with each other for exonuclease activity using the hairpin substrates, a low level of activity was seen in all of the protein preparations, Fig. 4-3. However, a lower amount of exonuclease activity is seen in the GST control lane when assayed using the 3' recessed end hairpin substrate, Fig, 4-3 (A), lane 2. In addition, no difference was detected between exonuclease activity in the GST control reactions and the checkpoint protein reactions using the 5' recessed end hairpin substrate. Therefore it is apparent that the checkpoint proteins Ddc1, Mec3 and Rad17 do not exhibit any exonuclease activity above background levels in these assays.

Discussion

Rad17 is required for the DNA damage checkpoint response and for cellular tolerance to UV and alkylation DNA damage(Lydall and Weinert, 1995; Weinert et al., 1994). In addition, Rad17 has been indicated to function in DNA processing as shown genetically through its affect on ssDNA generation in *cdc13-1* mutants(Lydall and Weinert, 1995). Rad17 protein has been shown to be homologous to the 3'->5' exonuclease Rec1 from *U.maydis* and to the replication protein PCNA(Lydall and Weinert, 1995; Venclovas and Thelen, 2000). These homology data suggest that Rad17 may act directly on DNA as an exonuclease.

Rad 17 is associated with low exonuclease activity.

Exonuclease activity was associated with Rad17 protein preparations when measured using TCA precipitation assays and a radio-labeled ssDNA substrate. Rad17 dependent exonuclease activity was observed to be above the background levels of the GST epitope control reaction. Although Rad17 is predicted to be a 3'->5' exonuclease based on the homology of Rad17 with Rec1, the directionality of Rad17 exonuclease activity could not be determined using the uniformly labeled ssDNA substrate. Rad 17 dependent exonuclease activity had a pH level preference, which varied based on the buffering conditions tested. The exonuclease activity that was detected was considered to be weak when compared to the reported robust exonuclease activity of Rec1 in other studies (Thelen et al., 1994).

Rad17 exonuclease activity was tested for whether it could be stimulated by different DNA structures. In addition, the checkpoint proteins Ddc1, Mec3 and Rad17 have been shown to interact with Rad17 either genetically or biochemically in other studies. They were tested for their ability to stimulate Rad17 exonuclease activity. Ddc1, Mec3 and Rad24 were tested for exonuclease activities using a DNA substrate that offered dsDNA, ssDNA and blunt end DNA structures. In addition to Rad17, Ddc1, Mec3 and Rad24 also had associated exonuclease activities when analyzed using denaturing PAGE analysis.

To further characterize the exonuclease activity associated with Ddc1, Mec3, Rad17 and Rad24, DNA substrates that formed hairpin structures through intra-molecular interactions were tested. These DNA hairpin substrates were chosen because the gapped DNA substrate used in the previous assays potentially formed the complete substrate at a

very low efficiency and therefore complicated interpretation of the data. A study in which the preparation of DNA substrates using intermolecular interactions indicated that the efficiency of complete DNA substrate is very low. However, exonuclease assays using the intra-molecularly annealed hairpin substrates was less convincing and difficult to interpret due to a higher background level of exonuclease activity associated with the GST epitope control reaction.

Is Rad 17 an exonuclease?

Further studies are required to determined if Rad17 is indeed a exonuclease or if it interacts with a exonuclease whose activity was detected in the exonuclease assays in this study. The latter hypothesis is supported by the finding that Ddc1, Mec3 and Rad24 all have associated exonuclease activities. In addition, point mutations made in amino acid residues thought to be critical for exonuclease activity based on the homology of Rad17 with Rec1 have no phenotype in regard to UV tolerance and DNA damage checkpoint function. This suggests that these residues thought to be critical for Rad17 exonuclease activity are not important for Rad17 function in regard to checkpoint activity or UV tolerance.

It is intriguing that Rec1 is an exonuclease, while Rad17 activity is very questionable. This conundrum has also been observed in the human homolog, hRad1. In one study hRad1 was found to have weak exonuclease activity, however a separate study found no associated hRad1 exonuclease activity (Freire et al., 1998; Parker et al., 1998). Thus, how can Rec1 be a homolog of such a weak exonuclease? One hypothesis may be that Rec1 may have acquired a novel function as an exonuclease in the fungus *U. maydis.*

Another reason may be that Rad17 and potentially hRad1 have lost their exonuclease functions and evolved novel functions in *S.cerevisiae*. For example, perhaps Rad17 exonuclease function had a role in DNA repair, which was lost as it became more specialized for the DNA damage checkpoint response.

Materials and Methods

Standard media conditions were used that included yeast extract-peptone and 2% dextrose (YEPD, Sherman e al., 1986) and –ura dropout media for strains containing plasmids.

Checkpoint mutants strains used in this study (Table 2-1) are isogenic with W303 and constructed using standard genetic techniques. Mutations were previously described for *mec3Δ, rad17Δ, and rad24* (Lydall and Weinert, 1995; Lydall and Weinert, 1997; Weinert and Hartwell, 1993), and *ddc1Δ* (Longhese et al., 1997). The *cdc13-1* and *cdc15-2* have been used in previous studies (Gardner et al., 1999; Lydall and Weinert, 1995). The protease deficient strain containing *pep4, prb1*, and *prc1* came from A.Adams. Yeast transformations were performed according to the LiAc TRAFO method (Schiestl and Gietz, 1989).

Plasmid constructions.

The construction of the plasmids used in this study are described in Chapter 1

G2/M cell cycle arrest assaying using *cdc13-1* DNA damage induction.

G2/M cycle arrest assays were performed as described (Lydall and Weinert, 1995). Yeast cells containing plasmids were grown for two days at 30°C in *-ura* dropout media and 2% raffinose. Overnight cultures were inoculated 1:50 dilution into *-ura* dropout media and

2% raffinose at 30°C. The following day cells were checked for cell density with a hemocytometer. Cells were counted as follows: one cell was counted as one and a budded cell counted as two. Cultures were adjusted to $6x10^6$ cells/ml if the cultures had not grown past $1.5x10^7$. α-factor (Sigma; St. Louis, MO) was then added to a final concentration of 20n*M*, except in the case of ddc1Δ cells which did not contain the bar1 mutation in which case the α-factor final concentration was 400n*M*. Cells were washed starting at t= -40 minutes to the zero time point and resuspended into YEP and 2% galactose media. At the zero time point cells were shifted to 36°C the restrictive temperature for *cdc13-1* and *cdc15-2*. Aliquots of the cultures were taken at the designated time points and fixed by adding 0.5 mls of cell culture to 1 ml 95% ethanol. Cell cycle arrest assays were quantitated by analyzing the nuclei of the cells to determine if nuclear division has occurred resulting in two nuclei, or if the G2/M checkpoint had been activated resulting in one visible nucleus. Nuclear morphologies were quantitated by scoring at least 100 cells that had been stained with 4,6-diamino-2-phenylindole (DAP1, 0,2 μg/ml) (Pringle et al., 1989) and visualized with a fluorescent microscope.

Cell survival following UV exposure.

Saturated cultures were grown as previously described in the section on cell cycle arrest assay. Cell cultures were adjusted to $2x10^6$ cells/ml grown for 6 hours with shaking at 23°C. Cells cultures were then adjusted to a final concentration of 2000 cells/ml. Duplicate 100μl aliquot were then plated in duplicate on YEPD agarose plates and the plates were allowed time to dry (approx. 20 min.). Plated cells were then exposed to appropriate does of UVC using a Stratalinker 1800. The plates were then incubated at

23°C for and counted on day 3 to determine viability. A control plate that had not been exposed to UVC defined 100% viability.

Protein preparation.

Protease deficient yeast cells containing plasmids were grown for two days at 30°C in 5.5 mls -ura dropout media and 2% raffinose. Eleven mls of saturated culture was inoculated into 1 liter of -ura and 2% raffinose and allowed to grow to midlog at 30°C with vigorous shaking. Once cells had reached midlog (4-6x10^6 cells/ml), protein expression was induced with 2% for 6 hours. Cells were pelleted, resuspended in 50% glycerol, flash frozen using liquid nitrogen, and stored in 50ml Falcon tubes at –70°C. Cell pellets were thawed on ice, pelleted, and resuspended in 4x the volume of the pellet of lysis buffer was added (50mM Tris-HCl [pH 7.4], 100mM NaCl, 2mM EDTA,1% NP-40, 1mM 2-mercaptoethanol, Aprotinin 2μg/ml, Leupeptin 2μg/ml, Pepstatin 1μg/ml). An equal volume to the lysis buffer of glass beads was added and cells lysed by vortexing at 4°C. Glass beads were washed with lysis buffer and the wash added to the supernatant. Cell lysates were clarified by centrifugation at 10,000x g and passed over a glutathione cellulose (Pharmacia) column (200μl bed volume) twice. Columns were washed with 10 column volumes with lysis buffer and GST fusion proteins eluted using elution buffer (30mM Hepes-K+[pH7.8], 7mM $MgCl_2$, 0.5 mM DTT, 10mM reduced glutathione). Protein preparations were separated on SDS-polyacrylamide gel electrophoresis (PAGE) of either 7.5% or 10% acrylamide concentration. The bis-acrylamide/acrylamide ratio was 1:37.5 respectively and visualized using Coomassie blue staining.

Western blotting.

Proteins were electroblotted onto nitrocellulose membrane and blocked for 1 hour in blocking solution (PBS-T and 5% w/v powder non-fat dry milk). The membranes were then washed once with PBS-T and then incubated for 1 hour with primary goat anti-GST antibody (Pharmacia) in PBS-T and 2.5% w/v powdered non-fat dry milk. Blots were then washed 3 times for 5 minutes each wash with PBS-T and then incubated for 1 hour with rabbit anti-goat HRP conjugated secondary antibody (Sigma) in PBS-T and 0.3% w/v powder non-fat dry milk. The blots were then washed 3 times for 5 minutes each wash with PBS-T. SuperSignal Substrate (Pierce) was used to detect the proteins. Thrombin cleavage was achieved by adding 10 units of thrombin (Sigma) to protein preparations and incubated for 20 min. at room temperature.

Exonuclease assay.

The tricholoroacetic acid procedure measures the conversion of DNA to an acid soluble form and has been described before (Thelen et al., 1994). Assay mixtures contained 1μg of a 1.6 kb DNA fragment containing the RAD17 gene that was synthesized using PCR, γP^{32}-dATP, dTTP, dGTP, and dCTP and the primers RAD17FP, 5'ATGAAAGGTGCATCTCAGGCT3' and RAD17RP, 5'TAACGCCAGAAAGGTTGTCG3'. Single-stranded DNA substrate was formed by boiling the substrate in a water bath for 5 min. to denature the linear duplex DNA, and then placed immediately on ice. Buffering conditions that varied by pH were (50mM Tris acetate [pH 7-9], 10mM Mg^{2+} acetate, 1mM dithiothreitol, 0.1mM EDTA), or (50mM Tris chloride [pH 7-9], 10mM Mg^{2+} chloride, 1mM dithiothreitol, 0.1mM EDTA). The 200μl reactions were started by the addition of 200-400ng of protein to the mixture and

incubated at 37°C for 10 minutes. To terminate the reactions ice-cold sonicated salmon sperm DNA (300 µl, 0.5mg/ml) and 10% trichloroacteric acid (500µl) were added. The terminated reactions were placed in ice for 10 min., centrifuged at 10,000 x g for 10min. and supernatant taken for measurement of the radioactivity that was present in it. All other exonuclease reaction mixtures contained 200-400ng of protein,30mM Hepes-K (pH7.8), 7mM $MgCl_2$, 0.5 mM DTT, 10mg/ml BSA, 20mM EDTA, 100mM NaCl, and 4fmoles of DNA substrate that had been gel and P^{32} labeled with Polynucleotide-Kinase (Roche Applied Science) in a 40µl volume. Reactions were incubated at 30°C for 20min, terminated by adding 5x reducing loading buffer, heated to 100°C for 5 min., and loaded onto Urea denaturing gels analyzed using a Molecular Dynamics 445 S1 PhoshporImager and the IP Lab Gel H program.

Figure 4-1. DNA substrates used to test for exonuclease activity. (A) Gapped DNA substrate offered a 20 nucleotide gap, 5' overhang, and a double-stranded DNA end. (B) Hairpin substrates that form intramolecular secondary structures at a higher efficiency than DNA substrates that form secondary DNA structures by intermolecular interactions. The two hairpin substrates resemble either a primer-template junction that can be recognized by replication proteins, or a primer-template of the opposite orientation. For substrate sequences see Table 4-3.

A.

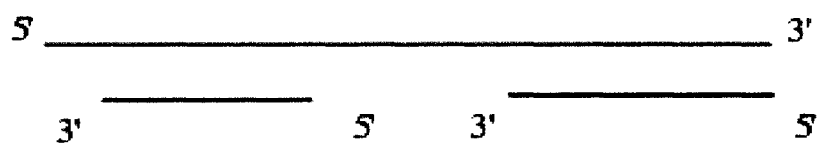

Gapped (20 nucleotides wide)
Blunt Ended
5' Overhang

B. DNA Hairpin substrate with 3' or 5' free end (29 nts. ssDNA).

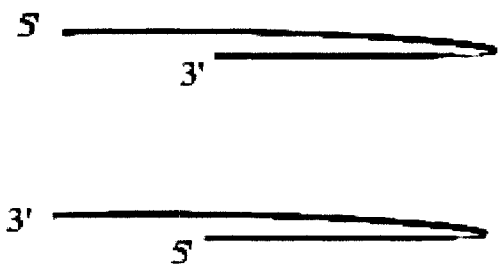

Figure 4-2. Checkpoint proteins have exonuclease activity above back ground level of detection. (A) Each checkpoint protein was assayed alone or in combination with the three other checkpoint proteins. (B) The addition of NaCl to a physiological concentration increased exonuclease activity. Exonuclease activity sensitivity to the addition of 20mM EDTA suggests a dependency for activity on the presence of magnesium. The majority of DNA degradation is seen in Lane 13 using the 80 nt substrate. For discussion of individual reactions see text.

A.

Lane	Reaction
1	- no protein control
2	- ssb
3	- GST
4	- GST-Ddc1
5	- GST-Mec3
6	- GST-Rad17
7	- GST-Rad24
8	- GST-Ddc1,GST-Mec3,GST-Rad17,GST-Rad24
9	- 20mM EDTA + GST-Ddc1,GST-Mec3,GST-Rad17,GST-Rad24
10	- 150 mM NaCl + GST-Ddc1,GST-Mec3,GST-Rad17,GST-Rad24
11	- 22 labeled only + GST-Ddc1,GST-Mec3,GST-Rad17,GST-Rad24
12	- 35 labeled only + GST-Ddc1,GST-Mec3,GST-Rad17,GST-Rad24
13	- 80 labeled only + GST-Ddc1,GST-Mec3,GST-Rad17,GST-Rad24

B.

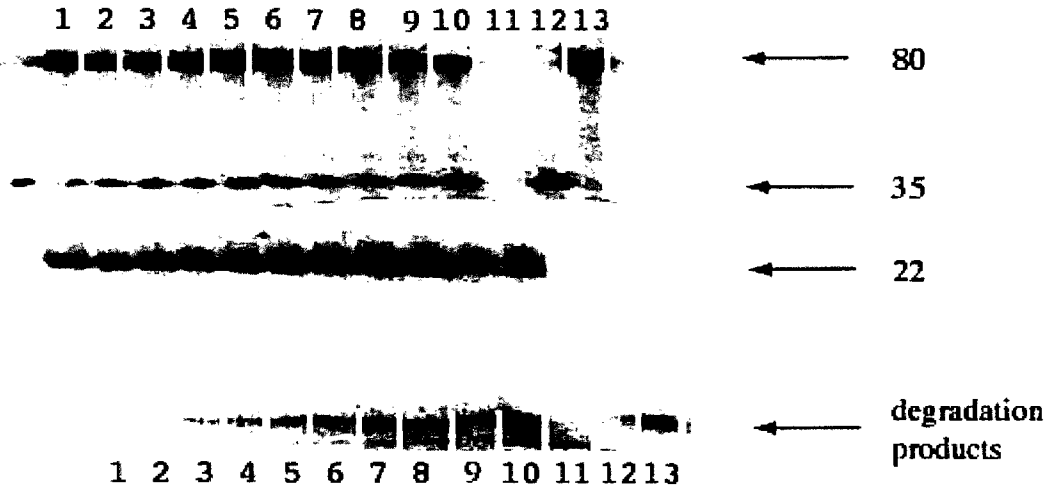

Figure 4-3. Associated exonuclease activity of checkpoint proteins with hairpin substrates. (A) Checkpoint proteins assayed for exonuclease activity alone or in combination using a 5'-^{32}P labeled hairpin substrate with a free 5' end and unlabeled recessed 3' end. (B) Same checkpoint protein preparations assayed for exonuclease activity but using a 5'-^{32}P labeled hairpin substrate with a free 3' end and labeled 5' recessed end. Assays were electrophoresed in a DNA sequencing gel under denaturing conditions.

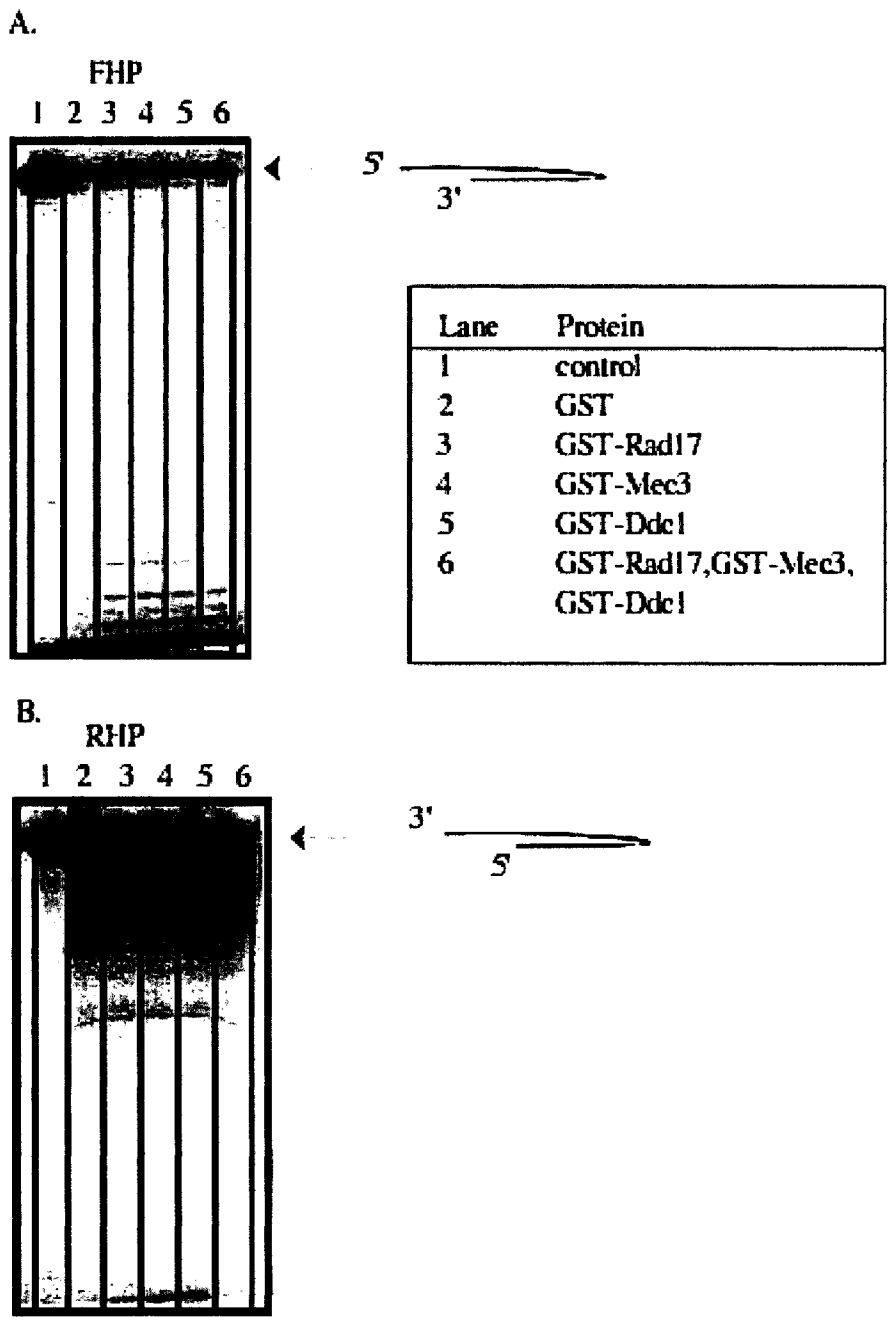

Lane	Protein
1	control
2	GST
3	GST-Rad17
4	GST-Mec3
5	GST-Ddc1
6	GST-Rad17,GST-Mec3, GST-Ddc1

Table 4-1. Characterization of low nuclease activity of GST-Rad17 preparation.

SAMPLE	BUFFER	CONDITION	ACTIVITY
			% max
ExoIII	Tris acetate	pH 9	100
GST	Tris acetate	pH 7	0.08
	Tris acetate	pH 8	0.91
	Tris acetate	pH 9	0.03
	Tris HCl	pH 7	0.10
	Tris HCl	pH 8	0.43
	Tris HCl	pH 9	0.16
GST-Rad17	Tris acetate	pH 7	0.28
	Tris acetate	pH 8	3.66
	Tris acetate	pH 9	0.06
	Tris HCl	pH 7	0.22
	Tris HCl	pH 8	0.06
	Tris HCl	pH 9	3.43

*Standard reaction conditions were at 37°C for 15 minutes in 25 mM Tris acetate pH 9.0 using 10 mM Mg^{++}. The table lists the changes to these conditions.
*Activity was measured using 0.1μg of total protein and 19.6 nmoles of heat denatured DNA substrate. The activity is given as a percentage of free nucleotides using the activity of ExoIII as the maximum activity.

Table 4-2. Repeated testing of GST-Rad17 dependent nuclease activity. (A) GST-Rad17 dependent nuclease activity is repeatedly stronger using Tris-acetate (pH 8) buffering conditions. Standard reaction conditions were assayed at 37°C for 15 minutes in 25mM Tris-acetate using 10mM Mg^{++}. The table lists the changes to these standard conditions. Activity was measured using 0.1mg of total protein and 19.6 nmoles of heat denatured DNA substrate. The activity is given as a percentage of free nucleotides using the activity of ExoIII as the maximum activity. (B) GST-Rad17 dependent exonuclease activity is stronger with an increased concentration of GST-Rad17 but not with an increase in GST concentration. Standard reaction conditions were assayed at 37°C for 15 minutes in 25mM Tris-acetate pH 8 using 10mM Mg^{++}.

A.

SAMPLE	CONDITION	ACTIVITY
		% max
ExoIII	pH 9	100
GST	pH 7	0.18
	pH 8	0.24
	pH 9	0.11
GST-Rad17	pH 7	0.74
	pH 8	1.04
	pH 9	0.39

B.

SAMPLE	ACTIVITY
	% max
ExoIII	100
GST (0.1μg)	1.38
GST-Rad17 (0.1μg)	1.01
GST (0.2μg)	1.16
GST-Rad17 (0.2μg)	3.08

Table 4-3.

Oligonucleotides used in this study.

gapped substrate construct	
EXO22	CAGGTACTTTGAACGAATGCAT
EXO35	TAGTTAATCATTGGCTCTTGTATTCGCGTATCTTG
EXO80	ATCATGCATTCGTTCAAAGTACCTGTCAAACTATT ATTCCGAGCACAAGATACGCGAATACAAGAGCCA ATGATTAACTA
hairpin oligonucleotide with 5' free end	
HPF96	CACACACACACACACACACACACACAGATCCC CGGGTACCGAGCTCGAATTCGTAATCATATGATTA CGAATTCGAGCTCGGTACCCGGGGATC
hairpin oligonucleotide with 3' free end	
HPR96	CTAGGGGCCCATGGCTCGAGCTTAAGCATTAGTAT ACTAATGCTTAAGCTCGAGCCATGGGCCCCTAGAC ACACACACACACACACACACACACAC

CHAPTER 5

EXPLORING RAD17 HOMOLOGY TO BOTH THE REPLICATION PROTEIN PROLIFERATING NUCLEAR CELL ANTIGEN, AND THE 3'->5' EXONUCLEASE FROM *USTILAGO MAYDIS* REC1 VIA MUTANT ANALYSIS.

Summary

RAD17, which is required for the DNA damage checkpoint response in *S.cerevisiae*, arrests cells at G2 following DNA damage. Homologs of Rad17 are reported to be 3'->5' exonucleases. Protein sequence analyses of Rad17 suggest that it is homologous to both 3'->5' proofreading exonucleases that function during DNA replication and that Rad17 is also homologous to the replication protein proliferating nuclear cell antigen (PCNA). Point mutations and protein truncation mutants were constructed and tested for their effects on Rad17 checkpoint and putative exonuclease activities.

A point mutation thought to be required for Rad17 exonuclease activity had no phenotype when tested for checkpoint activity and UV sensitivity. This suggests that Rad17 may not be an exonuclease or that the Rad17 exonuclease activity is not important for checkpoint function. Changes to conserved amino acid residues were also constructed in a leucine-rich domain found in all Rad17 homologs, which was shown to be required for UV tolerance and checkpoint activity in the Rad17 *S.pombe* homolog Rad1. Mutations made in this domain result in UV sensitivity, implying that this domain is important for Rad17 function. Lastly, carboxy-terminal truncations made past the PCNA homology region of Rad17 yielded mutants that are checkpoint defective, UV sensitive,

and defective for the *RAD17* dependent cell lethality of *cdc13-1* mutants. This implies that not only is the PCNA homology region of Rad17 not solely important for its function, but that the carboxy-terminal region of the protein not found in PCNA is also important for Rad17 activity in the DNA damage checkpoint response.

Introduction

Cells encounter constant DNA damage from both their internal and external environments that can result in the formation of DNA mutations. There are several DNA repair processes that prevent the accumulation of mutations, but these processes may at times require more time to repair the damage than the normal rate of cell cycle progression permits. The DNA damage checkpoint response delays the onset of mitosis to allow time for repair and to avoid passing along a damaged genome to the next cell generation. In addition, the DNA damage checkpoint response promotes the transcription of DNA repair genes, and also functions in DNA repair (Lydall and Weinert, 1995; Weinert et al., 1994).

Studies in *S.cerevisiae* have identified Rad17 as a protein required for the DNA damage checkpoint response that is also considered to be a direct sensor of DNA damage(Weinert et al., 1994). Checkpoint sensor proteins are thought promote the activation of the checkpoint response by localizing checkpoint kinases to the DNA to bring them into the proximity of their protein substrates (Melo and Toczyski, 2002; Zhou and Elledge, 2000). Molecular modeling analysis suggests that the checkpoint proteins Ddc1, Mec3 and Rad17 are homologous to PCNA (Venclovas and Thelen, 2000). PCNA functions during DNA replication as a homo-trimeric complex that is recruited by the replication protein complex RFC to promote DNA polymerase processivity (Tsurimoto, 1998; Tsurimoto and Stillman, 1991). Ddc1, Mec3 and Rad17 interact with each other and form a hetero-trimeric complex that is thought to be similar in structure to PCNA (Kondo et al., 1999). This suggests a model in which the checkpoint protein RFC-like

complex Rad24-RFC recruits the Ddc1/Mec3/Rad17 complex to the DNA (Venclovas and Thelen, 2000). However, how the recruitment of the Ddc1/Mec3/Rad17 complex leads to DNA checkpoint activation is still not understood.

Interestingly, the Rad17 homolog Rec1 from *Ustilago maydis* has been shown to be a 3'->5' exonuclease(Thelen et al., 1994). However, it is not known if all Rad17 homologs from various organisms are exonucleases. The Rad17 human homolog hRad1 has also been reported to be a 3'->5' exonuclease, although with a significantly lower specific activity than Rec1 (Parker et al., 1998). Preliminary data from a second report indicates that the Ddc1/Mec3/Rad17 human homolog complex 9-1-1 also has weak nuclease activity associated with it(Lindsey-Boltz et al., 2001). However, the data regarding the 9-1-1 nuclease activity has not yet been published. A second report regarding hRad1 nuclease activity independent of the previously mentioned study indicates that no nuclease activity is detectable from purified hRad1(Freire et al., 1998). In addition, no exonuclease activity has been published on the Rad17 homolog from *S.pombe* Rad1 or Rad17.

Another ambiguity is the two different homologies reported for Rad17, one to an 3'->5' exonuclease, and a second to PCNA that has no reported exonuclease activity. Although Rec1 has been reported to be homologous to 3'->5' proofreading exonucleases associated with DNA polymerases, a second report indicates that this is probably not correct and that the PCNA modeling data is probably closer to the truth (Venclovas and Thelen, 2000). This raises the question as to how the PCNA structure can accommodate nuclease activity? An example of an exonuclease whose structure forms a ring is the λ-

phage 5'->3- exonuclease(Kovall and Matthews, 1997). To function, λ-phage exonuclease is threaded onto duplex DNA from a free end and degrades the 5' strand of the DNA as the double-stranded DNA moves through the center of the exonuclease. The resulting single-stranded 3' end of the DNA continues through the protein and is a potential substrate for recombination(Kowalczykowski et al., 1994). The λ-phage exonuclease structure is a homo-trimeric protein complex that contains three exonuclease active sites within its ring structure, and is considered to be similar in both structure and sequence to the endonucleases PvuII and EcoRV(Kovall and Matthews, 1998). The catalytic site consists of α-helices that extend acidic amino acid residues towards the DNA as it passes through the center of the protein structure. Although λ-phage exonuclease forms a ring structure similar to PCNA, it is not considered to be homologous to PCNA in either amino acid sequence or protein structure. Both the PCNA and λ-phage exonuclease contain α-helices located inside the ring surface that contact the DNA. However, these two complexes differ in their secondary structures; lambda exonuclease contains more α-helices than PCNA, whose structure is comprised of mainly β-sheets (Fig. 5-1). Therefore, because the PCNA and λ-phage exonuclease structures are not considered to be related suggests that the Ddc1/Mec3/Rad17 complex is also not considered to be related to λ-phage exonuclease.

It is possible that the Ddc1/Mec3/Rad17 complex could both form a PCNA structure and function as an exonuclease via the α-helices that extend towards the DNA. Ddc1, Mec3 and Rad17 proteins consist of both regions that are homologous to PCNA and extensive carboxy-terminal regions of protein sequence that are not found in PCNA.

Thus, PCNA is substantially shorter than Ddc1, Mec3 and Rad17. This suggests the possibility that the Ddc1/Mec3/Rad17 complex exonuclease activity could reside in these extensive carboxy-terminal regions of the checkpoint proteins that are not involved in the formation of a toroidal structure.

To address the reported relevance of Rad17 homology to 3'->5' exonucleases and to PCNA, mutations were made in various regions of the protein. In this study, a Rad17 point mutation constructed at an amino acid site that is also conserved in Rec1 and other 3'->5' exonucleases and thought to be required for exonuclease activity was tested for its effect on checkpoint activity, UV sensitivity and *in vivo RAD17* dependent telomere degradation. Point mutations were also constructed at conserved amino acid residues located in a leucine-rich region of Rad17 and tested for UV sensitivity and telomere degradation. In addition, the location of the point mutations made in this study and their affect on the PCNA structure model is discussed. Lastly, Rad17 carboxy-terminal truncation mutants that lack regions of the protein immediately downstream of the region of Rad17 considered to be homologous to PCNA are tested for their effects on cell cycle arrest following DNA damage and UV sensitivity. One carboxy-terminal mutant with a hypomorphic DNA damage induced cell cycle arrest phenotype was tested for whether it is specifically defective for signaling through either the Pds1 or Rad53 branches of the checkpoint pathway.

Results

Test for *RAD17* exonuclease function *in vivo*.

D.Lydall and P.Skogg of the lab constructed a point mutation in one of the three proposed exonuclease domains at an acidic amino acid thought to be required for exonuclease activity based on alignments of Rad17 and Rec1 with the 3'->5' exonucleases PolA, and DNAQ, Fig. 5-2(Lydall and Weinert, 1995; Thelen et al., 1994). DNA proofreading exonucleases require these acidic amino acid residues to hold the positively charged magnesium cation for exonuclease activity (Moser et al., 1997; Thelen et al., 1994). If the Rad17 protein is an exonuclease and uses the same exonucleolytic mechanism as the 3'->5' exonuclease PolA, making a point mutation in this residue and testing it *in vivo* may help deduce what the importance of the exonuclease functions *in vivo*. However, the *rad17-E122A* mutation displayed no checkpoint defect when assayed by D.Lydall following DNA damage using the *cdc13-1* conditional mutant that allows *RAD17* dependent telomere degradation at the restrictive temperature (data not shown). Therefore, if the *rad17-E122A* mutation abolished Rad17 exonuclease activity it had no affect on its ability to induce cell cycle arrest following DNA damage.

Rapid death analysis of the *rad17-E122A* mutation.

In this study, the *rad17-E122A* mutant was tested for whether the *rad17-E122A* mutation affected the *RAD17* dependent DNA degradation observed in *cdc13-1* cells. Cells containing both *cdc13-1* and *rad9*Δ mutations die rapidly when grown at the restrictive temperature of 36°C, presumably due to the accumulation of single-stranded DNA at telomeres. *RAD9* has an inhibitory affect on *RAD17* dependent DNA degradation in *cdc13-1* cells and cell viability is dependent on the presence of *RAD9*. The rapid death assay was used to test whether the *rad17-E122A* mutant would cause lethality in

rad9Δ,cdc13-1 cells. As shown in Figure 5-3 (A), wild type and *rad17Δ* cells do not die when shifted to the restrictive temperature of 36°C to induce *cdc13-1* DNA damage, and *rad9Δ,cdc13-1* cells die over time at the restrictive temperature presumably due to the *RAD17* dependent DNA degradation at telomeres. However, the *rad17-E122A,rad9Δ,cdc13-1* cells also die when shifted to the restrictive temperature albeit at a slightly reduced rate suggesting that *rad17-E122A* may be slightly hypomorphic in the *RAD17* rapid death assay.

The *rad17-E122A* mutation had no affect on *RAD17* UV resistance.

In *U.maydis*, the *REC1* allele *rec1-1* retains greater than 70% of its nuclease activity although missing the last 15% of its amino acids from the carboxy-end of the protein. In addition, *rec1-1* mutant cells are UV sensitive. Therefore, since UV sensitivity and nuclease functions do not appear to be linked for Rec1, the *rad17-E122A* mutant was tested for UV sensitivity. As shown in Figure 5-3 (B), *rad17-E122A* cells are not sensitive to UV suggesting that the *rad17-E122A* mutation does not affect the function of *RAD17* in the UV resistance of cells.

UV sensitivity of mutations made in the *RAD17* leucine-rich domain.

Rad17 contains a leucine-rich domain, previously identified in Rec1, located C-terminally to the three proposed exonuclease domains, Fig. 5-4 (A)(Onel et al., 1995). This domain is found in all of the Rad17 homologs and in PCNA. Interestingly, a region of Polε, a polymerase that functions in the S-phase checkpoint response, also resembles this domain. The *rec1-1* mutant protein lacks half of this domain and the remaining C-terminus. Interestingly, although *rec1-1* is UV sensitive, the mutant protein retains 73%

of its exonuclease activity(Onel et al., 1995). To test whether the leucine-rich domain in Rad17 is also required for Rad17 UV resistance, point mutations were made in conserved amino acid residues. One mutation converts T241 to alanine, and the second more highly conserved residue R259 was changed to glutamic acid to induce a charge change or to isoluecine for a more neutral change. The UV sensitivities of these point mutants are shown in Figure 5-4 (B). The *rad17-T241A* and *rad17-R259I* mutations had greater UV sensitivities when compared to *rad17*Δ cells, and the *rad17-R259E* mutation UV sensitivity was similar to *rad17*Δ cells sensitivity. This suggests that the leucine-rich region of Rad17 is important for the UV resistance of cells.

Localization of *RAD17* point mutantions based on the PCNA structure.

It is possible that the Ddc1/Mec3/Rad17 protein complex can form both PCNA like toroidal structure and use the same catalytic mechanism that proofreading 3'->5' exonucleases use. However, further structure comparison indicates that this is probably not the case. The *RAD17* point mutation *rad17-E122A* was constructed based on the structure of the second exonuclease domain of Klenow exonuclease and was designed to knock out nuclease activity. Based on 3'->5' exonuclease structures the Rad17 residue E122 would cluster with other acidic amino acid residues in a catalytic site. Localization of the Rad17 E122 residue within the structure of PCNA shows that the mutation does not localize into what could be considered an exonuclease active site. As shown in Fig. 5-2, using the PCNA structure and homology alignments with Rad17, the amino acid E122 localized to the outside of the PCNA structure in a β-sheet distal from the center of the structure where PCNA contacts the DNA. Interestingly, the first characterized *RAD17*

mutant, *rad17-1*, was localized on the PCNA structure to a β-sheet that in PCNA forms an interface with another monomer to form the oligomeric structure. The mutation in *rad17-1* changes E128 to a lysine and disrupts Rad17 interaction with Mec3(Kondo et al., 1999). This point mutation is predicted by structural modeling to disrupt the Rad17 interaction with Mec3 (Venclovas and Thelen, 2000). The β-sheet containing residue E122 interacts directly with the β-sheet of E128. Therefore neither of these residues are thought to interact directly with DNA. The E122A mutation likely affects internal protein folding and, as previously mentioned the E128K mutation is thought to affect protein-protein interactions.

Mutations made in the leucine-rich region of Rad17 localize to different regions of the PCNA structure (Fig. 5-6). Amino acid R259 localized to the outside of the structure in a β-sheet that does not involve an interface between proteins but is involved in intra-molecular interactions. Thus, a mutation made at this site would most likely affect the overall fold of Rad17. Lastly, the T241 residue is the only mutant constructed that maps to a region in the PCNA structure that could contact the DNA and localize to an α-helix internal to the structure in an orientation that could confer DNA interaction. Therefore, the T241A mutation made at this site is the most likely mutation made in Rad17 to affect protein-DNA interactions.

DNA damage checkpoint and rapid death phenotype of *RAD17* carboxy-terminal deletion mutants.

Carboxy-terminal deletions of *RAD17* were constructed and their effect on DNA damaged induced cell cycle arrest, initially were characterized by D.Lydall of the

Weinert lab. The Rad17 protein is 401 amino acids in length. The *rad17-Δ2* truncation mutant contains the first 348 amino acids of Rad17, and the most severe truncation constructed *rad17-Δ3* results in a mutant protein 315 amino acids in length that includes only the region of Rad17 that is homologous to PCNA. The *rad17-Δ3* mutant had a *rad17Δ* phenotype in regard to cell cycle arrest; however, the *rad17-Δ2* mutant had a more ambiguous checkpoint defect when assayed by D.Lydall (data not shown).

In this study, these carboxy-terminal deletion alleles of *RAD17* were further characterized for their effects on the DNA damage checkpoint response. The *rad17-Δ2* and *rad17-Δ3* mutants were tested for DNA damage checkpoint arrest proficiency using *cdc13-1* DNA damage. As shown in Figure 5-7 (A), wild type cells arrest in the cell cycle at G2 following DNA damage induction and *rad17Δ* cells fail to arrest due to their checkpoint defect. *RAD17* was fully functional when integrated at the *TRP1* locus and served as a control because the truncation mutants were also integrated at the *TRP1* locus. The *rad17-Δ3* mutant displayed a complete loss of checkpoint function and did not arrest following DNA damage induction. Unexpectedly, the *rad17-Δ2* mutant initially arrested its cell cycle following DNA damage, but failed to maintain this arrest over time. This arrest phenotype is similar to what is seen in both *rad53-11* and *pds1Δ* cells, two checkpoint proteins that function downstream of Rad17. Rad53 and Pds1 function in parallel pathways for full cell cycle arrest following DNA damage.

The *rad17-Δ2* and *rad17-Δ3* mutants were next tested in the rapid death assay to determine how functional the mutants were in regard to the *RAD17* dependent telomeric degradation observed in *rad9Δ,cdc13-1* cells. As shown in Figure 5-7 (B), the *rad17-Δ3*

mutation had a phenotype similar to *rad17*Δ cells indicating a complete loss of function, whereas the *rad17*-Δ2 mutant was as functional as *RAD17* cells. This suggests that the region of Rad17 between amino acids 315 and 348 is potentially important for the *RAD17* dependent telomere degradation in *cdc13-1* cells.

Deletion of the *RAD17* carboxy-terminus results in a loss of checkpoint function.

It was initially hypothesized that *rad17*-Δ2 was defective in signaling through *RAD53* because *rad17*-Δ2 and *rad53-11* cells have similar cell cycle arrest profiles(Gardner et al., 1999). To test this, the *rad17*-Δ2,*rad53-11* double mutant was assayed for cell cycle arrest proficiency following *cdc13-1* DNA damage. As shown in Figure 5-8, the *rad17*-Δ2,*rad53-11*,*cdc13-1* mutant had the same, albeit reduced, defect in arrest as the *rad17*-Δ2,*cdc13-1* mutant. This data is inconclusive regarding whether *rad17*-Δ2 was defective in signaling the DNA damage checkpoint response through *RAD53*.

The *rad17*-Δ2 mutant was next tested for its ability to signal through *PDS1*. A *rad17*-Δ2,*pds1*Δ double mutant should be completely defective in its checkpoint response if it can signal through the *PDS1* pathway. However, this mutant was difficult to work with because *pds1*Δ stains are viable at 23°C but inviable at 30°C, and the lowest restrictive temperature of *cdc13-1* is 28°C. The *rad17*-Δ2,*pds1*Δ,*cdc13-1* cells were tested for their checkpoint response at 28°C, a semi-permissive temperature for the *pds1*Δ mutation but a high enough temperature for *cdc13-1* DNA damage activation. However, 28°C is the permissive temperature for *cdc15-2*, a mutation that at 30°C prevents cytokinesis and is used in all of the *cdc13-1* assays because it is helpful in the scoring of cells. Growth of the cells at the *cdc15-2* permissive temperature of 28°C allowed the

cells to continue cycling to the next cell cycle and resulted in difficulty when scoring cells. In two different attempts, both phenotypes of arrest and failure to arrest were observed, Figure 5-9 (A) and (B). This is probably due to the fact that the *rad17-Δ2,pds1Δ* phenotype was difficult to score due to *cdc15-2* and the unusual nuclear phenotypes seen in *pds1Δ* cells (Gardner et al., 1999). From these data it is inconclusive whether *rad17-Δ2* can signal through *PDS1* or is defective in signaling through *RAD53*.

UV sensitivity of *rad17-Δ2*.

As previously mentioned, the *rec1-1* protein is missing the last 15% of the full-length protein and is UV sensitive. Likewise, the *rad17-Δ2* mutation is also missing the last 15% of the full-length protein. However, there is low homology between the carboxy-terminals of Rad17 and Rec1 carboxyl to the leucine-rich domain. To test whether the last 15% of Rad17 is important for its function in UV resistance, the *rad17-Δ2* mutation was tested for UV sensitivity. As shown in Figure 5-10, the *rad17-Δ2* mutant has a hypomorphic defect in UV resistance following exposure, suggesting that this region of the protein is important for UV resistance. Another possibility is that overall the *rad17-Δ2* protein is slightly destabilized by the truncation but still functional to some degree.

Discussion

Rad17 is required for the DNA damage checkpoint response and the UV resistance of cells(Lydall and Weinert, 1995; Weinert et al., 1994). The Rad17 homolog Rec1 is a reported 3'->5' exonuclease which implies that Rad17 may also be an exonuclease(Thelen et al., 1994). The published alignment that includes Rec1 with other 3'->5' exonucleases that function in DNA proofreading lends potential insight into how

Rec1 might function as an exonuclease. In this study, a point mutation made in an amino acid residue thought to be important for the potential exonuclease function of Rad17 revealed that this reside was not important for *RAD17* dependent checkpoint cell cycle arrest, UV resistance, or the *RAD17* dependent lethality in *rad9Δ,cdc13*-1 cells. This suggests that either Rad17 is not an exonuclease, the amino acid residue mutated is not involved in Rad17 exonuclease activity, or that Rad17 exonuclease activity has no role in the functions of Rad17 that were tested.

Studies on Rec1 alleles support the hypothesis that if Rad17 were an exonuclease, that the exonuclease activity would not have an important role in the checkpoint response or UV resistance(Onel et al., 1995). The *rec1-1* allele is UV sensitive and checkpoint defective yet retains 73% of exonuclease function when tested *in vitro*. Rec1 exonuclease activity is important for the formation of spontaneous mutations. For example, the *rec1-1* mutant has a 10-fold higher spontaneous mutation rate. The *rec1-5* allele retains 42% of its exonuclease activity although it is missing the last 28% of the protein and has a 100-fold increase in spontaneous mutation rate. Therefore, the exonuclease activity of Rec1 does not appear to be important for the DNA damage checkpoint response in regard to cell cycle arrest or UV resistance, but is required for the prevention of mutations.

Further amino acid sequence analysis of Rad17 homologs suggests that the residues considered to be critical for Rec1 exonuclease activity based on structural analysis of the 3'->5' exonuclease of PolA are not conserved among its homologs (Fig. 5-7). The alignment predicts that only Rec1 could be an exonuclease because its

homologs do not contain all of the conserved residues required for exonuclease activity. Interestingly, the Rad17 human homolog hRad1 that is reported to be a weak 3'->5' exonuclease does not contain all of the residues predicted to be required for exonuclease function. The specific activities of Rad1 from human are very low when compared to Rec1, and one reason may be because the human and mouse homologs do not contain all the amino acids predicted to crucial for exonuclease activity. Another explanation may be that among this family of proteins some may be more stable during purification than others. It is interesting to note that Rec1 retains 45% of its exonuclease activity if is missing the third exonuclease domain, and 17% of its activity if it is missing both the second and third exonuclease domain. Therefore, not all of the amino acid residues thought to be required for the exonuclease activity of Rec1 are necessary. This also suggests that although Rad17 homologs do not contain all of the conserved residues for exonuclease activity, they still could function as exonucleases. The wide range of specific activities between Rec1 and the human homolog suggests that the nuclease activity may have evolved away from each other, becoming weaker or stronger exonucleases.

There are several explanations to reconcile how Rad17 could be both an exonuclease and homologous to PCNA. One is that Rad17 can flip in and out of exonuclease and PCNA structures. However, there does not appear to be any precedence for this among exonucleases or PCNA. A second hypothesis is that the PCNA structure can accommodate exonuclease activity, and that Rad17 is indeed an exonuclease, but the exonuclease domains or residues required for this activity have not been identified.

Finally, it may be that Rad17 is not an exonuclease and forms a PCNA-like structure to recruit other proteins such as exonucleases to the sites of damage to process the DNA. The DNA degradation seen in *cdc13-1* cells may be an example of Rad17 directly degrading the DNA, although *cdc13-1* DNA degradation proceeds in a 5'->3' direction, or *cdc13-1* DNA degradation could be an example of Rad17 recruiting an exonuclease that can degrade telomeres.

In addition to the three exonuclease domains located within the region of Rad17 that is also homologous to PCNA, Rad17 also contains a leucine-rich domain that is important for UV resistance(Onel et al., 1995). Based on the PCNA structure, the leucine-rich region spans three β-sheets located outside the structure, and an α-helix located near the center of the structure(Venclovas and Thelen, 2000). This domain is present in all of the Rad17 homologs identified and contains one amino acid residue that is absolutely conserved. Rad17 mutants containing amino acid substitutions in two of the conserved resides yielded mutants that were as, or more sensitive, to UV when compared to the *rad17*Δ mutant. A possible reason for the increased UV sensitivity is that the changes produced mutants with antimorphic effects, where the mutant protein could localize to sites of DNA damage, but somehow able to prevent repair. This could be by failing to localize repair proteins to the site or by physically blocking out repair proteins resulting in increased cell lethality. This is plausible because Rad17 has been shown to localize to sites of DNA damage. The importance of the leucine-rich region has also been studied in the Rad17 *S.pombe* homolog *Rad1*. The *Rad1* allele *rad1-S4* contains a small deletion in this region as shown in Fig. 5-4 (A) and is as UV sensitive as *rad1*Δ

cells, but more sensitive to γ-radiation than the null(Kanter-Smoler et al., 1995). In addition, *rad1-S4* is defective for signaling cell cycle arrest following exposure to γ-radiation or the replication inhibitor hydroxy-urea.

Although much attention has been given to the finding that Rad17 is homologous to PCNA, little has been done to analyze the region of Rad17 that is not homologous to PCNA. In this study, carboxy-terminal truncations were used to ascertain the importance of this region of Rad17 in the checkpoint response. The *rad17-Δ3* deletion mutant is missing the entire region of Rad17 that is not homologous to PCNA, and has a complete loss of function phenotype. This mutant was defective in both in cell cycle arrest following *cdc13-1* DNA damage and the *RAD17* dependent telomere degradation in *rad9Δ, cdc13-1* cells. It is interesting that while *rad17-Δ3* includes the entire PCNA and exonuclease domains of Rad17, it is completely defective in its ability to signal cell cycle arrest. This suggests that the PCNA region of Rad17 is not the only region of importance for Rad17 function and that the carboxyl-end has an undefined function in the checkpoint response. A potential function of the carboxy-end of Rad17 could be to interact with and localize DNA repair proteins or checkpoint kinases to the DNA. However, it is also possible that *rad17-Δ3* may not be able to fold properly and deletion of the carboxy-end of Rad17 could destabilize the overall structure of Rad17 resulting in a null phenotype.

The phenotype of the *rad17-Δ2* mutant is proficient in initiating cell cycle arrest following *cdc13-1* DNA damage, but cannot maintain arrest. This suggests that Rad17 is required for both the initiation and maintenance of arrest. On the less interesting side, this truncation mutant may merely be a hypomorph, but interestingly one with a

phenotype similar to *rad53-11* and *pds1*Δ mutants. *RAD53* and *PDS1* each function in a separate branch of the two parallel pathways that are thought to be involved in the signal transduction of the checkpoint response(Gardner et al., 1999). Both pathways are required for full cell cycle arrest and cells defective in one of these pathways have the same arrest profile as the *rad17*-Δ2 mutant. The *rad17*-Δ2 mutant was tested for whether it could signal through either *RAD53* or *PDS1*. Cells carrying the *rad17*-Δ2,*rad53-11* double mutation had a similar cell cycle arrest profile as the single mutants, suggesting that *rad17*-Δ2 is proficient for signaling through the *PDS1* pathway. However, the final analysis to test whether *rad17*-Δ2 is defective for signaling through the *RAD53* pathway was inconclusive. Therefore, it cannot be concluded that *rad17*-Δ2 is defective for signaling through the *RAD53* branch of the checkpoint signaling pathway. This is also supported by the observation that *rad17*-Δ2 is less sensitive to UV than *rad53-11*. If *rad17*-Δ2 were completely defective for the activation of *RAD53*, then this would predict that the two mutants would have similar UV sensitivities. However, this was not observed, and instead *rad17*-Δ2 is as sensitive to UV as *pds1*Δ, suggesting that the *RAD53* pathway is still activated. However, the further testing of UV sensitivities using the *rad17*-Δ2,*pds1*Δ and *rad17*Δ, *rad53-11* double mutants that would further this argument have not been done.

The *rad17*-Δ2 mutant does imply that *RAD17* can choose to signal through either *RAD53* or *PDS1* pathways, or that this mutant is a hypomorph. Currently, it is not known what the arrest profile is of a checkpoint hypomorph. Two possible hypomorph phenotypes are the *rad17*-Δ2 phenotype and the *TEL1* over-expression profile in which a

small percentage of cells activate and maintain cell cycle arrest. More interestingly, it is also not known why *rad17-Δ2, rad53-11* or *pds1Δ* cells initiate arrest but fail to maintain the arrest. There appears to be some synergy between *RAD53* and *PDS1* for the maintenance of arrest, because both are required for complete cell cycle arrest. However, it is not known how they interact with each other or other proteins to maintain arrest. The *rad17-Δ2* mutant indicates that perhaps *RAD17* has a role in this maintenance of arrest.

The current model regarding the activation of the DNA checkpoint response is that the Ddc1/Mec3/Rad17 complex is recruited to the DNA by Rad24-RFC. The Ddc1/Mec3/Rad17 complex then recruits other proteins that can then send the signal and can also recruit proteins for DNA repair. The potential exonuclease activity of the Ddc1/Mec3/Rad17 complex has not been characterized, but Rec1 studies indicate that the exonuclease activity is probably not important for the checkpoint response in *U.maydis.* The Ddc1/Mec3/Rad17 complex therefore probably functions in the checkpoint similar to how PCNA functions in replication, which is to recruit proteins to the DNA(Tsurimoto, 1998). What the proteins are that the Ddc1/Mec3/Rad17 complex recruits would certainly be important to identify to further our understanding of the DNA damage checkpoint response.

Materials and Methods

Yeast strains and media.

The budding yeast used in this study are isogenic with W303 and yeast strains constructed using standard genetic techniques (Table 5-1). The strains used in this study are *bar1* for greater sensitivity to α-factor. Mutations were previously described for

rad9Δ, rad17Δ, rad53-11 (Lydall and Weinert, 1995; Lydall and Weinert, 1997; Weinert and Hartwell, 1993)and *pds1Δ* (Gardner et al., 1999). The *cdc13-1* and *cdc15-2* have been used in previous studies (Gardner et al., 1999; Lydall and Weinert, 1995). The *rad17-Δ2* and *rad17-Δ3* mutations were constructed by D.Lydall, unpublished.

Construction of Point Mutations

A PCR-based method was used to create *rad17-T241A*, *rad17-R259E*, and *rad17-R259I*. This method takes advantage of the fact that *Pfu* polymerase (Stratagene) produces blunt ends. Three primers were designed that have the desired *RAD17* mutations flanked by homologous sequence, these are P447,5'TCTTCGATTTTGCCTCGTTTGATAA 3'; P448, 5'AAGTCCTTTTCAGGATGGATGTTCA3'; P449,5'AAGTCCTTTTCATCATGGATGTTCA3'. Another set of primers were designed to be oriented end to end with these primers with opposite directionality, primer 447PCR, 5'acccaattacagcaaaacca3' was used in reactions with primer P447, the primer 4489PCR, 5'tgcttgcaattttagtactctttc3' was using in reactions with primers P448 and P449. PCR reactions using these primers and ELP19 that contained the *RAD17* gene in the Bluescript SK- vector (Stratagene), resulted in amplified linear plasmid. The PCR produce was kinased Polynucleotide-Kinase (Roche Applied Science) and ligated with T4-Ligase (Roche Applied Science). Bacterial transformation and amplification of the plasmids were done using standard methods. The presence of the point mutations was confirmed by DNA sequencing. The *RAD17* point mutation containing plasmids ELP30 (*rad17-T241A*), ELP31 (*rad17-R259E*), and ELP32 (*rad17-R259I*) were cut with BamHI and transformed (Getz and Schiestl,1996) into DLY291 that had been marker swapped

with *URA3* at the *RAD17* locus, *Mata, cdc13-1, rad17Δ::leu2::URA3, his3, trp1, ura3, ade2, can1*. Cells were allowed to recover for 2 days at 23°C before being plated onto 5-fluoroortic acid (FOA) plates. PCR and DNA sequencing confirmed the presence of the integrated mutations.

G2/M cell cycle arrest assaying using *cdc13-1* DNA damage induction.

G2/M cycle arrest assays were performed as described (Lydall and Weinert, 1995). Cells were grown in yeast extract-peptone and 2% dextrose (YEPD) at 23°C for two days to saturation (Sherman, 1986). Overnight cultures were inoculated 1:50 dilution into YEPD@ 23°C. The following day cells were checked for cell density with a hemocytometer. Cells were counted as follows: one cell was counted as one and a budded cell counted as two. Cultures were adjusted to $6x10^6$ cells/ml if the cultures had not grown past $1.5x10^7$. α-factor (Sigma; St. Louis, MO) was then added to a final concentration of 20n*M*. Cell washing procedure started at t= -40 minutes to the zero time point. At the zero time point cells were shifted to 36°C (30°C for *pds1Δ* strains, Gardner et al.) the restrictive temperature for *cdc13-1* and *cdc15-2*. Aliquots of the cultures were taken at the designated time points and fixed by adding 0.5 mls of cell culture to 1 ml 95% ethanol. Cell cycle arrest assays were quantitated by analyzing the nuclei of the cells to determine if nuclear division has occurred resulting in two nuclei or if the G2/M checkpoint had been activated resulting in one visible nucleus. Nuclear morphologies were quantitated by scoring at least 100 cells that had been stained with 4,6-diamino-2-phenylindole (DAP1, 0,2 μg/ml) (Pringle et al., 1989) and visualized with a fluorescent microscope.

Rapid Death Assays

Cells were grown and arrested with α-factor as described previously for cell cycle arrest assays. The rapid death assay was performed as previously described (Lydall and Weinert, 1997). Cell viability was measured by diluting the cell culture to 2000 cells/ml in YEPD. Duplicate 100μl aliquots are then plated onto YEPD agarose plates and grown at 23°C for 3 days. Colonies that are visible are counted and the number of colonies that have grown at t=0 defines 100% viability.

Cell survival following UV exposure.

Saturated cultures were grown as previously described in the section on cell cycle arrest assay. Cell cultures were adjusted to $2x10^6$ cells/ml grown for 6 hours with shaking at 23°C. Cells cultures were then adjusted to a final concentration of 2000 cells/ml. Duplicate 100μl aliquot were then plated in duplicate on YEPD agarose plates and the plates were allowed time to dry (approx. 20 min.). Plated cells were then exposed to appropriate does of UVC using a Stratalinker 1800. The plates were then incubated at 23°C for and counted on day 3 to determine viability. A control plate that had not been exposed to UVC defined 100% viability.

Figure 5-1.

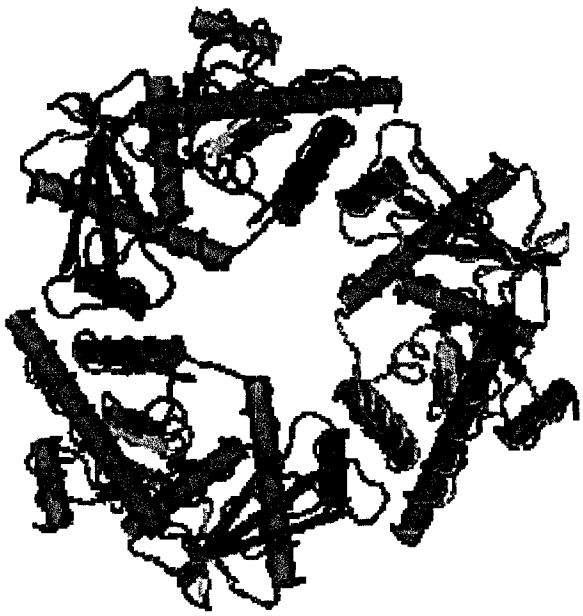

λ-exonuclease

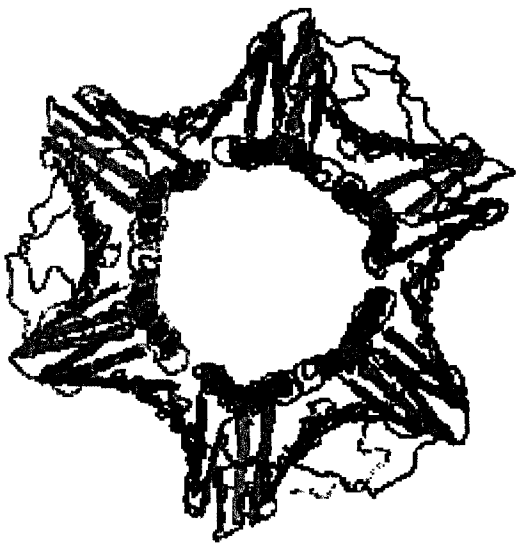

Human PCNA

Structures of λ phage exonuclease and *H.sapiens* proliferating nuclear cell antigen, PDB codes are 1AVQ and 1AXC respectively.

Figure 5-2.

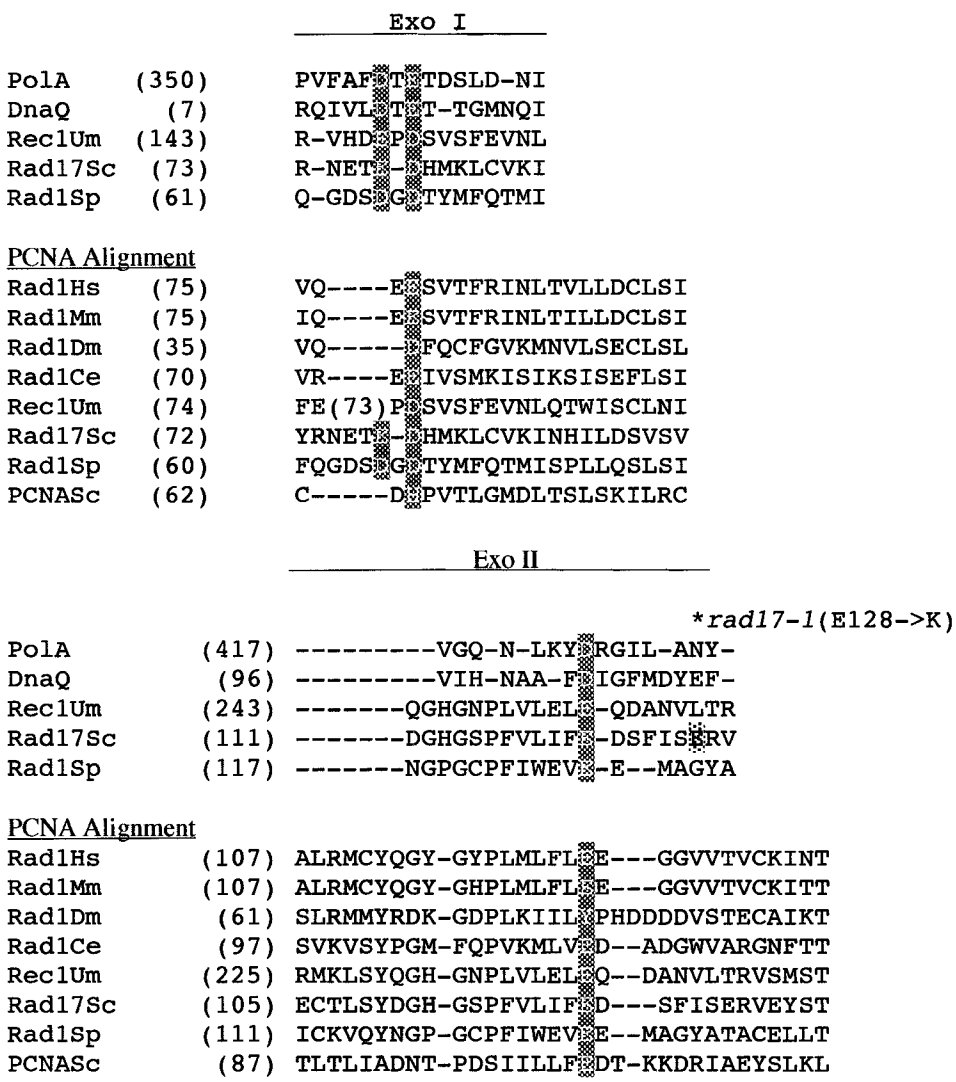
Exo I
PolA (350) PVFAF T TDSLD-NI
DnaQ (7) RQIVL T T-TGMNQI
Rec1Um (143) R-VHD P SVSFEVNL
Rad17Sc (73) R-NET - HMKLCVKI
Rad1Sp (61) Q-GDS G TYMFQTMI
PCNA Alignment
Rad1Hs (75) VQ----E SVTFRINLTVLLDCLSI
Rad1Mm (75) IQ----E SVTFRINLTILLDCLSI
Rad1Dm (35) VQ-----F QCFGVKMNVLSECLSL
Rad1Ce (70) VR----E IVSMKISIKSISEFLSI
Rec1Um (74) FE(73)P SVSFEVNLQTWISCLNI
Rad17Sc (72) YRNET - HMKLCVKINHILDSVSV
Rad1Sp (60) FQGDS G TYMFQTMISPLLQSLSI
PCNASc (62) C-----D PVTLGMDLTSLSKILRC
Exo II
*rad17-1(E128->K)
PolA (417) ---------VGQ-N-LKY RGIL-ANY-
DnaQ (96) ---------VIH-NAA-F IGFMDYEF-
Rec1Um (243) -------QGHGNPLVLEL -QDANVLTR
Rad17Sc (111) -------DGHGSPFVLIF -DSFIS RV
Rad1Sp (117) -------NGPGCPFIWEV -E--MAGYA
PCNA Alignment
Rad1Hs (107) ALRMCYQGY-GYPLMLFL E---GGVVTVCKINT
Rad1Mm (107) ALRMCYQGY-GHPLMLFL E---GGVVTVCKITT
Rad1Dm (61) SLRMMYRDK-GDPLKIIL PHDDDDVSTECAIKT
Rad1Ce (97) SVKVSYPGM-FQPVKMLV D--ADGWVARGNFTT
Rec1Um (225) RMKLSYQGH-GNPLVLEL Q--DANVLTRVSMST
Rad17Sc (105) ECTLSYDGH-GSPFVLIF D---SFISERVEYST
Rad1Sp (111) ICKVQYNGP-GCPFIWEV E--MAGYATACELLT
PCNASc (87) TLTLIADNT-PDSIILLF DT-KKDRIAEYSLKL

Figure 5-2 continued.

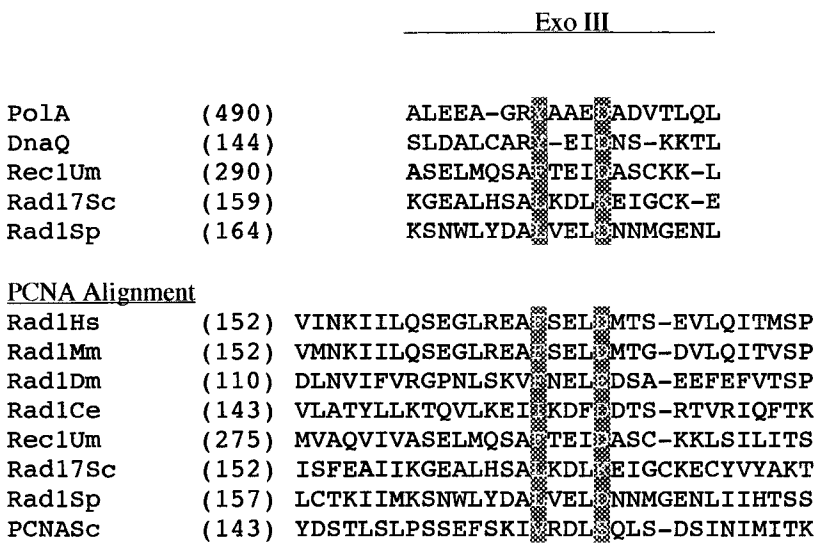

Figure 5-2. An alignment of Rad17 with both 3'->5' exonucleases and PCNA. Amino acids considered to be conserved for exonuclease activity are highlighted. The original *rad17-1* E128K point mutation is indicated. The alignments are adaptations from references (Thelen 2000, Thelen 1994). The sequences shown are as follows. PolA, *E.coli* DNA polymerase I; DnaQ, *E.coli*, ε-subunit of DNA polymerase III; RecIUm, *U.maydis* RecI; Rad17Sc, *S.cerevisiae* Rad17; Rad1Sp, *S.pombe* Rad1; Rad1Hs, *H.sapiens* Rad1; Rad1Mm, *M.musculus* Rad1; Rad1Dm, *D.melanogaster* Rad1; Rad1Ce, *C.elegans* Rad1;RecIUm, *U.maydis* RecI; PCNASc, *S.cerevisiae* proliferating nuclear cell antigen.

Figure 5-3. Cell viability of *rad17-E122A* mutants following *cdc13-1* DNA damage and UV radiation (A) Cell viablity of *rad17- E122A* indicate that the mutant protein is mildly defective in inducing rapid viability loss follwing *cdc13-1* DNA damage. (B) *rad17-E122A* cells are not sensitive to UV radiation.

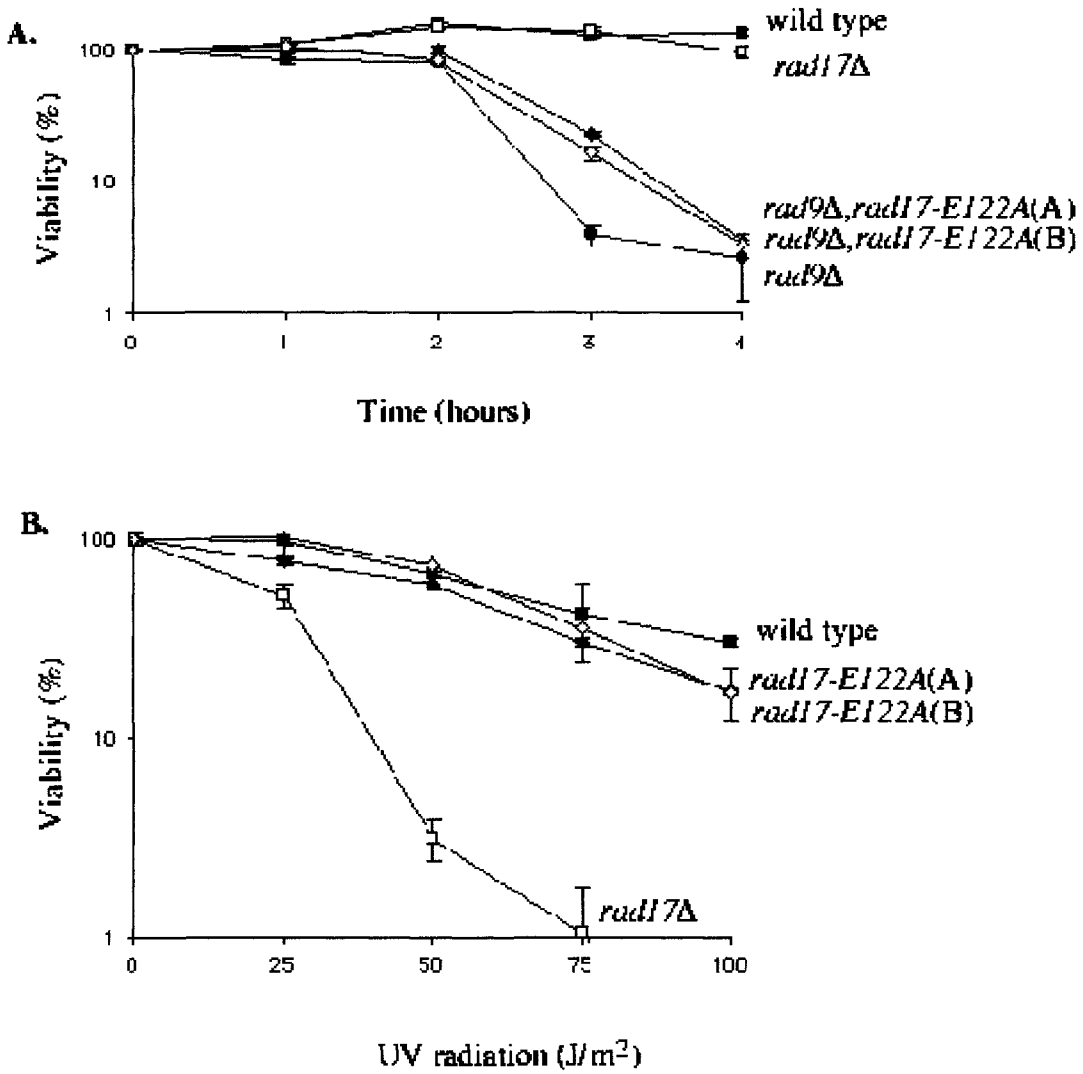

Figure 5-4.

A.

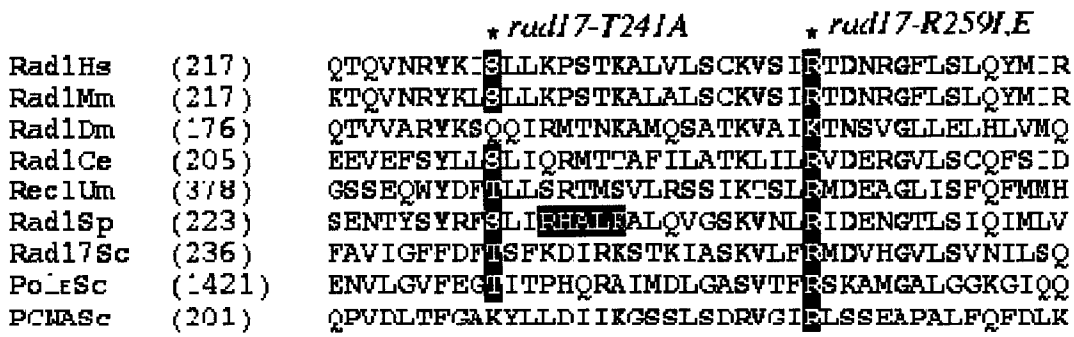

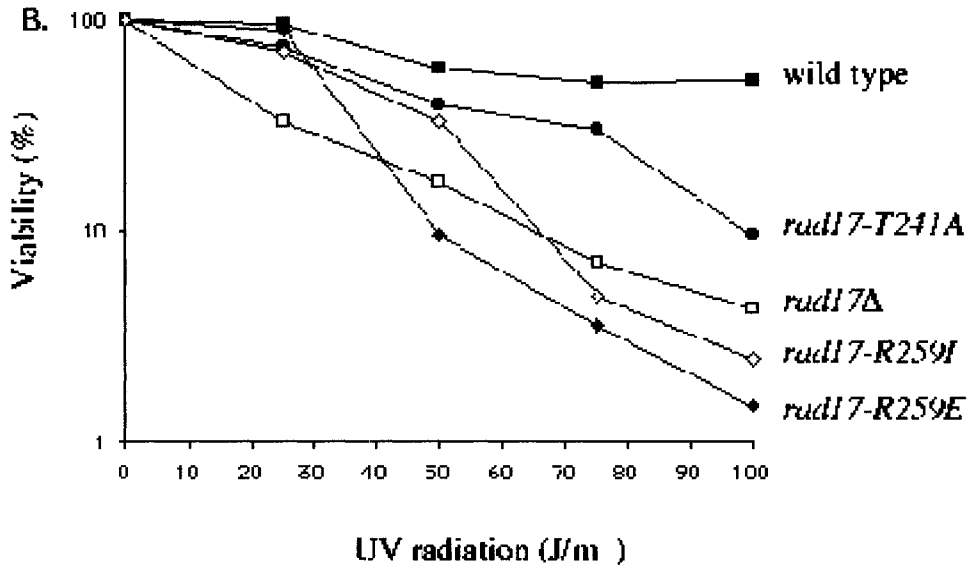

Figure 5-4. Alignment of Rad17 leucine-rich domain. Conserved amino amino acid residues are shown as black type on grey background. *RAD17* mutations *rad17-T241A*, *rad17-R259I*, and *rad17-R259E* are indicated by asterisks and their respective amino acid residues located in the alignment are indicated by white type on dark grey background. The *S.pombe* check-point small deletion mutant *rad1-S4* is indicated by white type on black background.The sequences shown are as follows. Rad1Hs, *H.sapiens* Rad1; Rad1Mm, *M.musculus* Rad1; Rad1Dm, *D.melanogaster* Rad1; Rad1Ce, *C.elegans* Rad1;Rec1Um, U.maydis Rec1; Rec1Um, U.maydis Rec1; Rad1Sp, *S.pombe* Rad1; Rad17Sc, *S.cerevisiae* Rad17; PolεSc, *S.cerevisiae* Polymerase ε; PCNASc, *S.cerevisiae* proliferating nuclear cell antigen.

Figure 5-5. Location of the *RAD17* mutants *rad17-E122A* and *rad17-1* based on the PCNA structure model. PDB code 1AXC.

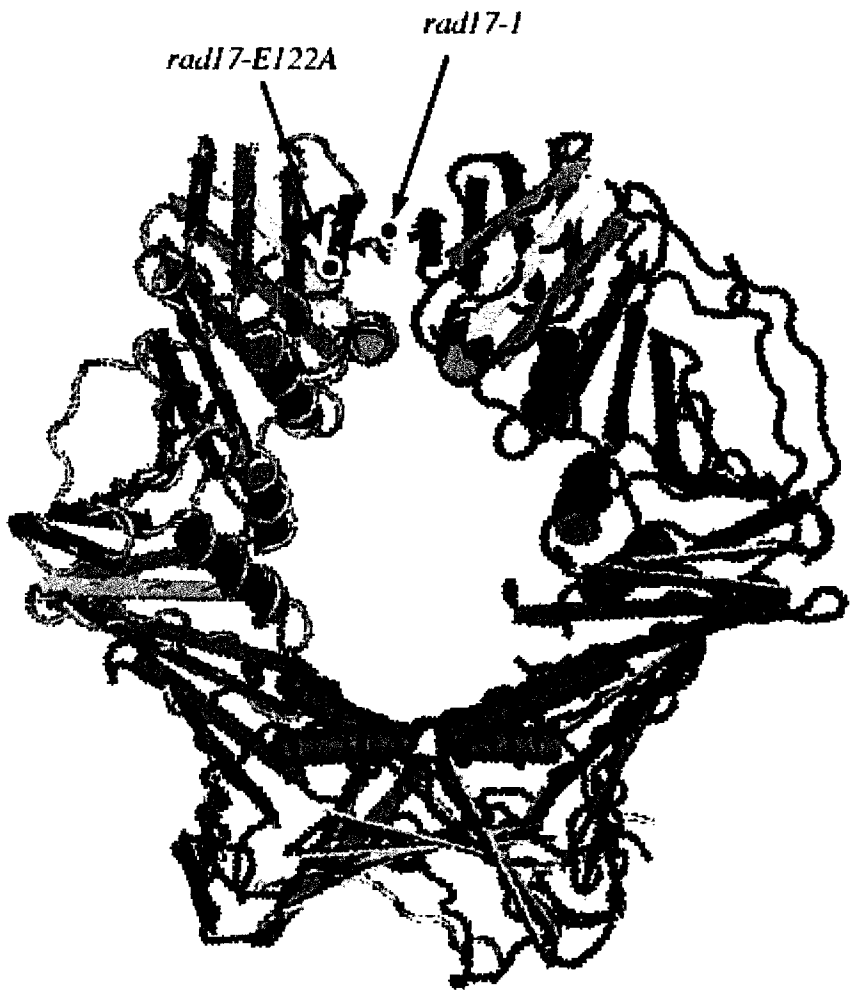

Figure 5-6. Location of *RAD17* mutants *rad17-T241A*, *rad17-R259E*, and *rad17-R259I* located in the leucine-rich region of the protein, based on the PCNA structure model PDB code 1AXC.

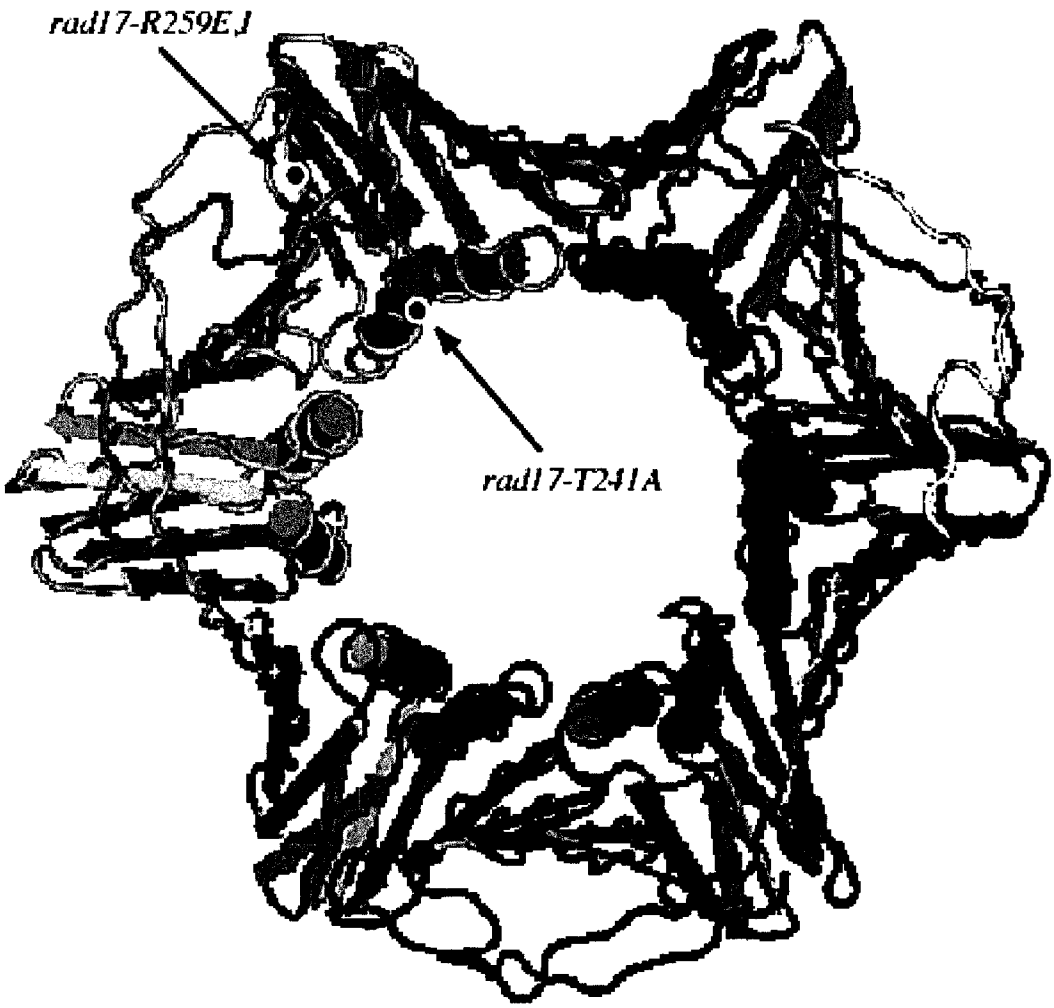

Figure 5-7. (A) Checkpoint function of *RAD17* carboxy-terminal deletion mutants following *cdc13-1* DNA damage induction at 36°C. (B) Cell viability of *rad9Δ*, *cdc13-1* mutant cells with or without the presence of *RAD17* carboxy-terminal deletion mutants following damage induction.

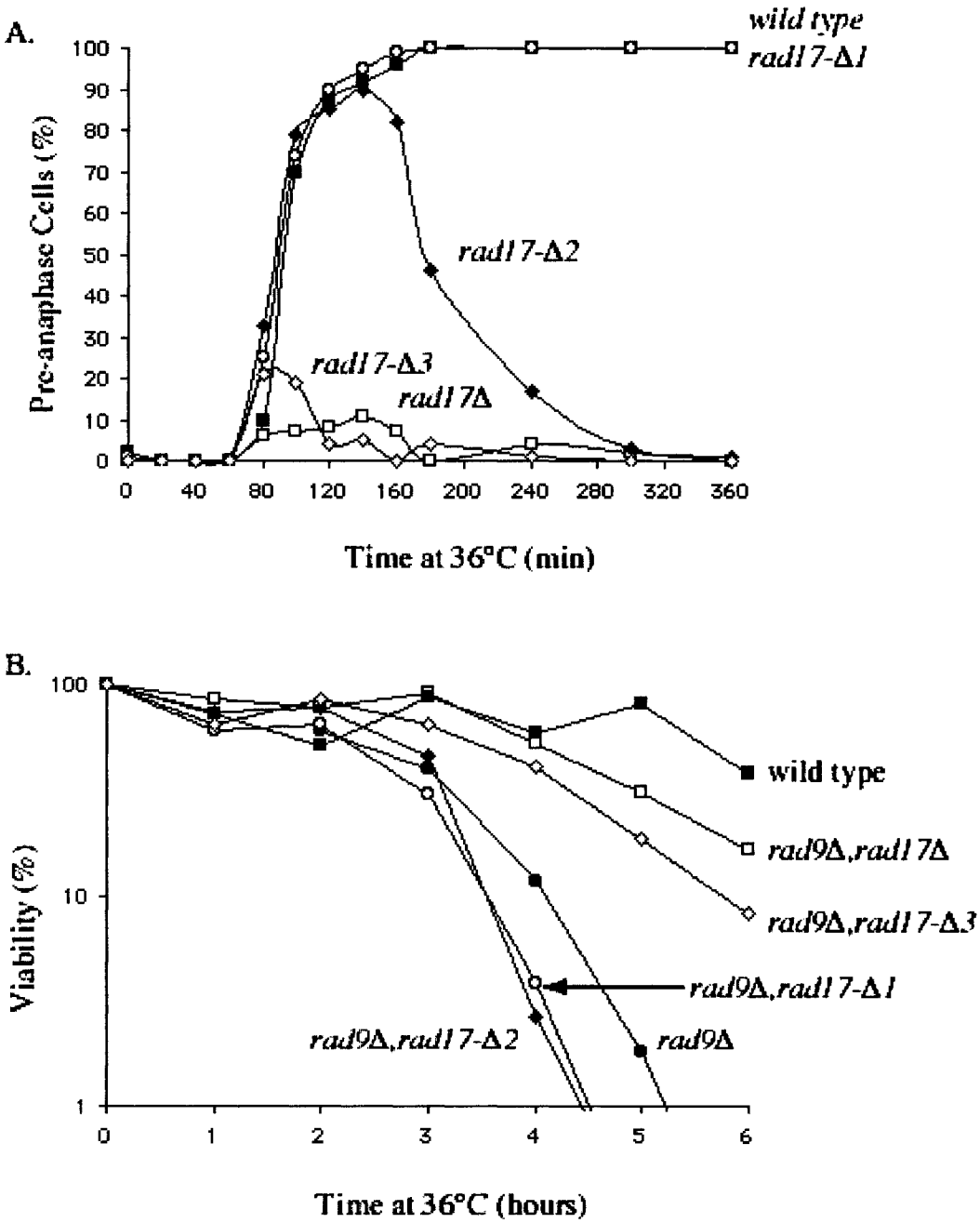

Figure 5-8. ***rad17-Δ2***, ***rad53-11*** **and** ***rad17-Δ2,rad53-11*** **cells have similar cell cylce arrest profiles following** ***cdc13-1*** **DNA damage. This suggests that** ***rad17-Δ2*** **cells are defective for signalling arrest through** ***RAD53.***

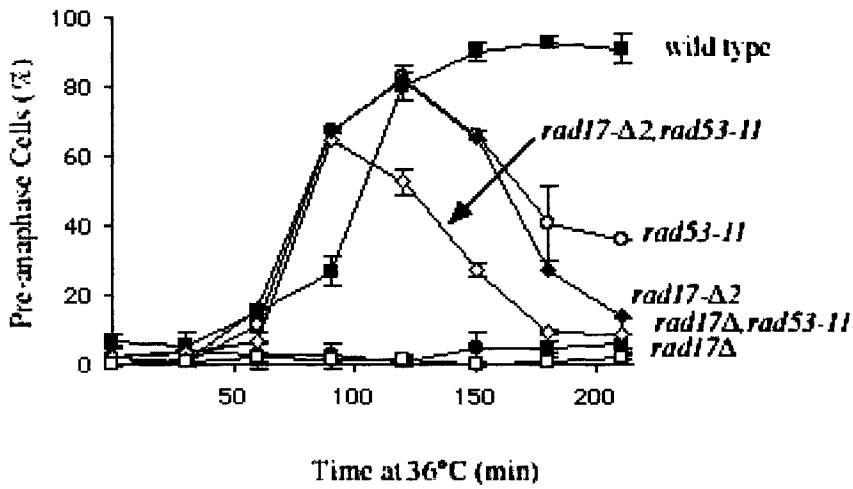

Figure 5-9. (A) and (B) are two independent cell cycle arrest assays testing *rad17-Δ2*, *pds1Δ*, and *rad17-Δ2,pds1Δ* mutant cycle arrest profiles following *cdc13-1* DNA damage. These results are inconclusive whether *rad17-Δ2,pds1Δ* mutant cell have a complete cell cycle arrest defect. The arrow in Figure A indicates a small difference first detected between *rad17-Δ2* and *rad17-Δ2,pds1Δ* mutants that was not able to be reproduced as shown in Figure B.

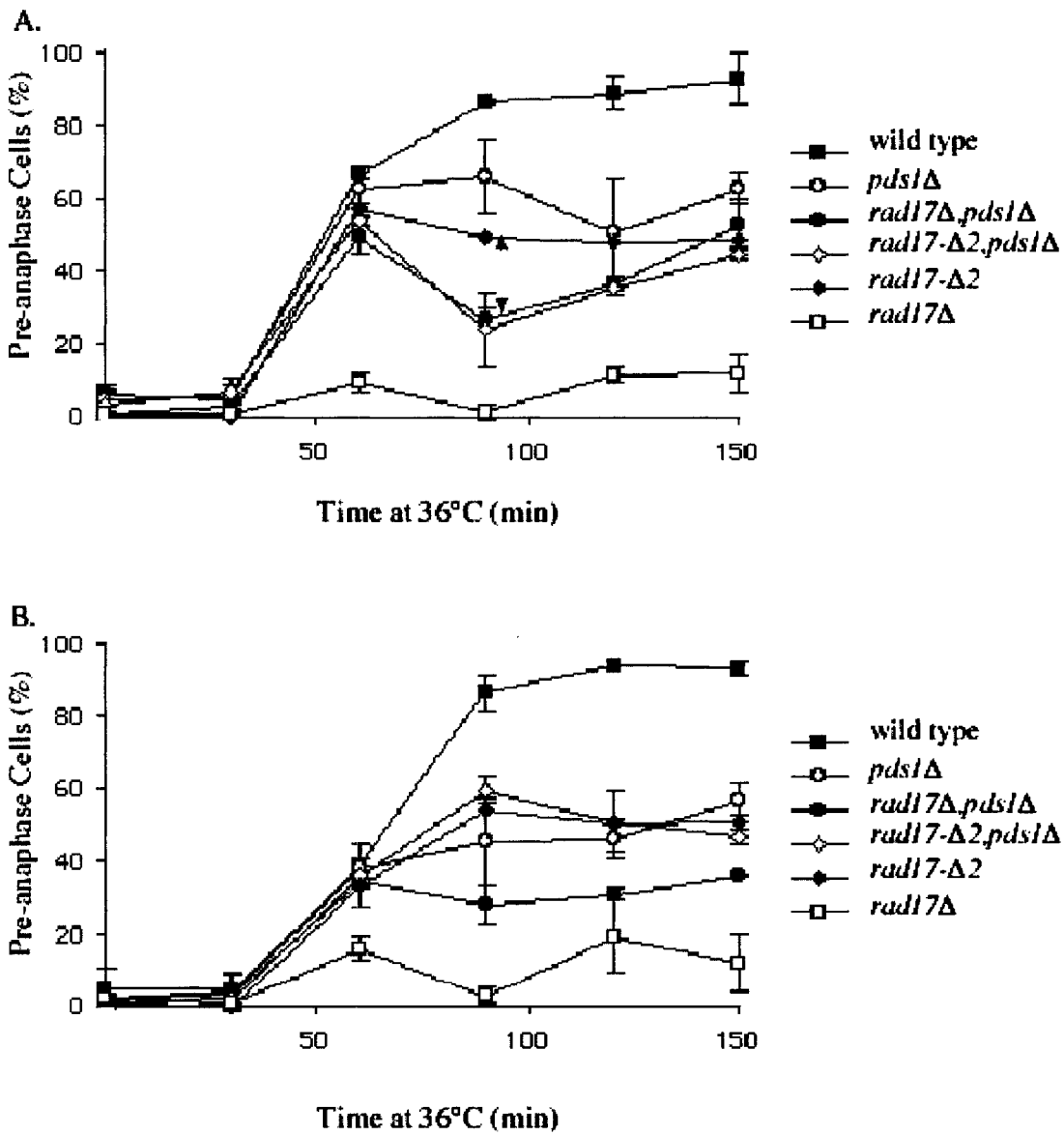

Figure 5-10. The *rad17*-Δ2 mutant is moderately sensitive to UV radiation, but does not have a *rad17*Δ phenotypic response.

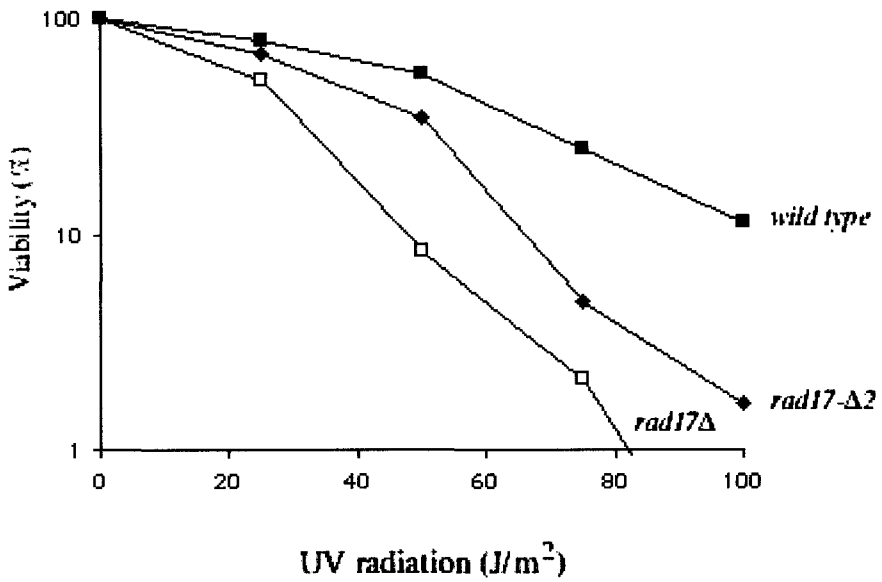

Table 5-1. Strains used in this study.

Strain	Genotype	Source
DLY291	*Mat**a**, rad17Δ::LEU2, cdc13-1, his3, trp1, ura3, ade2, can1*	D.Lydall
DLY835	*Mat**a**, rad9::HIS3, cdc13-1, ura3, leu2*	D.Lydall
DLY869	*Mat**a**, rad17-E122A::LEU2, rad9::HIS3, cdc13-1, ura3*	
DLY627	*Mat**a**, rad17-Δ1::TRP1, rad17Δ::LEU2, cdc13-1,cdc15-2 bar1, his3, ura3*	D.Lydall
DLY628	*Mat**a**, rad17-Δ2::TRP1, rad17Δ::LEU2, cdc13-1,cdc15-2 bar1, his3, ura3*	D.Lydall
DLY631	*Mat**a**, rad17-Δ3::TRP1, rad17Δ::LEU2, cdc13-1,cdc15-2 bar1, his3, ura3*	D.Lydall
ELY37	*Mat**a**, cdc13-1, cdc15-2 bar1, his3, leu2, trp1, ura3*	This study
ELY36	*Mat**a**, rad17::LEU2, cdc13-1, cdc15-2 bar1, his3, trp1, ura3*	This study
ELY38	*Mat**a**, rad17::LEU2, rad17-Δ1::TRP1, pds1Δ::LEU2, cdc13-1, cdc15-2 bar1, his3, trp1, ura3*	This study
ELY39	*Mat**a**, rad17::LEU2, rad17-Δ2::TRP1, pds1Δ::LEU2, cdc13-1, cdc15-2 bar1, his3, trp1, ura3*	This study
CPY277	*Mat**a**, pds1Δ::LEU2, cdc13-1, cdc15-2 bar1, his3, trp1, ura3*	C.Putnam
ELY41	*Mat**a**, pds1Δ::LEU2, rad17Δ::LEU2, cdc13-1, cdc15-2, bar1, his3, trp1, ura3*	This study
ELY42	*Mat**a**, rad17::LEU2, rad17-Δ1::TRP1, rad53-11,*	This study

Table 5-1 continued.

	cdc13-1, cdc15-2 bar1, his3, trp1, ura3	
	*Mat**a**, rad17::LEU2, rad17-Δ2::TRP1, rad53-11,*	This study
	cdc13-1, cdc15-2 bar1, his3, trp1, ura3	
ELY44	*Mat**a**, rad53-11, leu2, cdc13-1, cdc15-2 bar1, his3, trp1, ura3*	This study
ELY45	*Mat**a**, rad17Δ::LEU2, rad53-11, cdc13-1, cdc15-2 bar1,*	This study
	his3, trp1, ura3	
	*Mat**a**, rad17-Δ2::TRP1, rad17Δ::LEU2, rad53-11, cdc13-1,*	This study
	cdc15-2 bar1, his3, trp1, ura3	
	*Mat**a**, rad17-T24A::LEU2, cdc13-1, cdc15-2, bar1,*	This study
	his3, trp1, ura3	
	*Mat**a**, rad17-R259E::LEU2, cdc13-1, cdc15-2, bar1,*	This study
	his3, trp1, ura3	
	*Mat**a**, rad17-R259I::LEU2, cdc13-1, cdc15-2 bar1,*	This study
	his3, trp1, ura3	

Future Directions.

The DNA damage checkpoint response senses DNA damage to activate cell cycle arrest, DNA repair and gene transcription. This suggests that the checkpoint response uses sensor proteins that directly detect DNA damage. However, primary DNA damage has numerous forms such as UV dimers and double-stranded DNA breaks. The checkpoint response responds to all forms of DNA damage and could do this by either detecting all the various forms of DNA damage, or detecting the common intermediate structure for the repair of most forms of DNA damage, single stranded DNA. In this dissertation the checkpoint sensor proteins Rad9 and Rad24 were found to have associated single stranded DNA binding activity not found in other checkpoint proteins tested, supporting the hypothesis that the checkpoint responds to already processed DNA damage.

The observation from this dissertation is that Rad9 and Rad24 detect DNA damage in addition to the checkpoint protein Lcd1 that binds to DNA independent of Rad9 and Rad24(Rouse and Jackson, 2002b). This suggests a model in which all three proteins bind DNA to activate the response. The rationale for this may be for the cell to have multiple protein inputs to activate the checkpoint response and thus avoid any spurious checkpoint activation. However, now that these initial biochemical characterizations have been made, how these three proteins function at the DNA level and activate the checkpoint is an area for future research.

The different degrees of affinity that Rad24 DNA binding has for dsDNA and ssDNA may serve different functions for localization of Rad24 to DNA. Rad24 dsDNA affinity may keep Rad24 localized to the DNA in general in anticipation of DNA

damage, while Rad24 ssDNA affinity may target Rad24 to sites of DNA repair. Rad24 DNA binding shows no preference for ssDNA over primer-template junctions, an anticipated DNA substrate for Rad24. However, Rad24 DNA binding may be affected by the single stranded DNA binding protein RPA that promotes the specificity of RFC for primer-template junctions. In addition, the checkpoint complex Ddc1/Mec3/Rad17 may also affect the affinity of Rad24 for DNA substrates. This is based on a report that indicates RFC binding specificity is affected by PCNA (Tsurimoto and Stillman, 1991). These are all grounds for further experimentation, specifically a series of experiments looking at how both RPA and Ddc1/Mec3/Rad17 affect the substrate specificity of Rad24 –RFC.

The finding that Rad9 has its own associated DNA binding suggests that it can bind to DNA independent of the other checkpoint proteins. Chromatin association assays either using ChIP or GFP localization of Rad9 in either a Rad24 or Lcd1 mutant backgrounds would further support this finding, and the model in which three independent checkpoint protein inputs are required for a full checkpoint response.

Although it is alluring to hypothesize that Rad17 is an exonuclease that processes DNA to produce a DNA substrate that can be recognized by Rad9 and Lcd1, the biochemical analysis has not been forthcoming. In addition, Lcd1 has been shown to localize to DNA damage independent of Rad17. However, there are additional biochemical avenues to pursue to characterize the potential Rad17 exonuclease activity. Certainly various buffering conditions could be tested, and other DNA structures such as cruciform, DNA nicks, or UV dimers could be assayed for Rad17 exonuclease activity.

In addition, it was not tested for whether Rad17 truly formed the hetero-trimeric complex with Ddc1 and Mec3 that they form *in vivo*, and it may be that the Ddc1/Mec3/Rad17 trimeric complex is required for exonuclease activity.

Homology data that indicate that Rad 17 is homologous to PCNA is convincing. These data suggest that Rad17 functions with Ddc1 and Mec3 in a way similar to how PCNA functions to recruit proteins that are involved in DNA repair. The Ddc1/Mec3/Rad17 complex may function to recruit proteins to sites of DNA damage to activate the DNA damage checkpoint response and promote DNA repair. Therefore, a more intriguing question is what proteins does this trimeric complex interact with to initiate and also to maintain the cell cycle arrest until completion of repair. In addition, the investigation into the connection between the checkpoint response and DNA repair continues to be an area of inquiry that remains open.

The hypothesis that Ddc1, Mec3, and Rad17 can act as a potential polymerase recruiter in the checkpoint response and recruit polymerases not required for DNA replication to sites of DNA damage has yet to be addressed(Gomes et al., 2001). This is certainly supported by the finding in *S.pombe* that suggest that the checkpoint proteins specific for S-phase arrest doe not interfere with replications, as opposed to the G2/M checkpoint proteins whose functions may interfere with replication. Several alternative polymerases not thought to have a role in DNA replication have been identified that may be recruited to sites of DNA damage by Ddc1/Mec3/Rad17 complex for repair. Therefore the question is whether an alternative polymerase is required for the DNA damage checkpoint response.

Following this line of experimentation assays one could also address whether RFC is dislocated from sites of DNA damage not repaired during the S-phase arrest to allow Rad24-RFC binding would be informative. Intracellular localization studies using GFP or other antibody staining techniques on cells that sustained irreparable DNA damage in S-phase could address the temporal order of RFC versus Rad24-RFC analyzed at sites of 1 DNA damage. Does RFC fall off? Does RAd24-RFC replace RFC, and at what phase in the cell cycle?

In addition, these checkpoint proteins are conserved from yeast to humans appear in. Another interesting question is what stages of development are these proteins critical for in humans or other organisms other than yeast?

The DNA damage checkpoint response prevents the accumulation of mutations that could result in cell lethality, or in the case of multicellular organisms, cancer. Any increase in the knowledge of the proteins involved in the checkpoint response and how they function could identify potential targets for chemotherapy drug design. Therefore, the importance of continuing research on the checkpoint response remains important to both understanding events that can lead to cancer and potential cancer treatment.

REFERENCES

Abraham, R. T. (2001). Cell cycle checkpoint signaling through the ATM and ATR kinases. Genes Dev *15*, 2177-2196.

Allen, J. B., Zhou, Z., Siede, W., Friedberg, E. C., and Elledge, S. J. (1994). The SAD1/RAD53 protein kinase controls multiple checkpoints and DNA damage-induced transcription in yeast. Genes Dev *8*, 2401-2415.

Batty, D. P., and Wood, R. D. (2000). Damage recognition in nucleotide excision repair of DNA. Gene *241*, 193-204.

Brush, G. S., and Kelly, T. J. (2000). Phosphorylation of the replication protein A large subunit in the Saccharomyces cerevisiae checkpoint response. Nucleic Acids Res *28*, 3725-3732.

Brush, G. S., Morrow, D. M., Hieter, P., and Kelly, T. J. (1996). The ATM homologue MEC1 is required for phosphorylation of replication protein A in yeast. Proc Natl Acad Sci U S A *93*, 15075-15080.

Burack, W. R., and Shaw, A. S. (2000). Signal transduction: hanging on a scaffold. Curr Opin Cell Biol *12*, 211-216.

Cai, J., Yao, N., Gibbs, E., Finkelstein, J., Phillips, B., O'Donnell, M., and Hurwitz, J. (1998). ATP hydrolysis catalyzed by human replication factor C requires participation of multiple subunits. Proc Natl Acad Sci U S A *95*, 11607-11612.

Cullmann, G., Fien, K., Kobayashi, R., and Stillman, B. (1995). Characterization of the five replication factor C genes of Saccharomyces cerevisiae. Mol Cell Biol *15*, 4661-4671.

Dynan, W. S., and Yoo, S. (1998). Interaction of Ku protein and DNA-dependent protein kinase catalytic subunit with nucleic acids. Nucleic Acids Res *26*, 1551-1559.

Edwards, R. J., Bentley, N. J., and Carr, A. M. (1999). A Rad3-Rad26 complex responds to DNA damage independently of other checkpoint proteins. Nat Cell Biol *1*, 393-398.

Emili, A. (1998). MEC1-dependent phosphorylation of Rad9p in response to DNA damage. Mol Cell *2*, 183-189.

Freire, R., Murguia, J. R., Tarsounas, M., Lowndes, N. F., Moens, P. B., and Jackson, S. P. (1998). Human and mouse homologs of Schizosaccharomyces pombe rad1(+) and Saccharomyces cerevisiae RAD17: linkage to checkpoint control and mammalian meiosis. Genes Dev *12*, 2560-2573.

Gardner, R., Putnam, C. W., and Weinert, T. (1999). RAD53, DUN1 and PDS1 define two parallel G2/M checkpoint pathways in budding yeast. Embo J *18*, 3173-3185.

Garvik, B., Carson, M., and Hartwell, L. (1995). Single-stranded DNA arising at telomeres in cdc13 mutants may constitute a specific signal for the RAD9 checkpoint. Mol Cell Biol *15*, 6128-6138.

George, J., Castellazzi, M., and Buttin, G. (1975). Prophage induction and cell division in E. coli. III. Mutations sfiA and sfiB restore division in tif and lon strains and permit the expression of mutator properties of tif. Mol Gen Genet *140*, 309-332.

Gerald, J. N., Benjamin, J. M., and Kron, S. J. (2002). Robust G1 checkpoint arrest in budding yeast: dependence on DNA damage signaling and repair. J Cell Sci *115*, 1749-1757.

Gerik, K. J., Gary, S. L., and Burgers, P. M. (1997). Overproduction and affinity purification of Saccharomyces cerevisiae replication factor C. J Biol Chem *272*, 1256-1262.

Gilbert, C. S., Green, C. M., and Lowndes, N. F. (2001). Budding yeast Rad9 is an ATP-dependent Rad53 activating machine. Mol Cell *8*, 129-136.

Gomes, X. V., and Burgers, P. M. (2001). ATP utilization by yeast replication factor C. I. ATP-mediated interaction with DNA and with proliferating cell nuclear antigen. J Biol Chem *276*, 34768-34775.

Gomes, X. V., Schmidt, S. L., and Burgers, P. M. (2001). ATP utilization by yeast replication factor C. II. Multiple stepwise ATP binding events are required to load proliferating cell nuclear antigen onto primed DNA. J Biol Chem *276*, 34776-34783.

Green, C. M., Erdjument-Bromage, H., Tempst, P., and Lowndes, N. F. (2000). A novel Rad24 checkpoint protein complex closely related to replication factor C. Curr Biol *10*, 39-42.

Hall, M. C., Wang, H., Erie, D. A., and Kunkel, T. A. (2001). High affinity cooperative DNA binding by the yeast Mlh1-Pms1 heterodimer. J Mol Biol *312*, 637-647.

Hammarsten, O., and Chu, G. (1998). DNA-dependent protein kinase: DNA binding and activation in the absence of Ku. Proc Natl Acad Sci U S A *95*, 525-530.

Kanter-Smoler, G., Knudsen, K. E., Jimenez, G., Sunnerhagen, P., and Subramani, S. (1995). Separation of phenotypes in mutant alleles of the Schizosaccharomyces pombe cell-cycle checkpoint gene rad1+. Mol Biol Cell *6*, 1793-1805.

Kelman, Z., and Hurwitz, J. (1998). Protein-PCNA interactions: a DNA-scanning mechanism? Trends Biochem Sci *23*, 236-238.

Kim, H. S., and Brill, S. J. (2001). Rfc4 interacts with Rpa1 and is required for both DNA replication and DNA damage checkpoints in Saccharomyces cerevisiae. Mol Cell Biol *21*, 3725-3737.

Kondo, T., Matsumoto, K., and Sugimoto, K. (1999). Role of a complex containing Rad17, Mec3, and Ddc1 in the yeast DNA damage checkpoint pathway. Mol Cell Biol *19*, 1136-1143.

Kondo, T., Wakayama, T., Naiki, T., Matsumoto, K., and Sugimoto, K. (2001). Recruitment of Mec1 and Ddc1 checkpoint proteins to double-strand breaks through distinct mechanisms. Science *294*, 867-870.

Kovall, R., and Matthews, B. W. (1997). Toroidal structure of lambda-exonuclease. Science *277*, 1824-1827.

Kovall, R. A., and Matthews, B. W. (1998). Structural, functional, and evolutionary relationships between lambda-exonuclease and the type II restriction endonucleases. Proc Natl Acad Sci U S A *95*, 7893-7897.

Kowalczykowski, S. C., Dixon, D. A., Eggleston, A. K., Lauder, S. D., and Rehrauer, W. M. (1994). Biochemistry of homologous recombination in Escherichia coli. Microbiol Rev *58*, 401-465.

Krause, S. A., Loupart, M. L., Vass, S., Schoenfelder, S., Harrison, S., and Heck, M. M. (2001). Loss of cell cycle checkpoint control in Drosophila Rfc4 mutants. Mol Cell Biol *21*, 5156-5168.

Lee, J., Kumagai, A., and Dunphy, W. G. (2003). Claspin, a Chk1-regulatory protein, monitors DNA replication on chromatin independently of RPA, ATR, and Rad17. Mol Cell *11*, 329-340.

Leroy, D., Baldin, V., and Ducommun, B. (1994). Characterization of an active GST-human Cdc2 fusion protein kinase expressed in the fission yeast Schizosaccharomyces pombe: a new approach to the study of cell cycle control proteins. Yeast *10*, 1631-1638.

Liao, H., Yuan, C., Su, M. I., Yongkiettrakul, S., Qin, D., Li, H., Byeon, I. J., Pei, D., and Tsai, M. D. (2000). Structure of the FHA1 domain of yeast Rad53 and identification of binding sites for both FHA1 and its target protein Rad9. J Mol Biol *304*, 941-951.

Lindsey-Boltz, L. A., Bermudez, V. P., Hurwitz, J., and Sancar, A. (2001). Purification and characterization of human DNA damage checkpoint Rad complexes. Proc Natl Acad Sci U S A *98*, 11236-11241.

Liu, J. S., Kuo, S. R., McHugh, M. M., Beerman, T. A., and Melendy, T. (2000a). Adozelesin triggers DNA damage response pathways and arrests SV40 DNA replication through replication protein A inactivation. J Biol Chem *275*, 1391-1397.

Liu, Y., Vidanes, G., Lin, Y. C., Mori, S., and Siede, W. (2000b). Characterization of a Saccharomyces cerevisiae homologue of Schizosaccharomyces pombe Chk1 involved in DNA-damage-induced M-phase arrest. Mol Gen Genet *262*, 1132-1146.

Longhese, M. P., Neecke, H., Paciotti, V., Lucchini, G., and Plevani, P. (1996). The 70 kDa subunit of replication protein A is required for the G1/S and intra-S DNA damage checkpoints in budding yeast. Nucleic Acids Res *24*, 3533-3537.

Longhese, M. P., Paciotti, V., Fraschini, R., Zaccarini, R., Plevani, P., and Lucchini, G. (1997). The novel DNA damage checkpoint protein ddc1p is phosphorylated periodically during the cell cycle and in response to DNA damage in budding yeast. Embo J *16*, 5216-5226.

Lydall, D., and Weinert, T. (1995). Yeast checkpoint genes in DNA damage processing: implications for repair and arrest. Science *270*, 1488-1491.

Lydall, D., and Weinert, T. (1997). G2/M checkpoint genes of Saccharomyces cerevisiae: further evidence for roles in DNA replication and/or repair. Mol Gen Genet *256*, 638-651.

Mazin, A. V., and Kowalczykowski, S. C. (1996). The specificity of the secondary DNA binding site of RecA protein defines its role in DNA strand exchange. Proc Natl Acad Sci U S A *93*, 10673-10678.

Melo, J., and Toczyski, D. (2002). A unified view of the DNA-damage checkpoint. Curr Opin Cell Biol *14*, 237-245.

Melo, J. A., Cohen, J., and Toczyski, D. P. (2001). Two checkpoint complexes are independently recruited to sites of DNA damage in vivo. Genes Dev *15*, 2809-2821.
Mitchell, D. A., Marshall, T. K., and Deschenes, R. J. (1993). Vectors for the inducible overexpression of glutathione S-transferase fusion proteins in yeast. Yeast *9*, 715-722.

Moser, M. J., Holley, W. R., Chatterjee, A., and Mian, I. S. (1997). The proofreading domain of Escherichia coli DNA polymerase I and other DNA and/or RNA exonuclease domains. Nucleic Acids Res *25*, 5110-5118.

Mossi, R., and Hubscher, U. (1998). Clamping down on clamps and clamp loaders--the eukaryotic replication factor C. Eur J Biochem *254*, 209-216.

Naiki, T., Shimomura, T., Kondo, T., Matsumoto, K., and Sugimoto, K. (2000). Rfc5, in cooperation with rad24, controls DNA damage checkpoints throughout the cell cycle in Saccharomyces cerevisiae. Mol Cell Biol *20*, 5888-5896.

Naureckiene, S., and Holloman, W. K. (1999). DNA hydrolytic activity associated with the Ustilago maydis REC1 gene product analyzed on hairpin oligonucleotide substrates. Biochemistry *38*, 14379-14386.

Navas, T. A., Sanchez, Y., and Elledge, S. J. (1996). RAD9 and DNA polymerase epsilon form parallel sensory branches for transducing the DNA damage checkpoint signal in Saccharomyces cerevisiae. Genes Dev *10*, 2632-2643.

Noskov, V. N., Araki, H., and Sugino, A. (1998). The RFC2 gene, encoding the third-largest subunit of the replication factor C complex, is required for an S-phase checkpoint in Saccharomyces cerevisiae. Mol Cell Biol *18*, 4914-4923.

Nyberg, K. A., Michelson, R. J., Putnam, C. W., and Weinert, T. A. (2002). TOWARD MAINTAINING THE GENOME: DNA Damage and Replication Checkpoints. Annu Rev Genet *36*, 617-656.

Onel, K., Thelen, M. P., Ferguson, D. O., Bennett, R. L., and Holloman, W. K. (1995). Mutation avoidance and DNA repair proficiency in Ustilago maydis are differentially lost with progressive truncation of the REC1 gene product. Mol Cell Biol *15*, 5329-5338.

Paciotti, V., Clerici, M., Lucchini, G., and Longhese, M. P. (2000). The checkpoint protein Ddc2, functionally related to S. pombe Rad26, interacts with Mec1 and is regulated by Mec1-dependent phosphorylation in budding yeast. Genes Dev *14*, 2046-2059.

Paciotti, V., Lucchini, G., Plevani, P., and Longhese, M. P. (1998). Mec1p is essential for phosphorylation of the yeast DNA damage checkpoint protein Ddc1p, which physically interacts with Mec3p. Embo J *17*, 4199-4209.

Painter, R. B., and Young, B. R. (1980). Radiosensitivity in ataxia-telangiectasia: a new explanation. Proc Natl Acad Sci U S A *77*, 7315-7317.

Parker, A. E., Van de Weyer, I., Laus, M. C., Oostveen, I., Yon, J., Verhasselt, P., and Luyten, W. H. (1998). A human homologue of the Schizosaccharomyces pombe rad1+ checkpoint gene encodes an exonuclease. J Biol Chem *273*, 18332-18339.

Paull, T. T., Cortez, D., Bowers, B., Elledge, S. J., and Gellert, M. (2001). Direct DNA binding by Brca1. Proc Natl Acad Sci U S A *98*, 6086-6091.

Paulovich, A. G., Margulies, R. U., Garvik, B. M., and Hartwell, L. H. (1997). RAD9, RAD17, and RAD24 are required for S phase regulation in Saccharomyces cerevisiae in response to DNA damage. Genetics *145*, 45-62.

Pringle, J. R., Preston, R. A., Adams, A. E., Stearns, T., Drubin, D. G., Haarer, B. K., and Jones, E. W. (1989). Fluorescence microscopy methods for yeast. Methods Cell Biol *31*, 357-435.

Rauen, M., Burtelow, M. A., Dufault, V. M., and Karnitz, L. M. (2000). The human checkpoint protein hRad17 interacts with the PCNA-like proteins hRad1, hHus1, and hRad9. J Biol Chem *275*, 29767-29771.

Rouse, J., and Jackson, S. P. (2000). LCD1: an essential gene involved in checkpoint control and regulation of the MEC1 signalling pathway in Saccharomyces cerevisiae. Embo J *19*, 5801-5812.

Rouse, J., and Jackson, S. P. (2002a). Interfaces between the detection, signaling, and repair of DNA damage. Science *297*, 547-551.

Rouse, J., and Jackson, S. P. (2002b). Lcd1p recruits Mec1p to DNA lesions in vitro and in vivo. Mol Cell *9*, 857-869.

Sanchez, Y., Bachant, J., Wang, H., Hu, F., Liu, D., Tetzlaff, M., and Elledge, S. J. (1999). Control of the DNA damage checkpoint by chk1 and rad53 protein kinases through distinct mechanisms. Science *286*, 1166-1171.

Sanchez, Y., Desany, B. A., Jones, W. J., Liu, Q., Wang, B., and Elledge, S. J. (1996). Regulation of RAD53 by the ATM-like kinases MEC1 and TEL1 in yeast cell cycle checkpoint pathways. Science *271*, 357-360.

Santocanale, C., Neecke, H., Longhese, M. P., Lucchini, G., and Plevani, P. (1995). Mutations in the gene encoding the 34 kDa subunit of yeast replication protein A cause defective S phase progression. J Mol Biol *254*, 595-607.

Schiestl, R. H., and Gietz, R. D. (1989). High efficiency transformation of intact yeast cells using single stranded nucleic acids as a carrier. Curr Genet *16*, 339-346.

Schmidt, S. L., Pautz, A. L., and Burgers, P. M. (2001). ATP utilization by yeast replication factor C. IV. RFC ATP-binding mutants show defects in DNA replication, DNA repair, and checkpoint regulation. J Biol Chem *276*, 34792-34800.

Sherman, R. H., Fink, G. R. and Hicks, J. B. (1986). Methods in yeast genetics (Cold Spring Harbor, Cold Sprink Harbor Laboratory Press).

Shimada, M., Okuzaki, D., Tanaka, S., Tougan, T., Tamai, K. K., Shimoda, C., and Nojima, H. (1999). Replication factor C3 of Schizosaccharomyces pombe, a small subunit of replication factor C complex, plays a role in both replication and damage checkpoints. Mol Biol Cell *10*, 3991-4003.

Shiomi, Y., Shinozaki, A., Nakada, D., Sugimoto, K., Usukura, J., Obuse, C., and Tsurimoto, T. (2002). Clamp and clamp loader structures of the human checkpoint protein complexes, Rad9-1-1 and Rad17-RFC. Genes Cells *7*, 861-868.

Siede, W., Friedberg, A. S., Dianova, I., and Friedberg, E. C. (1994). Characterization of G1 checkpoint control in the yeast Saccharomyces cerevisiae following exposure to DNA-damaging agents. Genetics *138*, 271-281.

Soulier, J., and Lowndes, N. F. (1999). The BRCT domain of the S. cerevisiae checkpoint protein Rad9 mediates a Rad9-Rad9 interaction after DNA damage. Curr Biol *9*, 551-554.

Sugimoto, K., Shimomura, T., Hashimoto, K., Araki, H., Sugino, A., and Matsumoto, K. (1996). Rfc5, a small subunit of replication factor C complex, couples DNA replication and mitosis in budding yeast. Proc Natl Acad Sci U S A *93*, 7048-7052.

Sun, Z., Fay, D. S., Marini, F., Foiani, M., and Stern, D. F. (1996). Spk1/Rad53 is regulated by Mec1-dependent protein phosphorylation in DNA replication and damage checkpoint pathways. Genes Dev *10*, 395-406.

Thelen, M. P., Onel, K., and Holloman, W. K. (1994). The REC1 gene of Ustilago maydis involved in the cellular response to DNA damage encodes an exonuclease. J Biol Chem *269*, 747-754.

Toh, G. W., and Lowndes, N. F. (2003). Role of the Saccharomyces cerevisiae Rad9 protein in sensing and responding to DNA damage. Biochem Soc Trans *31*, 242-246.
Tsurimoto, T. (1998). PCNA, a multifunctional ring on DNA. Biochim Biophys Acta *1443*, 23-39.

Tsurimoto, T., and Stillman, B. (1991). Replication factors required for SV40 DNA replication in vitro. I. DNA structure-specific recognition of a primer-template junction by eukaryotic DNA polymerases and their accessory proteins. J Biol Chem *266*, 1950-1960.

Uhlmann, F., Cai, J., Flores-Rozas, H., Dean, F. B., Finkelstein, J., O'Donnell, M., and Hurwitz, J. (1996). In vitro reconstitution of human replication factor C from its five subunits. Proc Natl Acad Sci U S A *93*, 6521-6526.

Uhlmann, F., Cai, J., Gibbs, E., O'Donnell, M., and Hurwitz, J. (1997). Deletion analysis of the large subunit p140 in human replication factor C reveals regions required for complex formation and replication activities. J Biol Chem *272*, 10058-10064.

Venclovas, C., Colvin, M. E., and Thelen, M. P. (2002). Molecular modeling-based analysis of interactions in the RFC-dependent clamp-loading process. Protein Sci *11*, 2403-2416.

Venclovas, C., and Thelen, M. P. (2000). Structure-based predictions of Rad1, Rad9, Hus1 and Rad17 participation in sliding clamp and clamp-loading complexes. Nucleic Acids Res *28*, 2481-2493.

Vialard, J. E., Gilbert, C. S., Green, C. M., and Lowndes, N. F. (1998). The budding yeast Rad9 checkpoint protein is subjected to Mec1/Tel1-dependent hyperphosphorylation and interacts with Rad53 after DNA damage. Embo J *17*, 5679-5688.

Waga, S., and Stillman, B. (1998). The DNA replication fork in eukaryotic cells. Annu Rev Biochem *67*, 721-751.

Wakayama, T., Kondo, T., Ando, S., Matsumoto, K., and Sugimoto, K. (2001). Pie1, a Protein Interacting with Mec1, Controls Cell Growth and Checkpoint Responses in Saccharomyces cerevisiae. Mol Cell Biol *21*, 755-764.

Wang, H., Liu, D., Wang, Y., Qin, J., and Elledge, S. J. (2001). Pds1 phosphorylation in response to DNA damage is essential for its DNA damage checkpoint function. Genes Dev *15*, 1361-1372.

Weinert, T. A., and Hartwell, L. H. (1988). The RAD9 gene controls the cell cycle response to DNA damage in Saccharomyces cerevisiae. Science *241*, 317-322.

Weinert, T. A., and Hartwell, L. H. (1993). Cell cycle arrest of cdc mutants and specificity of the RAD9 checkpoint. Genetics *134*, 63-80.

Weinert, T. A., Kiser, G. L., and Hartwell, L. H. (1994). Mitotic checkpoint genes in budding yeast and the dependence of mitosis on DNA replication and repair. Genes Dev *8*, 652-665.

Wold, M. S. (1997). Replication protein A: a heterotrimeric, single-stranded DNA-binding protein required for eukaryotic DNA metabolism. Annu Rev Biochem *66*, 61-92.

Xu, X., Tsvetkov, L. M., and Stern, D. F. (2002). Chk2 activation and phosphorylation-dependent oligomerization. Mol Cell Biol *22*, 4419-4432.

Yuzhakov, A., Kelman, Z., Hurwitz, J., and O'Donnell, M. (1999). Multiple competition reactions for RPA order the assembly of the DNA polymerase delta holoenzyme. Embo J *18*, 6189-6199.

Zhou, B. B., and Elledge, S. J. (2000). The DNA damage response: putting checkpoints in perspective. Nature *408*, 433-439.

Zhou, Z., and Elledge, S. J. (1993). DUN1 encodes a protein kinase that controls the DNA damage response in yeast. Cell *75*, 1119-1127.